

**Creative Synthesis of Novel
Optically-Functional Materials
by Modified BODIPYs with Unique Structures**

Honami YAMANE

2017

**Creative Synthesis of Novel
Optically-Functional Materials
by Modified BODIPYs with Unique Structures**

Honami YAMANE

2017

Department of Polymer Chemistry

Graduate School of Engineering

Kyoto University

Preface

The studies presented in this thesis have been carried out under the direction of Professor Yoshiki Chujo at Department of Polymer Chemistry, Graduate School of Engineering, Kyoto University from April 2011 to March 2017. The studies are concerned with “Creative Synthesis of Novel Optically-Functional Materials by Modified BODIPYs with Unique Structures”.

The author wishes to express her sincerest gratitude to Professor Yoshiki Chujo for his kind guidance, valuable suggestions and warm encouragement throughout this work. The author is deeply grateful to Dr. Kazuo Tanaka for his constant advices and helpful discussions during this work. The author would like to thank Professor Yasuhiro Morisaki, Dr. Ryousuke Yoshii, Dr. Takahiro Kakuta, and Dr. Masayuki Gon for their valuable suggestions and discussions. The author is also grateful to Mr. Shunichiro Ito and Mr. Shunsuke Ohtani for their great contribution to this work. The author is thankful to all members of Professor Chujo’s group. The author is obliged to Ms. Masako Kakutani for her assistance during the author’s laboratory life.

Furthermore, the author wishes to acknowledge Professor Takayuki Yanagida, Dr. Kimihiro Matsukawa, Dr. Seiji Watase, Dr. Koji Mitamura, Dr. Hiroshi Kita, Dr. Hideo Taka, Dr. Atsushi Nagai, and Mr. Amane Hirose for great collaboration in this study. The author wishes to express her special thanks to Professor Richard M. Laine and Dr. Joseph Furgal at University of Michigan for their hospitable supports and valuable suggestions during the author’s stay in USA. The author is grateful to Japan Society for the Promotion of Science (JSPS) for financial support from April 2014 to March 2017.

Finally, the author expresses her deep appreciation to her friends and family, especially her parents, Tetsuhiro Yamane, Teruyo Yamane, and her brother, Kensuke Yamane for their continuous assistance and encouragement.

Honami Yamane

March 2017

Contents

General Introduction ----- 1

Chapter 1 ----- 13

Simple and Valid Strategy for the Enhancement of the Solid-Emissive Property of Boron
Dipyrromethene

Chapter 2 ----- 37

Preservation of Main-Chain Conjugation through BODIPY-Containing Alternating Polymers from
Electronic Interactions with Side-Chain Substituents by Cardo Boron Structures

Chapter 3 ----- 81

The Dual-Emissive Polymer Based on BODIPY Homopolymer Bearing Anthracene on Cardo
Boron

Chapter 4 ----- 97

Efficient Light Absorbers Based on Thiophene-Fused Boron Dipyrromethene (BODIPY) Dyes

Chapter 5 ----- 115

Synthesis of Furan-Substituted Aza-BODIPYs Having Strong Near-Infrared Emission

Chapter 6 ----- 131

Synthesis of the Near-Infrared Light-Absorbing Polymer Based On Thiophene-substituted Aza-BODIPY

Chapter 7 ----- 149

Liquid Scintillators with Near Infrared Emission Based on Organoboron Conjugated Polymers

List of Publications ----- 165

General Introduction

1. Conjugated Organoboron Polymers

π -Conjugated polymers (Figure 1) are versatile candidates for various applications because of their unique electronic properties, low manufacturing cost and capability for flexible conditions. Specifically, they are supposed to be suitable for optoelectronic applications such as organic light emitting diodes, photovoltaic cells, field effect transistors, etc.¹ The character of conjugated polymers can be tuned for each application. To tune the character of conjugated polymers, introduction of hetero atoms is one of the modulation methods. Therefore, various conjugated polymers including hetero atoms were developed. For example, polythiophene, polypyrrole, polyaniline, etc. are well-known hetero atom-containing conjugated polymers and applied to organic devices (Figure 2).²

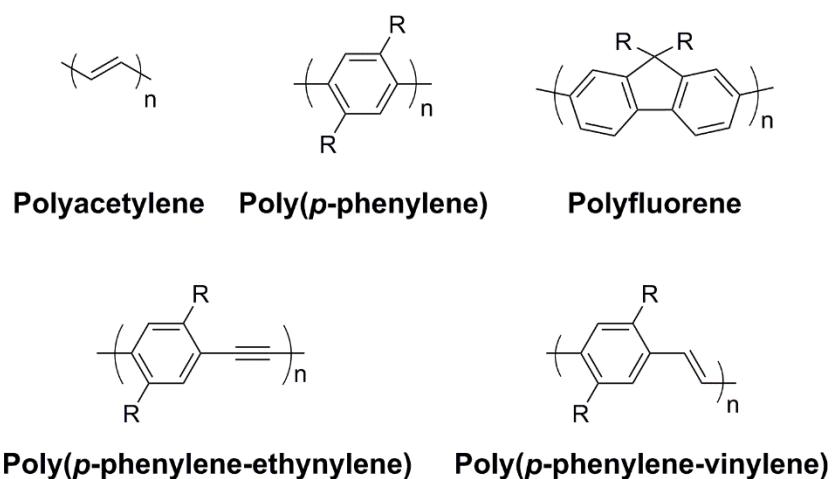


Figure 1. Structures of π -conjugated polymers.

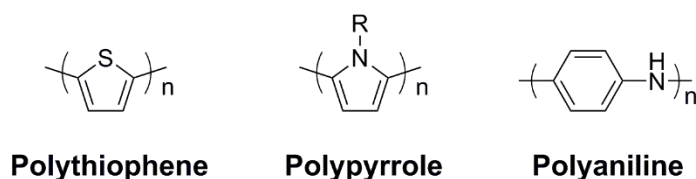
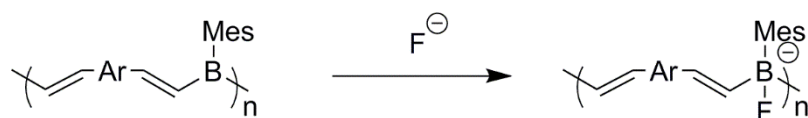


Figure 2. Hetero atom containing π -conjugated polymers.

General Introduction

Boron was also introduced into conjugated systems. The conjugated polymers including tricoordinate boron complexes are promising materials for fabrication of electronic devices as an n-type semiconductor. Tricoordinate boron complexes have vacant p-orbital, and the conjugation of polymer can expand through via this vacant orbital.³ Moreover, tricoordinate boron have Lewis acidity and sensitivity to Lewis base. In the previous work, the conjugated polymer having tricoordinate boron in the main-chain acted as optical sensors for fluoride anion (Scheme 1).^{3c} The coordination of fluoride anions to boron atoms interrupt the main-chain conjugation of the polymer, then the blue emission disappeared.

Scheme 1. Reaction of fluoride anion sensing with organoboron polymer



Boron can also form tetracoordinate structures such as boron quinolate, boron diketonete, boron ketoiminate, boron dipyrromethene (BODIPY) (Figure 3). They have higher stability than tricoordinate boron compounds because a vacant p-orbital of boron atom are filled by a lone pair. Therefore, it is easy to handle tetracoordinate boron compounds under ambient conditions, and it is expected to be useful for material applications. Especially, they are attractive for optoelectronic materials because they have good absorption and emission properties. Examples are shown below.

The conjugated polymer based on boron quinolate showed not only strong emission but also high electron mobility.⁴ This value was comparable to the value of Alq₃ which is the most well-

known electron-transport and luminescent material for OLEDs. Boron ketoiminates exhibits aggregation induced emission (AIE).⁵ The conjugated polymer including boron ketoiminates in main chain showed emission in films.⁶ These results indicate that the conjugated polymer including organoboron compounds have possibility to be used as optoelectronic materials in various fields.

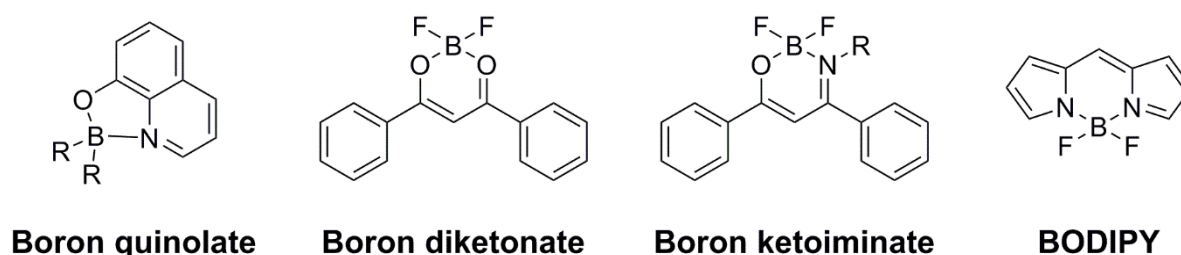


Figure 3. Examples of tetracoordinate organoboron compounds.

2. Boron Dipyrromethenes

Boron dipyrromethenes (BODIPYs) are one of the most famous luminescent dyes, and it is known that they have various advantages such as large absorption and luminescent abilities in the narrow wavelength regions, high photo-stability, and environment-resistant emissive properties.⁷ BODIPYs can be modified with their structures easily to modulate the character, especially optical properties. Therefore, various BODIPY derivatives have been developed by modification with substituents so far (Figure 4). Aza-BODIPYs have nitrogen atoms at the *meso*-position and lower LUMO energy levels than those of common BODIPYs because of the strong electronegativity of the nitrogen atom in the *meso*-position.⁸ Therefore, aza-BODIPYs showed absorption and

General Introduction

emission bands in the longer wavelength region than common BODIPYs. From these properties, the conjugated polymers based on aza-BODIPYs can work as a near-infrared (NIR) dyes⁹ or electron-transporting materials.¹⁰ BODIPYs usually have two fluorine atoms on their boron atoms. These fluorine atoms can be replaced by other substituents. For example, the aryl substituents can be introduced into the boron center of BODIPYs by organometallic reagents.¹¹ By selecting the organometallic reactions, the number of substituents in the boron center in BODIPY can be modulated. Ring-fused structures are also adopted for BODIPYs. The conjugation of BODIPY can be expanded by a fused ring. The ring-fused BODIPYs and their polymers were developed to show strong emission in the NIR region.¹² As stated above, BODIPYs have possibility to be applied in various applications via tuning properties with modification of their structures.

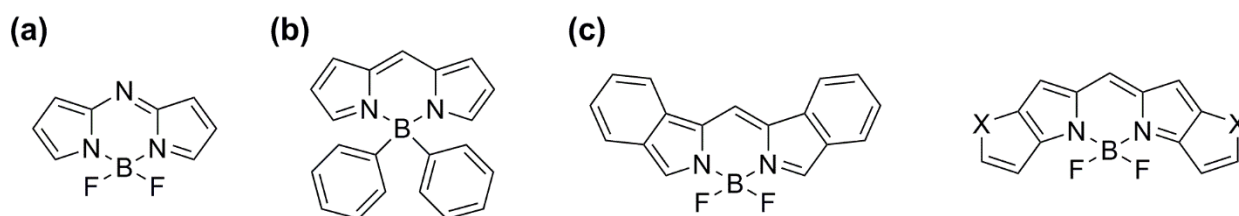
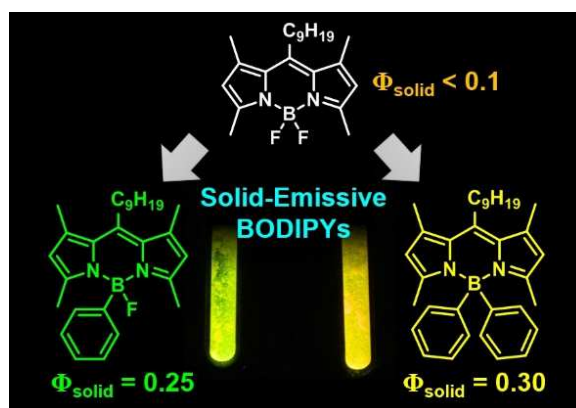


Figure 4. Examples of modified BODIPYs. (a) Aza-BODIPY, (b) BODIPY bearing aromatic groups on boron center, (c) ring-fused BODIPYs.

3. Survey of this Thesis

This thesis describes the synthesis and characterization of novel optically-functional materials by modified BODIPYs with unique structures. Details will be discussed in the following chapters.

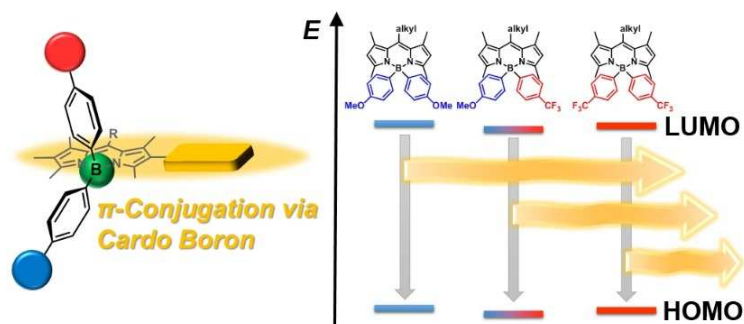
In Chapter 1, solid-emissive BODIPYs are presented. By the organometallic reactions, single- or dual-phenyl groups were introduced into the boron center in BODIPY. These substituents were valid for avoiding the concentration quenching in the solid state. In the solution state, the dual-phenyl substituted BODIPY provided broad and red-shifted photoluminescence spectrum, however the emission property was recovered not only in the solid state but also in the viscous solvent. It was revealed that the suppression of the molecular motion should play a crucial role in the enhancement of the emission properties of the dual-substituted BODIPY.



Chapter 1

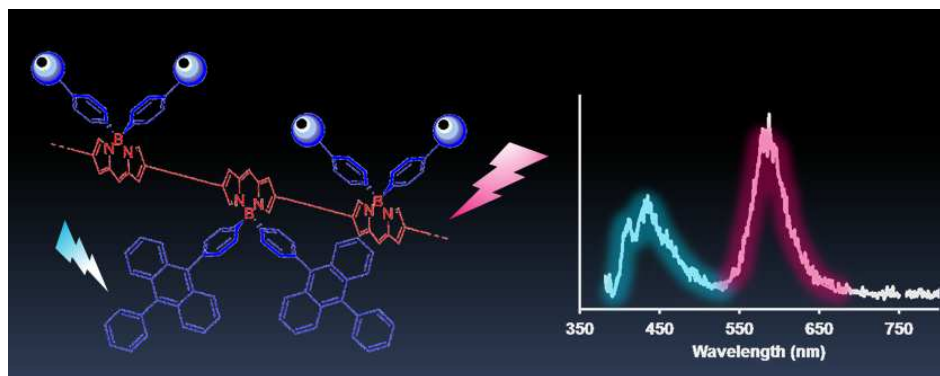
In Chapter 2, the synthesis and electronic structures of the modified BODIPY derivatives containing the cardo boron are shown. The aryl substituents with electron-donating groups and/or electron-withdrawing groups were introduced into boron atoms of BODIPYs. By the optical and electrochemical measurements, it was clarified that the cardo boron can efficiently isolate the main-chain conjugation from the electronic interaction with the side chains.

General Introduction



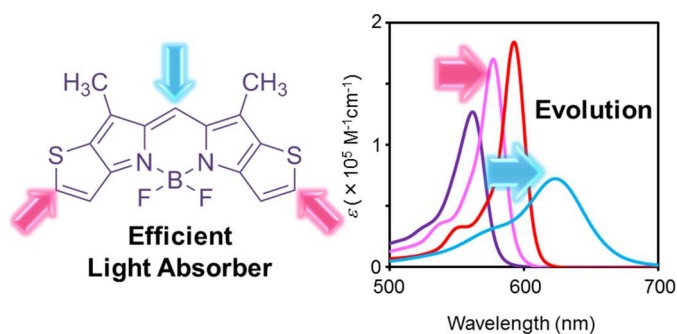
Chapter 2

In Chapter 3, the synthesis and optical properties of the dual-emissive polymer based on the cardo BODIPYs are presented. From the results of Chapter 2, the electronic structure of the main-chain conjugation in the polymer can be isolated from influence of the side-chains. Therefore, the conjugated polymer having anthracenes via the cardo substituents was designed to obtain dual emission. The synthetic polymer showed emission in red and blue regions derived from polymer main-chain and anthracene moieties, respectively.



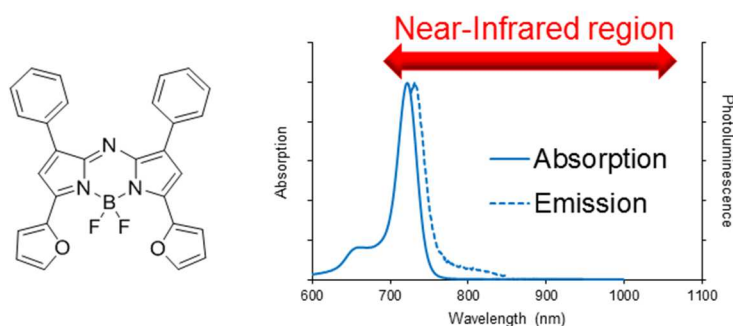
Chapter 3

In Chapter 4, the thiophene-fused BODIPY derivatives are presented. The absorption wavelength was tuned by substituents. By introducing iodine groups, the bathochromic shifts of the peak positions (+15 nm) and the enhancement of molar extinct coefficients. The trifluoromethyl group also contributed to the large bathochromic shift (+60 nm). They are useful for efficient light absorbers because of their absorption properties.



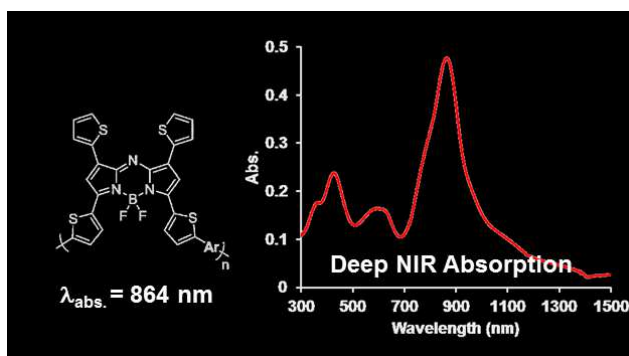
Chapter 4

In Chapter 5, furan-substituted aza-BODIPY with strong and sharp NIR emission was developed. Comparing with the well-known aza-BODIPY, the furan-substituted aza-BODIPY showed emission band in the longer wavelength with the peak at 735 nm, and the quantum yield was similar value. From these results, the introduction of furanyl groups into aza-BODIPY is an effective strategy to realize strong emission in the NIR region.



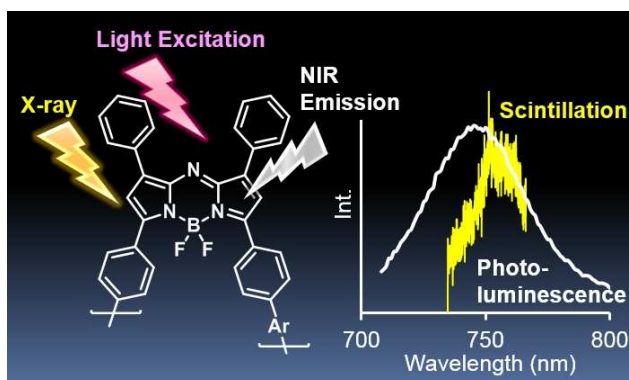
Chapter 5

In Chapter 6, the strong and deep NIR absorbing conjugated polymer was synthesized based on thiophene-substituted aza-BODIPY. From the optical measurement, it was revealed that the absorption band of the polymer reached to more than 800 nm. The cyclic voltammetry analyses revealed that the polymer had a low-lying LUMO energy level which was similar to the LUMO of monomer aza-BODIPYs.



Chapter 6

In Chapter 7, the organic liquid scintillators based on the emissive polymers are reported. BODIPY-based conjugated polymers showed emission in the NIR region by both photo- and X-ray excitations, and the emission bands were observed in similar regions regardless of excitation methods. These data propose that the organoboron conjugated polymers are attractive platforms to obtain an organic liquid scintillator with the emission in the NIR region.



Chapter 7

Refereneces

1. (a) Brabec, C. L.; Sariciftci, N. S.; Hummelen, J. C. *Adv. Funct. Mater.* **2001**, *11*, 15–26. (b) Cheng, Y.-J.; Yang, S.-H.; Hsu, C.-S. *Chem. Rev.* **2009**, *109*, 5868–5923. (c) Friend, R. H.; Gymer, R. W.; Holmes, A. B.; Burroughes, J. H.; Marks, R. N.; Taliani, C.; Bradley, D. D. C.; Dos Santos, D. A.; Brédas, J. L.; Lögdlund, M.; Salaneck, W. R. *Nature* **1999**, *397*, 121–128. (d) Mitschke, U.; Bäuerle, P. *J. Mater. Chem.* **2000**, *10*, 14715–1507. (e) Grimsdale, A. C.; Chan, K. L.; Martin, R. E.; Jokisz, P. G.; Holmes, A. B. *Chem. Rev.* **2009**, *109*, 897–1091. (f) Zhao, X.; Zhang, X. *Chem. Soc. Rev.* **2011**, *40*, 3728–3743.
2. (a) Roncali, J. *Chem. Rev.* **1992**, *92*, 711–738. (b) Wang, C.; Zheng, W.; Yue, Z.; Too, C. O.; Wallace, G. G. *Adv. Mater.* **2001**, *23*, 3580–3584. (c) Camurlu, P. *RSC Adv.* **2014**, *4*, 55832–55845. (d) Lee, S.-J.; Lee, D.-H.; Lee, K.; Lee, C.-W. *Adv. Funct. Mater.* **2005**, *15*, 1495–1500. (e) Bejbouji, H.; Vignau, L.; Miane, J. L.; Dang, M.-T.; Oualim, E. M.; Harmouchi, M.; Mouhsen, A. *Solar Energy Materials and Solar Cells*, **2010**, *94*, 176–181.
3. (a) Matsumi, N.; Naka, K.; Chujo, Y. *J. Am. Chem. Soc.* **1998**, *120*, 5112–5113. (b) Kobayashi, H.; Sato, N.; Ichikawa, I.; Miyata, M.; Chujo, Y.; Matsuyama, T. *Synthetic Metals* **2003**, 393–394. (c) Miyata, M.; Chujo, Y. *Polym. J.* **2002**, *34*, 967–969.
4. Nagai, A.; Kobayashi, S.; Nagata, Y.; Kokado, K.; Taka, H.; Kita, H.; Suzuri, Y.; Chujo, Y. *J. Mater. Chem.* **2010**, *20*, 5196–5201.
5. Yoshii, R.; Nagai, A.; Tanaka, K.; Chujo, Y. *Chem. Eur. J.* **2013**, *19*, 4506–4512.
6. (a) Yoshii, R.; Nagai, A.; Tanaka, K.; Chujo, Y. *Macromol. Rapid Commun.* **2014**, *35*, 1315–

General Introduction

1319. (b) Yoshii, R.; Tanaka, K.; Chujo, Y. *Macromolecules* **2014**, *47*, 2268–2278.
7. (a) Loudet, A.; Burgess, K. *Chem. Rev.* **2007**, *107*, 4891–4932. (b) Ulrich, G.; Ziesel, R.; Harriman, A. *Angew. Chem. Int. Ed.* **2008**, *47*, 1184–1201. (c) Ziesel, R.; Ulrich, G.; Harriman, A. *New J. Chem.* **2007**, *31*, 469–501. (d) Bones, N.; Leen, V.; Dehaen, W. *Chem. Soc. Rev.* **2012**, *41*, 1130–1172.
8. (a) Gorman, A.; Killoran, J.; O'Shea, C.; Kenna, T.; Gallagher, W. M.; O'Shea, D. F. *J. Am. Chem. Soc.* **2004**, *126*, 10619–10631. (b) Loudet, A.; Bandichhor, R.; Wu, L.; Burgess, K. *Tetrahedron* **2008**, *64*, 3642–3654. (c) Ge, Y.; O'Shea, D. F. *Chem. Soc. Rev.* **2016**, *45*, 3846–3864.
9. (a) Yoshii, R.; Nagai, A.; Chujo, Y. *J. Polym. Sci. A: Polym. Chem.* **2010**, *48*, 5348–5356. (b) Ma, X.; Mao, X.; Zhang, S.; Huang, X.; Cheng, Y.; Zhu, C. *Polym. Chem.* **2013**, *4*, 520–527.
10. Yoshii, R.; Yamane, H.; Nagai, A.; Tanaka, K.; Taka, H.; Kita, H.; Chujo, Y. *Macromolecules* **2014**, *47*, 2316–2323.
11. (a) Goze, C.; Ulrich, G.; Mallon, L. J.; Allen, B. P.; Harriman, A.; Ziesel, R. *J. Am. Chem. Soc.* **2006**, *128*, 10231–10239. (b) Kubota, Y.; Uehara, J.; Funabiki, K.; Ebihara, M.; Matsui, M. *Tetrahedron Lett.* **2010**, *51*, 6195–6198.
12. (a) Nagai, A.; Chujo, Y. *Macromolecules* **2010**, *43*, 193–200. (b) Yoshii, R.; Nagai, A.; Tanaka, K.; Chujo, Y. *J. Polym. Sci. Part A: Polym. Chem.* **2013**, *51*, 1726–1733. (c) Umezawa, K.; Nakamura, Y.; Makino, H.; Citterio, D.; Suzuki, J. *J. Am. Chem. Soc.* **2008**, *130*, 1550–1551. (d) Umezawa, K.; Matsui, A.; Nakamura, Y.; Citterio, D.; Suzuki, K. *Chem. Eur. J.* **2009**, *15*,

1096–1106. (e) Okujima, T.; Tomimori, Y.; Nakamura, J.; Yamada, H.; Uno, H.; Ono, N.

Tetrahedron **2010**, *66*, 6895–6900. (f) Wakamiya, A.; Murakami, T.; Yamaguchi, S. *Chem Sci.*

2013, *4*, 1002–1007.

General Introduction

Chapter 1

Simple and Valid Strategy for the Enhancement of the Solid-Emissive Property of Boron Dipyrromethenes

ABSTRACT: This manuscript presents the strategy for obtaining solid-emissive properties from the BODIPY dyes. It is demonstrated that the emission properties can be preserved from the aggregation-caused quenching (ACQ) by introducing the phenyl groups into their boron center. The author established the synthetic procedures for the introduction of single or dual phenyl groups into the boron center in BODIPYs. The synthesized BODIPYs having single and dual-phenyl groups showed unimodal photoluminescence spectra both in the solution and solid states with sufficient quantum yields. The pristine and the single-phenyl substituted BODIPYs showed similar optical properties in the solution state. In contrast, the dual-phenyl substituted BODIPY provided broad and red-shifted photoluminescence spectrum. Interestingly, the emission property of the dual-substituted BODIPY was recovered not only in the solid state but also in the viscous solvent. It was revealed that the suppression of the molecular motion should play a crucial role in the enhancement of the emission properties of the dual-substituted BODIPY. Furthermore, it is also presented that the steric hindrance by the phenyl groups can inhibit ACQ in the condensed state.

Chapter 1

Introduction

Boron dipyrromethenes (BODIPYs) are well known as a commodity luminescent dye because of their various advantages such as large absorption and luminescent abilities in the narrow wavelength regions, high photo-stability, and environment-resistant emissive properties.¹ Based on these useful characteristics, Chujo *et. al.* regarded BODIPY derivatives as an attractive element block which is defined as a functional building block including heteroatoms for constructing advanced materials.² Indeed, BODIPYs and their derivatives have been applied not only for emissive materials in an organic optical device³ but also for the molecular probes as a biotechnical tool.⁴ However, optical properties of BODIPYs would be drastically changed in the aggregation state^{5a,b} and sometimes spoiled in the condensed states via the aggregation-induced quenching (ACQ).^{5c,d} The planarity of the dipyrromethene ligand can be greatly enhanced by the complexation with boron. Subsequently, specific or non-specific intermolecular interactions via stacking and adhesion readily occur in the condensed states, resulting in the undesired changes or the loss of the bright green-light emission.^{5c,d} In particular, since materials are used as a thin film in the common organic devices, the crucial changes in the optical properties of BODIPYs in the solid materials should be still the emerging problem to be solved.

One of the most common strategies for avoiding ACQ is to introduce the bulky substituents into the molecules. There are the series of successful examples based on conjugated molecules for realizing solid emissions based on this strategy.⁶ By combining the bulky groups or other units which can hardly influence on the electronic state of the conjugation system, the emission

properties in the diluted solution were maintained in the condensed state. Chujo *et al.* recently reported the validity of the cardo structure in polyfluorene for improving the emissive properties in the film state.⁷ The introduction of the dual-phenyl groups into the fluorene moiety played a crucial role in the preservation of the emissions even in the film state. Furthermore, this strategy was also applied for obtaining the solid-emissive BODIPYs.⁸ The modified BODIPYs with the bulky substituents at the ligand moiety showed significant emissions even in the solid state in the previous reports.⁸ Although the emission quantum efficiencies were apparently maintained in the solid state in these researches, the shapes of the emission spectra were often divergent from that of the general BODIPY dyes. Therefore, the molecular design strategy to preserve the optical properties of BODIPYs is still required for realizing the highly-efficient emissive solid materials.

Most of BODIPYs have two fluorine atoms on their boron atoms. In particular, these fluorine atoms can be replaced by other substituents. Ziessel *et al.* reported the BODIPYs bearing aryl substituents at the boron center.⁹ Matsui *et al.* reported the solid-emissive BODIPY by introducing two phenyl groups at boron atom.¹⁰ However, to the best of the author's knowledge, the report on the solid emission of the modified BODIPY with heterogeneous types of the aryl substituents at the boron center was still very few although several synthetic routes for have been established.¹¹

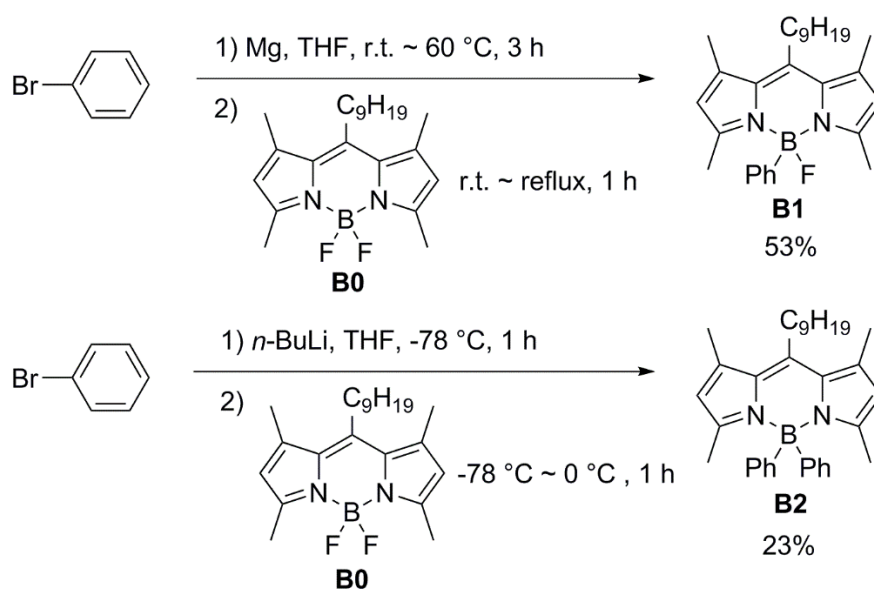
Herein, the author presents syntheses and optical properties of the phenyl-substituted BODIPYs. Initially, the synthetic procedures were established for preparing the BODIPY derivatives having single or dual phenyl groups at the boron center. Next, with the series of optical measurements, the emissive properties of the synthesized BODIPYs were examined. Especially, the influence of

Chapter 1

the phenyl groups on the emissive properties in the solid state was evaluated. The mechanisms on the solid emissive properties were also mentioned in this manuscript

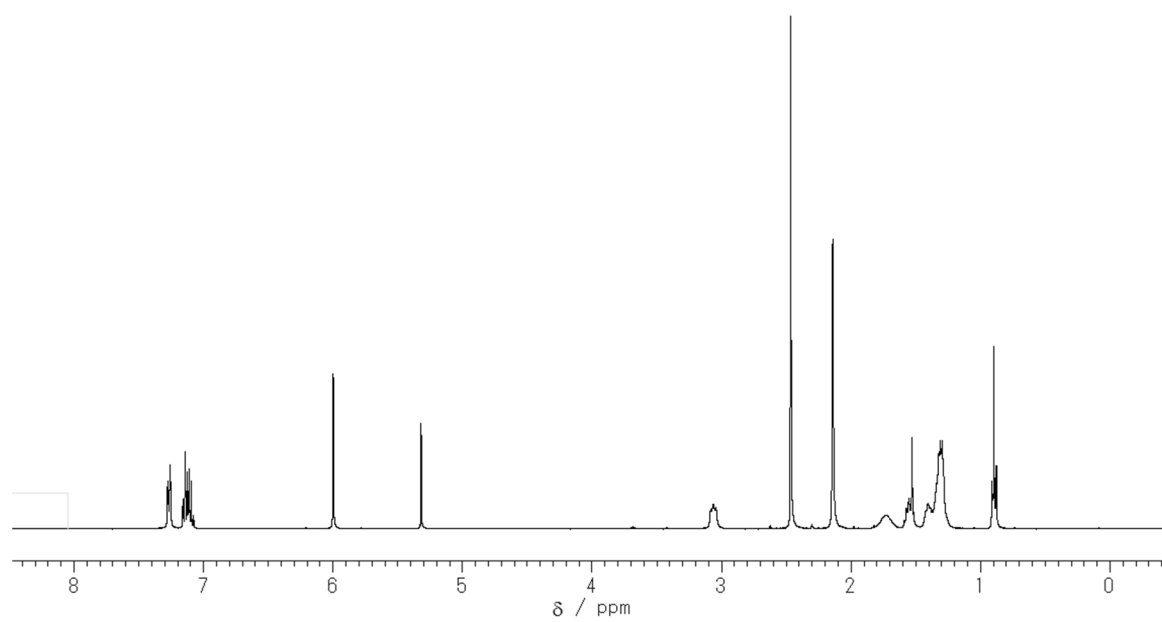
Results and Discussion

The modification of the boron in the BODIPYs is outlined in Scheme 1. The author used the difluorinated compound **B0** as a starting material.¹² The bright emission was obtained from the solid state in the Matsui's work.¹⁰ However, the multi-modal emission bands were observed. In this report, it was suggested that the local inhomogeneity such as crystal formation could provide the diverse emission bands. To achieve homogeneous amorphous state in the solid sample, the longer alkyl chains were introduced into the *meso* position. The introduction of the single phenyl group required the sensitive control of the reaction condition. In the reference 9, the substitution reaction proceeded at 0 °C in the presence of 2 eq. of a Grignard reagent. On the other hand, the reaction hardly occurred at 0 °C in this case. In addition, the dual substitution was observed by increasing reaction time. Thus, the author performed the reaction with reflux temperature for 1 h. Finally, the single-substituted BODIPY **B1** was obtained from **B0** with a good yield. To proceed the substitution reaction for obtaining the dual-substituted BODIPY **B2**, the lithiation with *n*-butyllithium was applied. The products showed good solubility in the common organic solvents such as chloroform, THF, and ethanol. The structures of all compounds were confirmed by ¹H, ¹¹B, ¹³C NMR spectroscopies and ionization mass measurements (Figures 1 and 2).

Scheme 1. Modifications of the boron atoms for preparing phenyl-substituted BODIPYs

Chapter 1

(a)



(b)

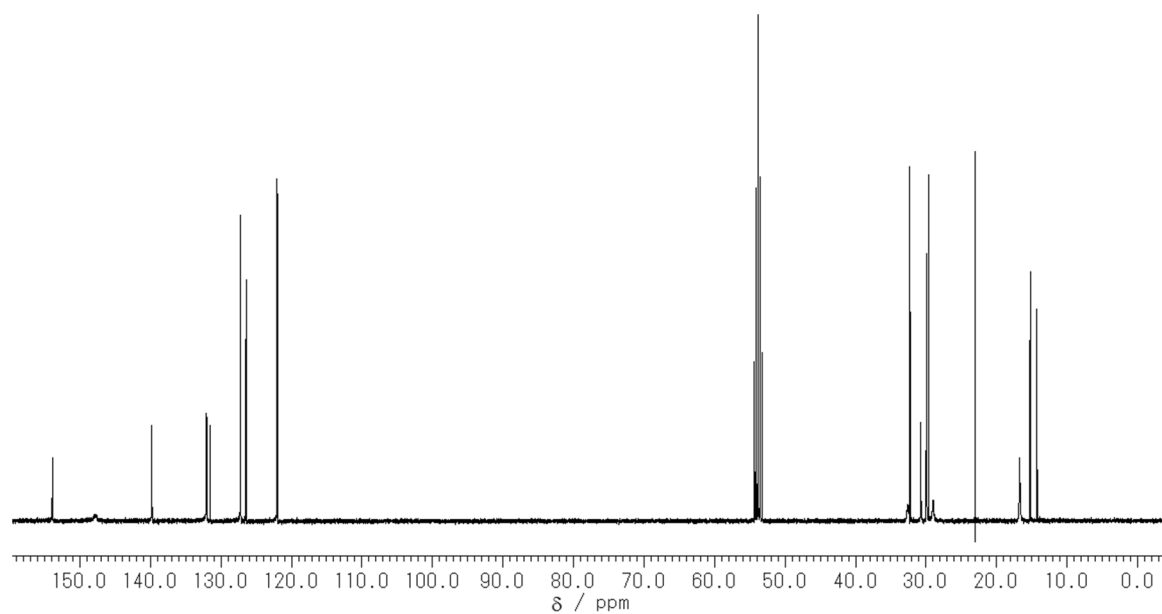
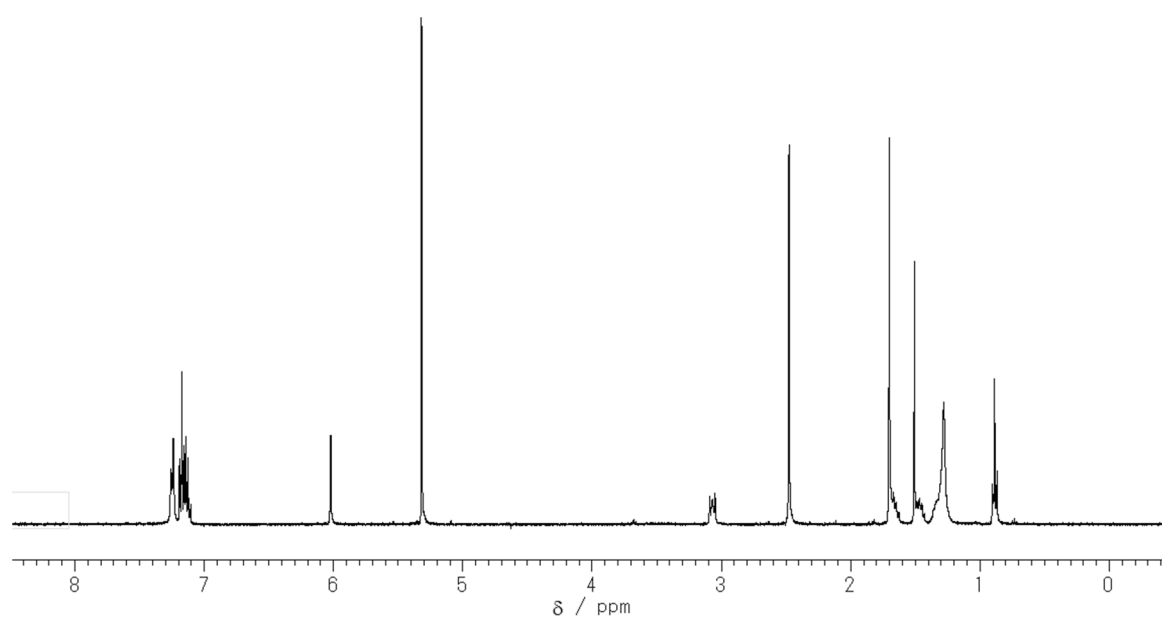


Figure 1. (a) ^1H and (b) ^{13}C NMR spectra of **B1** in dichloromethane.

(a)



(b)

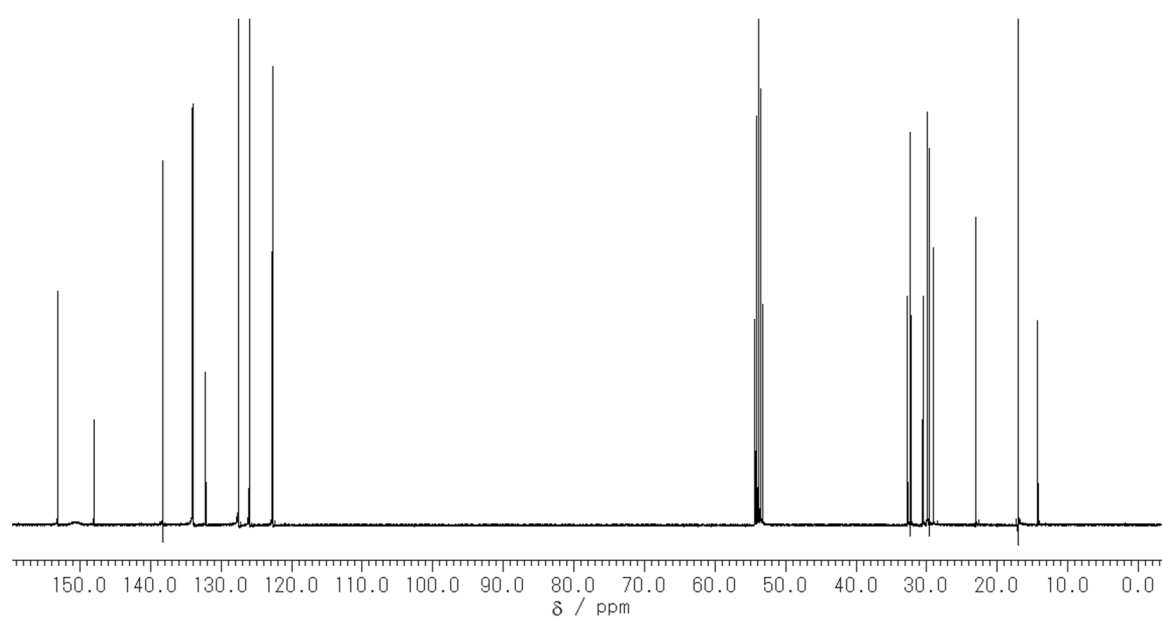


Figure 2. (a) ^1H and (b) ^{13}C NMR spectra of **B2** in dichloromethane.

Chapter 1

Initially, the UV–vis absorption spectra were compared to evaluate the influence of the modification at the boron center on the electronic states in the ground state (Figure 3a). The optical properties are listed in Table 1. From the solutions in chloroform (1.0×10^{-5} mol/L), similar absorption spectra were obtained from all three BODIPYs. Typical spectra to the common BODIPYs were observed; large molar extinction coefficients and sharp absorption bands with the peaks at 500 nm attributable to $S_0 \rightarrow S_1$ ($\pi \rightarrow \pi^*$) transition. These data indicate that the electronic structures in the ground state should be hardly influenced by the substituents.

Figure 3b shows the photoluminescence spectra of the modified BODIPYs in chloroform (1.0×10^{-5} mol/L). Interestingly, the emission spectrum of **B2** was different from those of **B0** and **B1**. **B0** and **B1** showed typical emission properties of BODIPYs. In contrast, **B2** showed a broad and red-shifted emission band. The emission color of **B2** was varied from those of **B0** and **B1**. The quantum yield of **B2** was crucially lower than those of **B0** and **B1**. From the lifetime measurements, it was confirmed that all BODIPYs showed fluorescence emission. Significantly, **B2** presented the shorter lifetime than those of **B0** and **B1** (Table 1). From these data, it can be summarized that the second phenyl substituent in **B2** should perturb the electronic structure of BODIPY only in the excited state.

Table 1. Optical properties of the modified BODIPYs in the solutions^a

	$\lambda_{\text{abs}}(\text{nm})$	$\varepsilon(\text{M}^{-1}\text{cm}^{-1})^b$	$\lambda_{\text{em}}(\text{nm})^c$	Φ_{PL}^d	$\tau(\text{ns})^e$
B0	500	92,000	511	0.81	6.35
B1	500	89,200	511	0.79	6.22
B2	497	88,000	539	0.34	3.36

^aIn chloroform (1.0×10^{-5} M). ^bDetermined at the peak in the longest wavelength band. ^cExcited at 473 nm (for **B0** and **B1**) and 469 nm (for **B2**). ^dDetermined as an absolute value. ^eExcited at 375 nm.

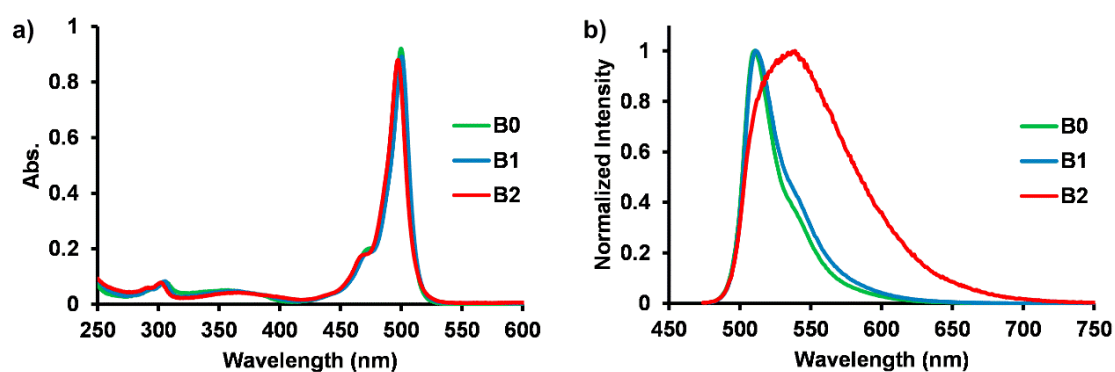


Figure 3. (a) UV-vis absorption and (b) photoluminescence spectra of the modified BODIPY in chloroform (1×10^{-5} M).

Chapter 1

To receive the information on the electronic states of the synthesized compounds, the computer calculations were performed. The author optimized the geometries of the modified BODIPYs by the density functional theory (DFT) and calculated their transitions from S_0 to S_1 by the time-dependent DFT (TD-DFT). The calculation results are shown in Figure 4. It was clearly shown that all highest occupied molecular orbitals (HOMOs) and lowest unoccupied molecular orbitals (LUMOs) delocalized through the whole dipyrromethene ligands in all three BODIPYs. Moreover, the energy level of HOMO or LUMO and energy band gap were very similar in all three compounds. These data corresponded to the experimental results obtained from the similar absorption spectra from all three BODIPYs.

Next, the author performed the theoretical calculation using TD-DFT to presume the most stable structure at the excited state (Figure 5). The phenyl ring at boron of **B1** hardly moves from the original position before and after the transition. In contrast, it is revealed that the one phenyl ring at boron center in **B2** should rotate at the excited state. This result suggests that the broadening of the emission band and the decrease of quantum yield of **B2** should be derived from molecular motion at the phenyl group induced by the excitation. The electron acceptability of the boron in **B1** could be still remained by the strong electron withdrawing from the single fluorine substitution. Therefore, the mobility of the phenyl group on the boron should be suppressed via the tight coordination with the dipyrromethene ligand. The boron atom in **B2** could have slight longer electron acceptability because of two phenyl substituents. Consequently, it is proposed that the flexibility around boron center could be enhanced. As a result, the perpendicular phenyl group to

the dipyrromethene ligand can obtain the mobility in the excited state. To confirm the structural alteration in the excited state, the author carried out further experiments.

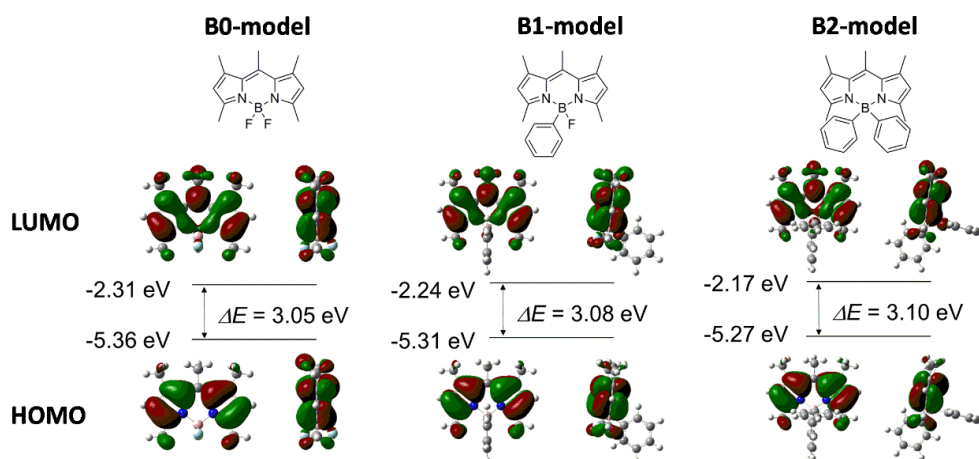


Figure 4. Structures and molecular orbital diagrams for LUMO and HOMO of **B0-model**, **B1-model** and **B2-model** calculated with DFT (B3LYP/6-31G(d)//B3LYP/6-31G(d)).

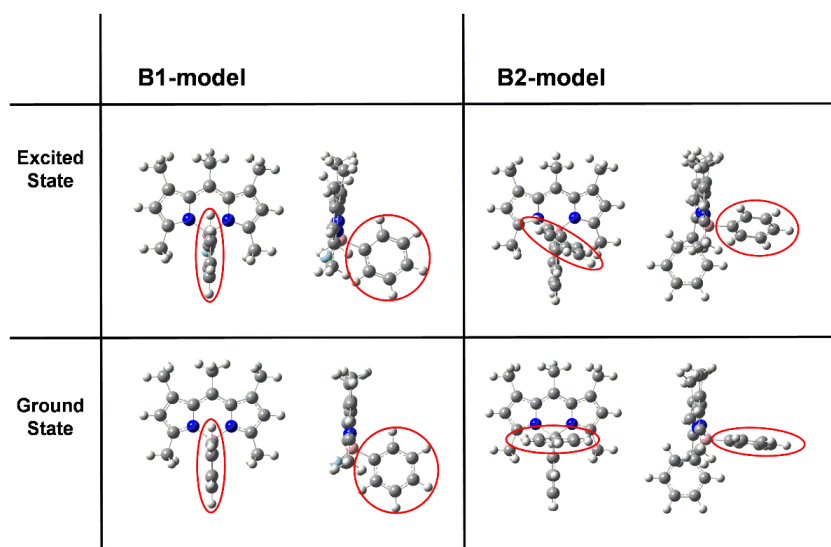


Figure 5. Structural changes of **B1** and **B2** during excitation. Optimized geometries in the excited states were estimated with TD-DFT (B3LYP/6-31+G(d)).

Chapter 1

To understand the mechanism of the differences in the emission properties according to the theoretical investigation, the effect of molecular motion was experimentally examined. Optical measurements by altering the solvent viscosity were performed. Glycerin-ethanol mixture system with various proportions of each component was used for modulating the solvent viscosity. Similarly in chloroform, the absorption spectra were almost same in all proportions (Figure 6). In addition, the photoluminescence spectra of **B0** and **B1** were also almost same in all proportions (Figures 7a and 7b). In contrast, it was observed that the emission intensity of **B2** increased when the viscosity of solvents increased (Figures 7c and 7d). Moreover, the spectrum was similar to those of **B0** and **B1** in relatively-higher viscosity solvent (80 vol% of glycerin content). From these results, it is strongly supported that the broad spectra of **B2** should be caused by the molecular motion of the one phenyl group induced only in the excited state.

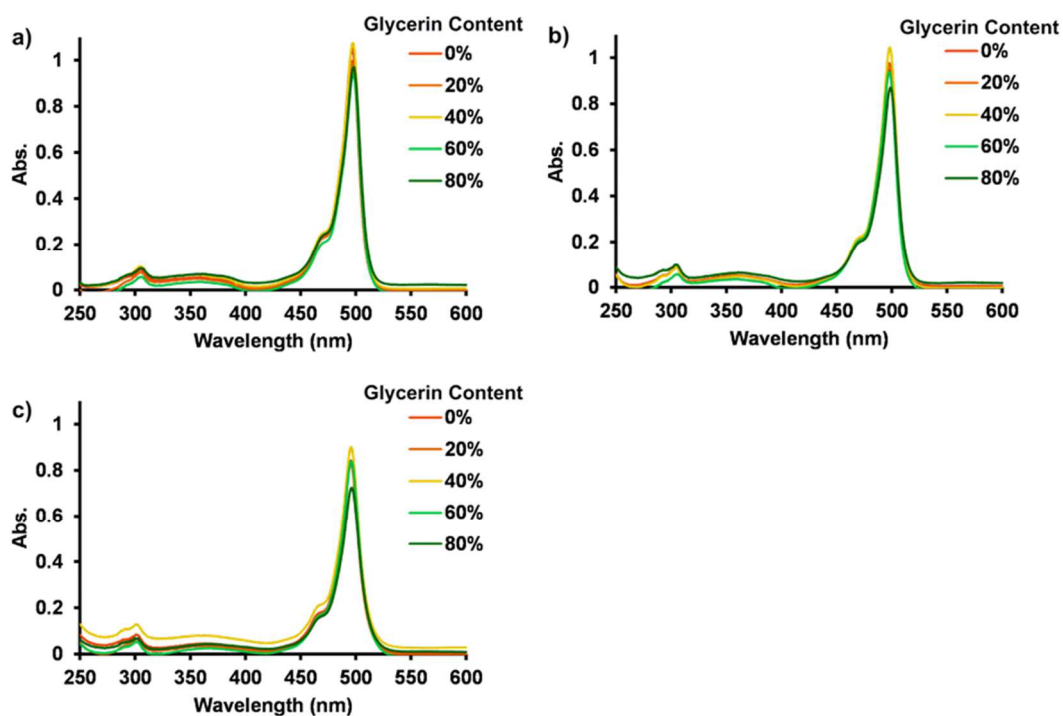


Figure 6. UV-vis absorption spectra of (a) **B0**, (b) **B1** and (c) **B2** in variable viscosity solutions.

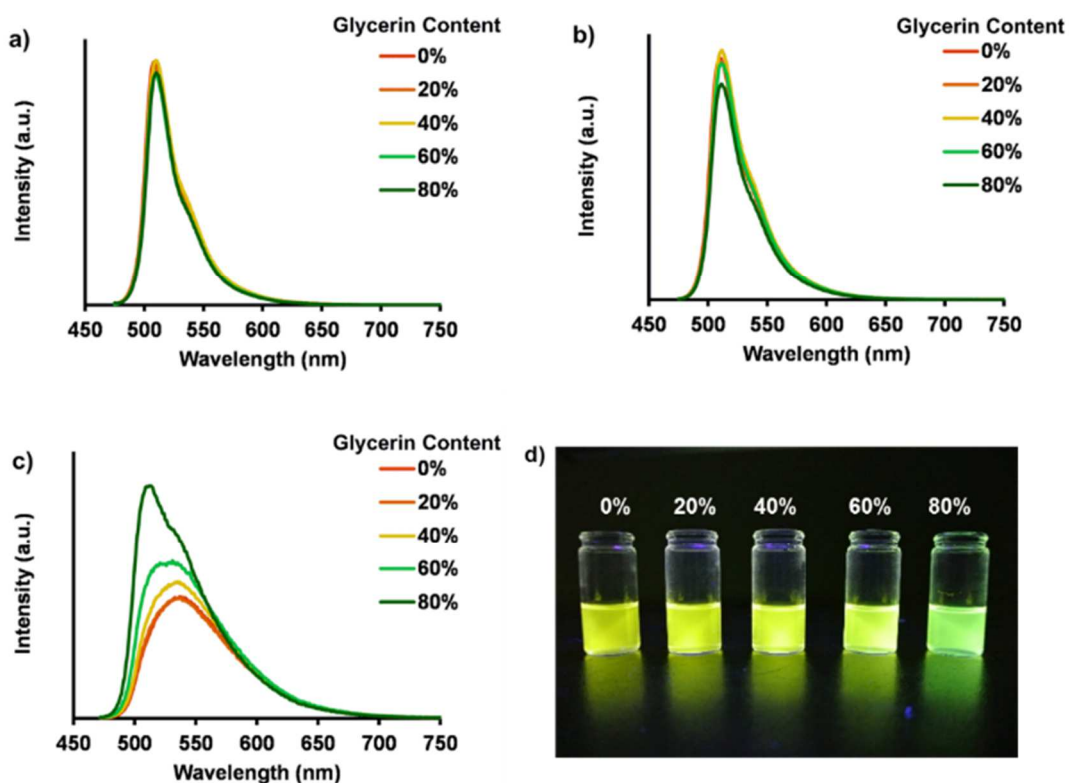


Figure 7. PL spectra of (a) **B0**, (b) **B1** and (c) **B2** in variable viscosity solutions. (d) Photographs of the solution samples of **B2** under UV irradiation (365 nm).

Chapter 1

Finally, the solid-emissive properties were examined with the powder samples of the modified BODIPYs. Figure 8 shows the photoluminescence spectra of **B0**, **B1** and **B2** in the solid state, and the optical properties are listed in Table 2. From **B0**, the typical behavior was observed: Very weak emission with quite low quantum yield ($\Phi = 0.09$) was detected. This value was almost 10% of that in solution. The spectrum of **B0** in the solid state shifted much longer wavelength than that in solution. The shape of spectrum of **B0** was broad and multimodal. Because of high planarity of **B0**, stacking and non-specific aggregation should readily occur in the amorphous state, resulting in the peak shifts and ACQ of the emission. On the other hand, **B1** and **B2** showed bright photoluminescence in the solid state. **B1** and **B2** presented narrow emission bands with good quantum yields ($\Phi = 0.25$ and 0.30 , respectively). It should be mentioned that the quantum yield of **B2** in the solid state was similar to that in the solution state ($\Phi = 0.34$). Furthermore, narrow and unimodal emission bands were observed. From these data, the introduction of phenyl groups into the boron center in BODIPY should be valid for enhancing the solid-emissive property. It is proposed that the steric hindrance of the phenyl group could play a significant role in the inhibition of ACQ of BODIPY.

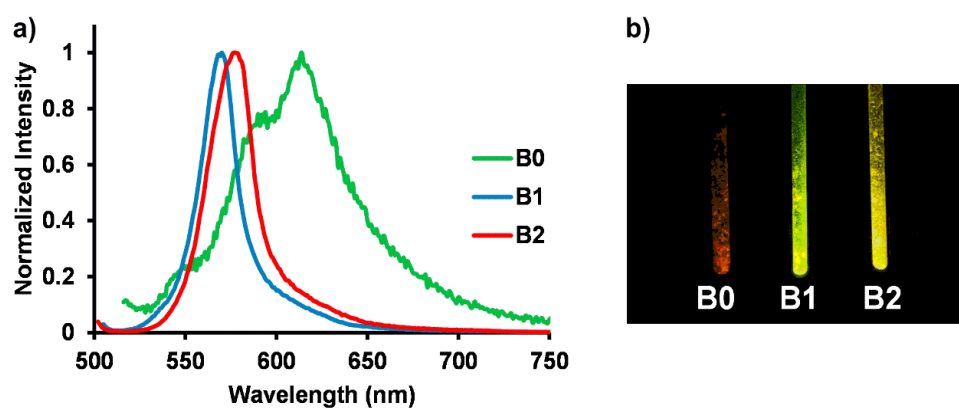


Figure 8. (a) PL spectra of **B0**, **B1** and **B2** in the solid state. (b) Photographs of the powder samples of **B0**, **B1** and **B2** under UV irradiation (365 nm).

Table 2. Emission properties of the modified BODIPYs in the solid state

	λ_{em} (nm) ^a	Φ_{PL} ^b		τ (ns) ^c
B0	614	0.09		4.46
B1	569	0.25	4.10 (52%)	7.37 (48%)
B2	577	0.30	3.50 (76%)	22.5 (24%)

^aExcited at the corresponding λ_{abs} in their solutions. ^bDetermined as an absolute value. ^cExcited at 375 nm. Parentheses represent the proportion of each element.

Chapter 1

Conclusion

This manuscript describes the valid strategy for obtaining the solid-emissive property from BODIPYs. By selecting the organometallic reactions, the number of substituents in the boron center in BODIPY can be modulated. By introducing phenyl groups into the boron atom in the BODIPY, the planarity of the six-membered ring including boron was lowered. In addition, because of the molecular motion at the phenyl group, the peak broadening and the decrease of emission quantum yields were induced in the solution state. However, interestingly, these substituents played a favorable role in improving the solid-emissive properties of BODIPY. It was clearly demonstrated that the introduction of the phenyl groups were valid for avoiding the concentration quenching by inhibiting the intermolecular interaction in the solid state. In addition, the molecular motion was suppressed in the solid state. As a result, the solid emission with the sharp and unimodal peak can be accomplished. From these data, it can be said that the minimum modification method was accomplished for solid emission based on BODIPY without modification at the ligand moiety. It is implied that the solid emission might be obtained with the strategy based on the conventional BODIPY derivatives such as deep red or NIR-emissive molecules which are useful for the direct application not only to organic opto-electronics devices but also to the bioimaging probes.

Experimental Section

General: ^1H (400 MHz), ^{13}C (100 MHz) and ^{11}B (128 MHz) NMR spectra were recorded on a JEOL JNM EX400 spectrometer. ^{11}B NMR spectra were referenced externally to $\text{BF}_3\cdot\text{OEt}_2$ (sealed capillary). Analytical thin-layer chromatography (TLC) was performed with silica gel 60 Merck F254 plates. Column chromatography was performed with Wakogel C-300 silica gel. UV-vis spectra were recorded on a Shimadzu UV-3600 spectrophotometer. Fluorescence emission spectra were recorded on a HORIBA JOBIN YVON Fluoromax-4 spectrofluorometer, and the absolute quantum yield was calculated by integrating sphere method on the HORIBA JOBIN YVON Fluoromax-4 spectrofluorometer in chloroform. Fluorescence lifetime analysis was carried out on a HORIBA FluoreCube spectrofluorometer system; excitation at 375 nm was carried out using a UV diode laser (NanoLED-375L).

Computational Details: The Gaussian 09 program package¹³ was used for computation. The author optimized the structures of BODIPYs in the ground S_0 and excited S_1 states with the density functional theory (DFT) at the B3LYP/6-31G(d)//B3LYP/6-31G(d) level and the time-dependent DFT (TD-DFT) at the B3LYP/6-31+G(d) level, respectively.

Synthesis of B0: The synthesis and identification of **B0** were performed according to the previous literature (Vincent *et al. Tetrahedron Lett.* **2013**, *54*, 2050). Decanoyl Chloride (5.0 g, 26 mmol) was added to the solution of 2,4-dimethylpyrrole (5.0 g, 53 mmol) in dichloromethane solution at r.t under argon atmosphere. After the reaction mixture was stirred at 50 °C for 2 h, the solvent was removed by a rotary evaporator. To the residue, dry toluene (150 mL) and dry dichloromethane

Chapter 1

(50 mL) were added under argon, and then triethylamine (17 mL, 0.12 mol) was added. After the mixture was stirred at r. t. for 30 min, boron trifluoride diethyl etherate (29 mL, 0.44 mmol) was added. After the mixture solution was stirred at 50 °C for 3 h, water (300 mL) was added to the reaction mixture to quench the reaction. After the mixture was stirred for overnight, the product was extracted with toluene and washed with water and brine. After the organic phase was dried over MgSO₄, the solvent was removed by a rotary evaporator. The product was purified by column chromatography with hexane/ethyl acetate (9:1). The eluent was recrystallized from methanol to give desired product as a metallic orange solid **B0** (4.0 g, 40%). ¹H NMR (CDCl₃): δ = 6.04 (2H, s), 2.95 (2H, t, *J* = 10.23 Hz), 2.51 (6H, s), 2.41 (6H, s), 1.67–1.58 (2H, m), 1.52–1.42 (2H, m), 1.35–1.28 (10H, m), 0.88 (3H, t, *J* = 6.94 Hz) ppm. Melting point: 84–85 °C.

Synthesis of B1: Bromobenzene (0.67 g, 4.3 mmol) in THF (40 mL) was added to magnesium (0.11 g, 4.7 mmol) at r.t. under argon atmosphere. The reaction solution was stirred at 60 °C for 2 h. The resulting solution was cooled to r.t. and transferred via cannula to a solution of **B0** (0.8 g, 2.1 mmol) in THF. After the mixture solution was stirred at reflux temperature for 1 h, water (100 mL) was added to the reaction mixture to quench the reaction. The solution was extracted with dichloromethane and washed with water and brine. After the organic phase was dried over MgSO₄, the solvent was removed by a rotary evaporator. The product was purified by column chromatography with hexane/dichloromethane (3:1). The isolated product was dissolved in a small amount of dichloromethane, and the product was precipitated from methanol to give pure **B1** as a metallic orange solid (0.67 g, 53%). ¹H NMR (CD₂Cl₂): δ = 7.27 (2H, dd, *J*₁ = 7.8 Hz, *J*₂ = 1.5

Hz), 7.16–7.07 (3H, m), 6.00 (2H, s), 3.06 (2H, t, $J = 8.3$ Hz), 2.47 (6H, s), 2.14 (6H, s), 1.73 (2H, s), 1.59–1.52 (2H, m), 1.41–1.30 (10H, m), 0.90 (3H, t, $J = 9.1$ Hz) ppm. ^{13}C NMR (CD_2Cl_2): $\delta = 153.9, 147.8, 139.8, 132.04, 132.02, 131.5, 127.2, 126.4, 122.0, 32.6, 32.3, 30.7, 30.0, 29.9, 29.7, 29.0, 23.1, 16.7, 15.3, 15.2, 14.3$ ppm. ^{11}B NMR (CDCl_3): $\delta = 2.54$ (br) ppm. HRMS (ESI): Calcd. for $[\text{M}+\text{H}]^+$, 433.3185; found, m/z 433.3179. Melting point: 79–82 °C.

Synthesis of B2: *n*-BuLi (5.5 mL, 1.60 mol/L in hexane) was added to the solution of bromobenzene (1.4 g, 8.8 mmol) in THF (18 mL) at -78 °C under argon atmosphere. The reaction mixture was stirred for 1 h. Then, the solution of **B0** (1.5 g, 4.0 mmol in 38 mL of THF) was added to the reaction mixture via cannula. After the reaction mixture was stirred for 1h at -78 °C and subsequently for 10 min at 0 °C, cooled saturated ammonium chloride aqueous solution was added. The solution was extracted with dichloromethane and washed with water and brine. After the organic phase was dried over MgSO_4 , the solvent was removed by a rotary evaporator. The product was purified by column chromatography with hexane/dichloromethane (4:1). The isolated product was dissolved in a small amount of CH_2Cl_2 , and the product was precipitated from methanol to give pure **B2** as a metallic orange solid (0.45 g, 23%). ^1H NMR (CD_2Cl_2): $\delta = 7.25$ (4H, d, $J = 6.3$ Hz), 7.20–7.10 (6H, m), 6.02 (2H, s), 3.07 (2H, t, $J = 8.4$ Hz), 2.48 (6H, s), 1.70 (6H, s), 1.67–1.60 (2H, m), 1.48–1.42 (2H, m), 1.28 (10H, br), 0.89 (3H, t, $J = 6.9$ Hz) ppm. ^{13}C NMR (CD_2Cl_2): $\delta = 153.2, 150.5, 148.0, 138.3, 134.0, 132.2, 127.8, 127.5, 126.0, 32.7, 32.3, 30.6, 30.0, 29.9, 29.7, 29.1, 23.1, 17.1, 17.0, 14.3$ ppm. ^{11}B NMR (CDCl_3): $\delta = -0.49$ (br) ppm. HRMS (ESI): Calcd. for $[\text{M}+\text{H}]^+$, 491.3592; found, m/z 491.3583. Melting point: 100–103 °C.

Chapter 1

References

1. (a) Ulrich, G.; Ziessel, R.; Harriman, A. *Angew. Chem. Int. Ed.* **2008**, *47*, 1184–1201. (b) Ziessel, R.; Ulrich, G.; Harriman, A. *New J. Chem.* **2007**, *31*, 496–501. (c) Bones, N.; Leen, V.; Dehaen, W. *Chem. Soc. Rev.* **2012**, *41*, 1130–1172.
2. Chujo, Y.; Tanaka, K. *Bull. Chem. Soc. Jpn* **2015**, *88*, 633–643.
3. (a) Yoshii, R.; Yamane, H.; Nagai, A.; Tanaka, K.; Taka, H.; Kita, H.; Chujo, Y. *Macromolecules* **2014**, *47*, 2316–2323. (b) Kajiwara, Y.; Nagai, A.; Tanaka, K.; Chujo, Y. *J. Mater. Chem. C* **2013**, *1*, 4437–4444. (c) Yoshii, R.; Nagai, A.; Tanaka, K.; Chujo, Y. *J. Polym. Sci. Part A: Polym. Chem.* **2013**, *51*, 1726–1733. (d) Yoshii, R.; Yamane, H.; Tanaka, K.; Chujo, Y. *Macromolecules* **2014**, *47*, 3755–3760. (e) Tanaka, K.; T. Yanagida, H. Yamane, A. Hirose, R. Yoshii, Chujo, Y. *Bioorg. Med. Chem. Lett.* DOI:10.1016/j.bmcl.2015.09.037. (f) Tanaka, K.; Yamane, H.; Yoshii, R.; Chujo, Y. *Bioorg. Med. Chem.* **2013**, *21*, 2715–2719.
4. (a) Kobayashi, T.; Komatsu, T.; Kamiya, M.; Campos, C.; González-Gaitán, M.; Terai, T.; Hanaoka, K.; Nagano, T.; Urano, Y. *J. Am. Chem. Soc.* **2012**, *134*, 11153–11160. (b) Komatsu, T.; Oshiki, D.; Takeda, A.; Miyamura, M.; Ueno, T.; Terai, T.; Hanaoka, K.; Urano, Y.; Mineno, T.; Nagano, T. *Chem. Commun.* **2011**, *47*, 10055–10057. (c) Komatsu, T.; Urano, Y.; Fujikawa, Y.; Kobayashi, T.; Kojima, H.; Terai, T.; Hanaoka, K.; Nagano, T. *Chem. Commun.* **2009**, 7015–7017.
5. (a) Spies, C.; Huynh, A.-M.; Huch, V.; Jung, G. *J. Phys. Chem. C* **2013**, *117*, 18163–18169. (b) Bergström, F.; Mikhalyov, I.; Hägglöf, P.; Wortmann, R.; Ny, T.; Johansson, L. B.-Å. *J.*

- Am. Chem. Soc.* **2002**, *124*, 196–204. (c) Kajiwara, Y.; Nagai, A.; Chujo, Y. *Bull. Chem. Soc. Jpn* **2011**, *84*, 471–481. (d) Kajiwara, Y.; Nagai, A.; Chujo, Y. *J. Mater. Chem.* **2010**, *20*, 2985–2992.
6. (a) Figueira, T. M.; Rosso, P. G. D.; Trattnig, R.; Sax, S.; List, E. J. W.; Müllen, K. *Adv. Mater.* **2010**, *22*, 990–993. (b) Shiraishi, K.; Kashiwabara, T.; Sanji, T.; Tanaka, M. *New J. Chem.* **2009**, *33*, 1680–1684. (c) Miyake, J.; Chujo, Y. *Macromol. Rapid Commun.* **2008**, *29*, 86–92. (d) Swager, T. M. *Acc. Chem. Res.* **2008**, *41*, 1181–1189. (e) Satrijo, A.; Kooi, S. E.; Swager, T. M. *Macromolecules* **2007**, *40*, 8833–8841. (f) Zhao, C. H.; Wakamiya, A.; Yamaguchi, S. *Macromolecules* **2007**, *40*, 3898–3900. (g) Amrutha, S. R.; Jayakannan, M. *Macromolecules* **2007**, *40*, 2380–2391. (h) Wang, J.; Zhao, Y.; Dou, Y. C.; Sun, H.; Xu, P.; Ye, K.; Zhang, J.; Jiang, S.; Li, F.; Wang, Y. *J. Phys. Chem. B* **2007**, *111*, 5082–5089. (i) Pu, K. Y.; Zhang, B.; Ma, Z.; Wang, P.; Qi, X. Y.; Chen, R. F.; Wang, L. H.; Fan, Q. L.; Huang, W. *Polymer* **2006**, *47*, 1970–1978. (j) Wu, C. W.; Tsai, C. M.; Lin, H. C. *Macromolecules* **2009**, *39*, 4298–4305. (k) Hecht, S.; Fréchet, J. M. J. *Angew. Chem. Int. Ed.* **2001**, *40*, 74–91. (l) Zhao, C. H.; Sakuda, E.; Wakamiya, A.; Yamaguchi, S. *Chem. Eur. J.* **2009**, *15*, 10603–10612.
7. (a) Yeo, H.; Tanaka, K.; Chujo, Y. *J. Polym. Sci. Part A: Polym. Chem.* **2012**, *50*, 4433–4442. (b) Yeo, H.; Tanaka, K.; Chujo, Y. *Macromolecules* **2013**, *46*, 2599–2605. (c) Yeo, H.; Tanaka, K.; Chujo, Y. *Polymer* **2015**, *60*, 228–233. (d) Yeo, H.; Tanaka, K.; Chujo, Y. *J. Polym. Sci. A: Polym. Chem.* **2015**, *53*, 2026–2035.

Chapter 1

8. (a) Zhang, D.; Wen, Y.; Xiao, Y.; Yu, G.; Liu, Y.; Qian, X. *Chem. Commun.* **2008**, *44*, 4777–4779. (b) Ozdemir, T.; Atilgan, S.; Kutuk, I.; Yildirim, L. T.; Tulek, A.; Bayindir, M.; Akkaya, E. U. *Org. Lett.* **2009**, *11*, 2105–2107. (c) Gai, L.; Lu, H.; Zou, B.; Lai, G.; Shen, Z.; Li, Z. *RSC Adv.* **2012**, *2*, 8840–8846. (d) Lu, H.; Wang, Q.; Gai, L.; Li, Z.; Deng, Y.; Xiao, X.; Lai, G.; Shen, Z. *Chem. Eur. J.* **2012**, *18*, 7852–7861. (e) Liu, C.-L.; Chen, Y.; Shelar, D. P.; Li, C.; Cheng, G.; Fu, W.-F. *J. Mater. Chem. C* **2014**, *2*, 5471–5478.
9. Goze, C.; Ulrich, G.; Mallon, L. J.; Allen, B. P.; Harriman, A.; Ziessele, R. *J. Am. Chem. Soc.* **2006**, *128*, 10231–10239.
10. Kubota, Y.; Uehara, J.; Funabiki, K.; Ebihara, M.; Matsui, M. *Tetrahedron Lett.* **2010**, *51*, 6195–6198.
11. (a) Hundnall, T. W.; Lin, T.-P.; Gabbai, F. P. *J. Fluor. Chem.* **2010**, *131*, 1182–1186. (b) Li, Z.; Lin, T.-P.; Liu, S.; Huang, C.-W.; Hundnall, T. W.; Gabbai, F. P.; Conti, P. S. *Chem. Commun.* **2011**, *47*, 9324–9326. (c) Haefele, A.; Zedde, C.; Retailleau, P.; Ulrich, G.; Ziessele, R. *Org. Lett.* **2010**, *12*, 1672–1675. (d) Bonnier, C.; Piers, W. E.; Ali, A. A.-S.; Thompson, A.; Parvez, M. *Organometallics* **2009**, *28*, 4845–4851. (e) Ulrich, G.; Goze, C.; Goeb, S.; Retailleau, P.; Ziessele, R. *New J. Chem.* **2006**, *30*, 982–986. (f) Landrum, M.; Smertenko, A.; Edwards, R.; Hussey, P. J.; Steel, P. G. *Plant J.* **2010**, *62*, 529–538.
12. Vincent, M.; Beabout, E.; Benett, R.; Hewavitharanage, P. *Tetrahedron Lett.* **2013**, *54*, 2050–2054.

13. Gaussian 09, Revision D.01, Frisch, M. J.; Trucks, G. W.; Schlegel, H. B.; Scuseria, G. E.; Robb, M. A.; Cheeseman, J. R.; Scalmani, G.; Barone, V.; Mennucci, B.; Petersson, G. A.; Nakatsuji, H.; Caricato, M.; Li, X.; Hratchian, H. P.; Izmaylov, A. F.; Bloino, J.; Zheng, G.; Sonnenberg, J. L.; Hada, M.; Ehara, M.; Toyota, K.; Fukuda, R.; Hasegawa, J.; Ishida, M.; Nakajima, T.; Honda, Y.; Kitao, O.; Nakai, H.; Vreven, T.; Montgomery, J. A., Jr.; Peralta, J. E.; Ogliaro, F.; Bearpark, M.; Heyd, J. J.; Brothers, E.; Kudin, K. N.; Staroverov, V. N.; Kobayashi, R.; Normand, J.; Raghavachari, K.; Rendell, A.; Burant, J. C.; Iyengar, S. S.; Tomasi, J.; Cossi, M.; Rega, N.; Millam, M. J.; Klene, M.; Knox, J. E.; Cross, J. B.; Bakken, V.; Adamo, C.; Jaramillo, J.; Gomperts, R.; Stratmann, R. E.; Yazyev, O.; Austin, A. J.; Cammi, R.; Pomelli, C.; Ochterski, J. W.; Martin, R. L.; Morokuma, K.; Zakrzewski, V. G.; Voth, G. A.; Salvador, P.; Dannenberg, J. J.; Dapprich, S.; Daniels, A. D.; Farkas, Ö.; Foresman, J. B.; Ortiz, J. V.; Cioslowski, J.; Fox, D. J. Gaussian, Inc., Wallingford CT, **2009**. (b) NBO Version 3.1, Glendening, E. D.; Reed, A. E.; Carpenter, J. E.; Weinhold, F.

Chapter 1

Chapter 2

Preservation of Main-Chain Conjugation through BODIPY-Containing Alternating Polymers from Electronic Interactions with Side-Chain Substituents by Cardo Boron Structures

ABSTRACT: This manuscript describes the synthesis and electronic structures of the modified boron dipyrromethene derivatives containing the cardo boron. By the organometallic reagents, the replacements of fluorine groups to the aryl substituents with electron-donating groups and/or electron-withdrawing groups were accomplished, resulting in the formation of the cardo boron. From the theoretical calculations and optical measurements, electronic structures in the main-chain conjugation were evaluated. In summary, it was clearly shown that the cardo boron can efficiently isolate the main-chain conjugation from the electronic interaction with the side chains since the optical properties were highly preserved from the introduction of the side-chain substituents. These findings should be fundamentally significant for the application of the cardo boron-containing conjugated polymers as a scaffold to construct the multi-functional unit by the assembly of functional units.

Chapter 2

Introduction

By using the cardo structure as a platform for assembling functional units in the conjugated polymers, multi-functionalities can be introduced based on the preprogrammed design.¹ For example, the series of the conjugated polymers composed of the modified cardo fluorenes have been synthesized, and their unique emissive behaviors were revealed.² It was shown that significant emission from the main-chain conjugation can be maintained even in the film state from the aggregation-caused quenching (ACQ) owing to the substituents connected via the cardo carbon. Especially, it was found that the main-chain conjugation can be efficiently preserved even in the presence of the electron-donating and/or -withdrawing units at the end of the side groups via the cardo carbons. In addition, by placing several dyes with orthogonal directions of each transition moment, the energy transfer between the fluorescent dyes at the side chains and the main-chain conjugation can be modulated.^{3,4} Finally, by selecting the type of the fluorescent dyes at the side chains and the copolymers in the main chain, not only the light-harvesting materials but also the multi-emissive polymer films were readily obtained.^{3,4} These results suggest that the construction of the cardo structure in the conjugated molecules including polymers should be feasible for realizing the multi-functional materials as the preprogrammed designs.

The nano-building blocks composed of heteroatoms are called as an “element-block”.⁵ The class of conjugated molecules and polymers containing functional “element-blocks” such as organoboron complexes and their unique optical properties have attracted much attention particularly to the applications for producing advanced opto-electric devices. For instance,

commodity emissive dyes readily show ACQ in the solid state. On the contrary, it was found that some kinds of organoboron emissive materials involving conjugated polymers presented the strong emission only in the aggregation state.⁶ Thus, versatility of the organoboron conjugation is vigorously increasing for the emissive materials. Boron dipyrromethene (BODIPY) is known to be one of stable and highly-emissive organoboron complexes.⁷ Since BODIPYs intrinsically have large light-absorption abilities and emissive properties, BODIPYs have been applied in wide variety fields including material chemistry⁸ and biomedical⁹. Although BODIPYs also showed critical ACQ, several valid strategies to maintain the optical properties have been developed by the chemical modifications.^{10,11} Moreover, by replacing from fluorine atoms to other functional units such as aryl groups,¹² various types of optical properties have been achieved such as energy-transfer donors or acceptors¹³ and solid emission^{14,15}. I focused on the boron atom in BODIPYs as a scaffold for constructing the cardo structure. In particular, we expected that the interesting optical and electronic characteristics could be obtained from the assembly of the emissive functional units on the cardo boron in the BODIPY-containing conjugated polymers to obtain useful functions for organic opto-electronic devices.¹⁶ However, to design the functional materials based on the cardo structure in BODIPYs, it is preliminary essential to examine the influence of the substituent effect on the electronic state of the main-chain conjugation. In particular, the degree of perturbation toward the main-chain conjugation should be evaluated by introducing the electron-donating (EDG) and/or -withdrawing (EWG) groups into the cardo boron.

Herein, the construction of the cardo boron in BODIPY and fundamental properties of the

Chapter 2

modified BODIPYs bearing the EDG and/or EWG to the boron center are reported to prove the isolation of the main-chain conjugation in the conjugated polymers from the electronic interaction with the side chains by the cardo boron. The series of modified BODIPYs with trifluoromethylphenyl groups as an EWG and/or methoxyphenyl groups as an EDG at the boron atom and the alternating polymers of these BODIPYs using fluorene and bithiophene as a comonomer unit were prepared. From the optical measurements, the electronic states of the BODIPY ligand and the main-chain conjugation through the polymers were evaluated by changing the substituents via the cardo boron. The energy diagrams and orbital shapes from the theoretical calculation support the discussions on the electronic substituent effect. This is the first example, to the best of the author's knowledge, to offer the systematic study from a new standpoint about the electronic states of BODIPY-containing conjugated materials.

Results and Discussion

To estimate the electronic correlation between the polymer main-chain and side-chains via the cardo structure, the quantum calculation was performed with the models of the polymers using density-functional theory (DFT). The optimized structures and the electronic transitions were calculated at the B3LYP/6-31G(d) level by DFT and time-dependent DFT (TD-DFT), respectively. The models of the polymers were composed of the single repeat unit linked to the BODIPY moiety at both sides. Figures 1-5 exhibit highest occupied molecular orbitals (HOMOs), lowest unoccupied molecular orbitals (LUMOs), the values of energy levels and optimized structures of

the models. It was shown that both of the HOMOs and LUMOs in the models were located on the ligand moiety. The HOMOs and LUMOs of models containing the cardo structures hardly localize on their phenyl groups. It should be mentioned that the electron orbitals and the energy levels were slightly influenced by the types of the substituents at the cardo boron. From this fact, it is assumed that the conjugation systems on the BODIPY ligand and the BODIPY-containing polymers could be independent from the side-chain substituents.

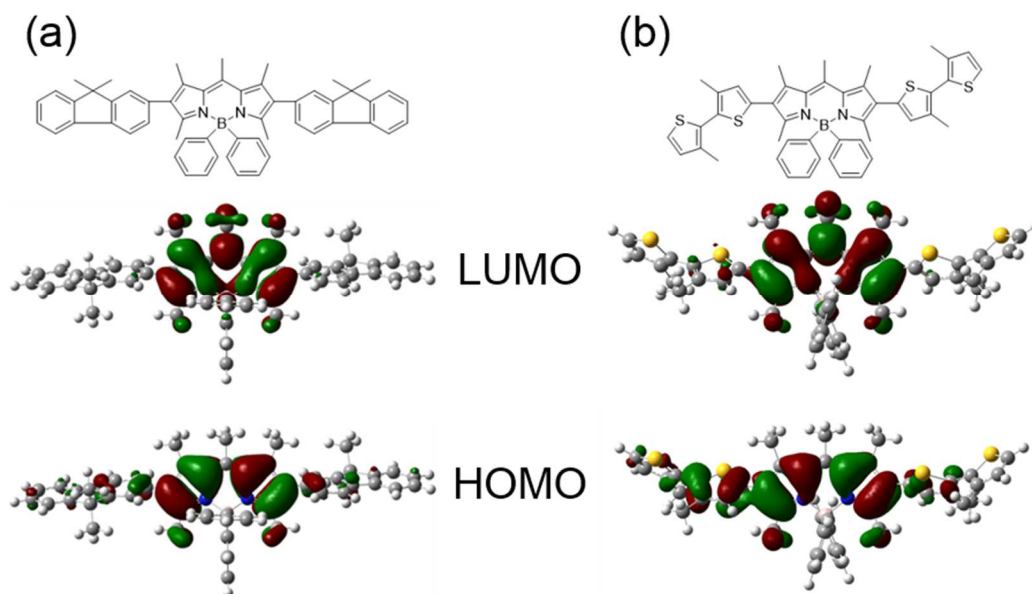


Figure 1. Structures and frontier orbitals of the model compounds of (a) **PFB2** and (b) **PTB2** (B3LYP/6-31G(d)// B3LYP/6-31G(d)).

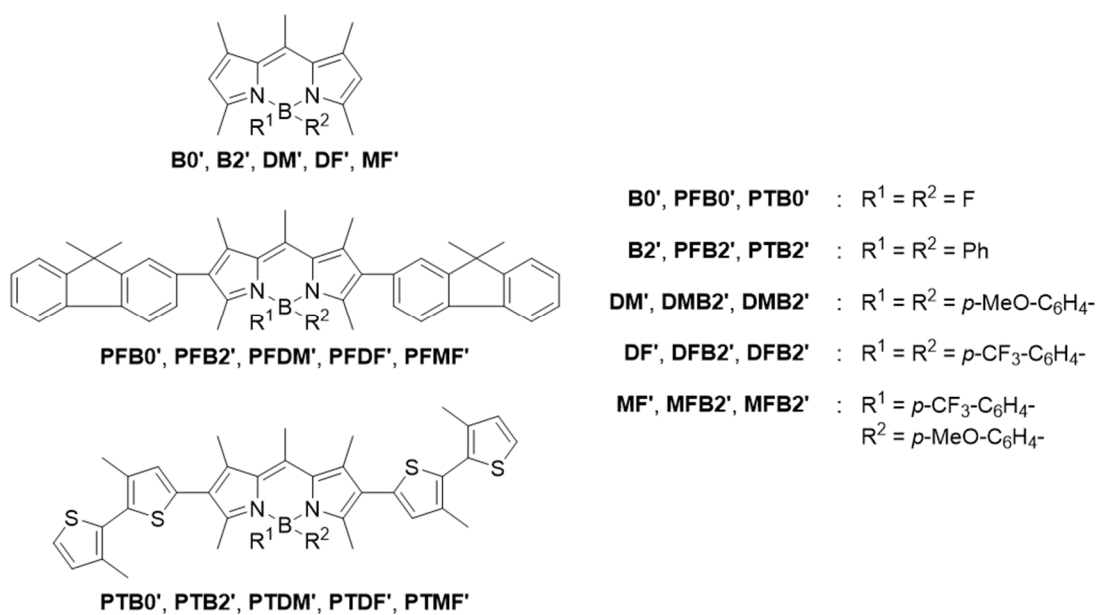


Figure 2. Structure of the model compounds for DFT calculation.

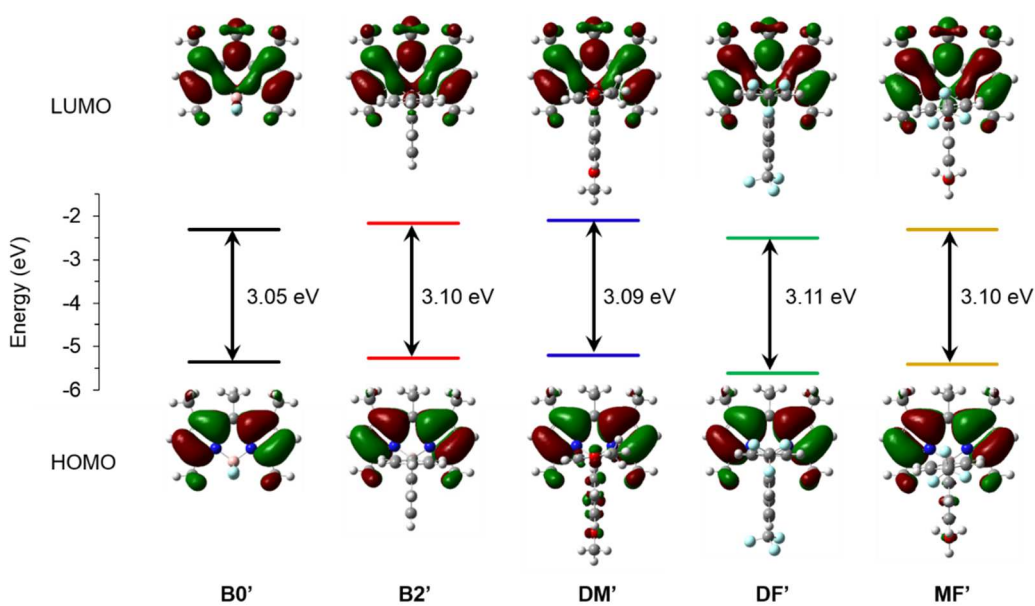


Figure 3. Frontier orbitals and energy diagrams of **B0'**, **B2'**, **DM'**, **DF'** and **MF'**.

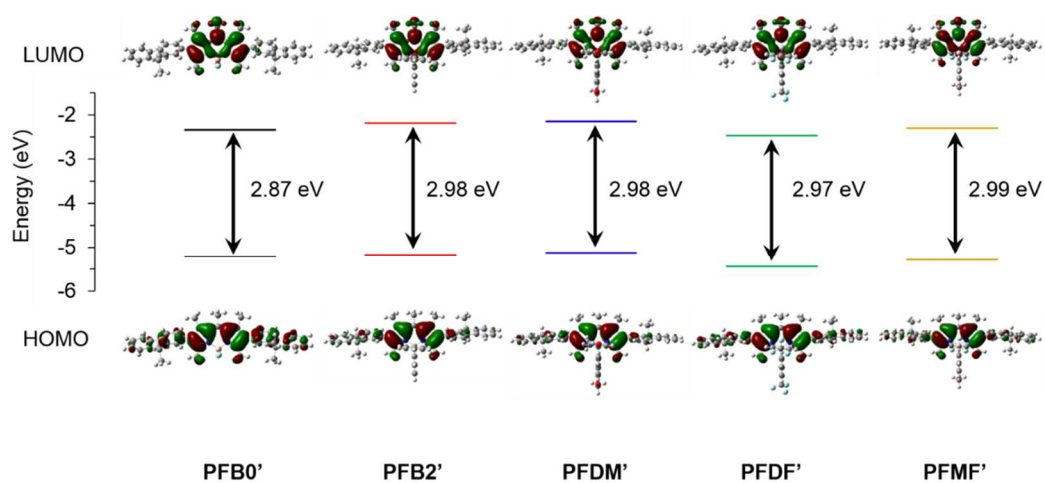


Figure 4. Frontier orbitals and energy diagrams of **PFBO'**, **PFB2'**, **PFDM'**, **PFDF'** and **PFMF'**.

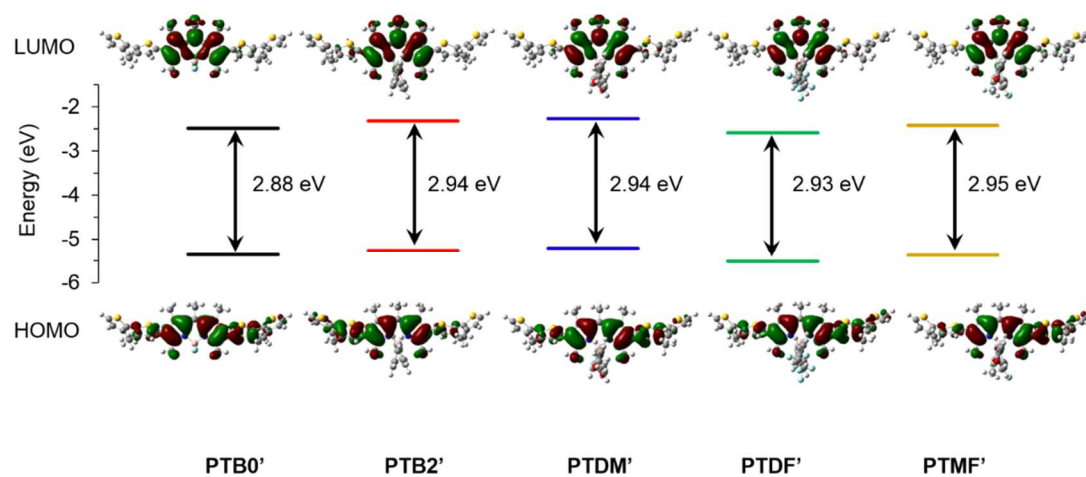
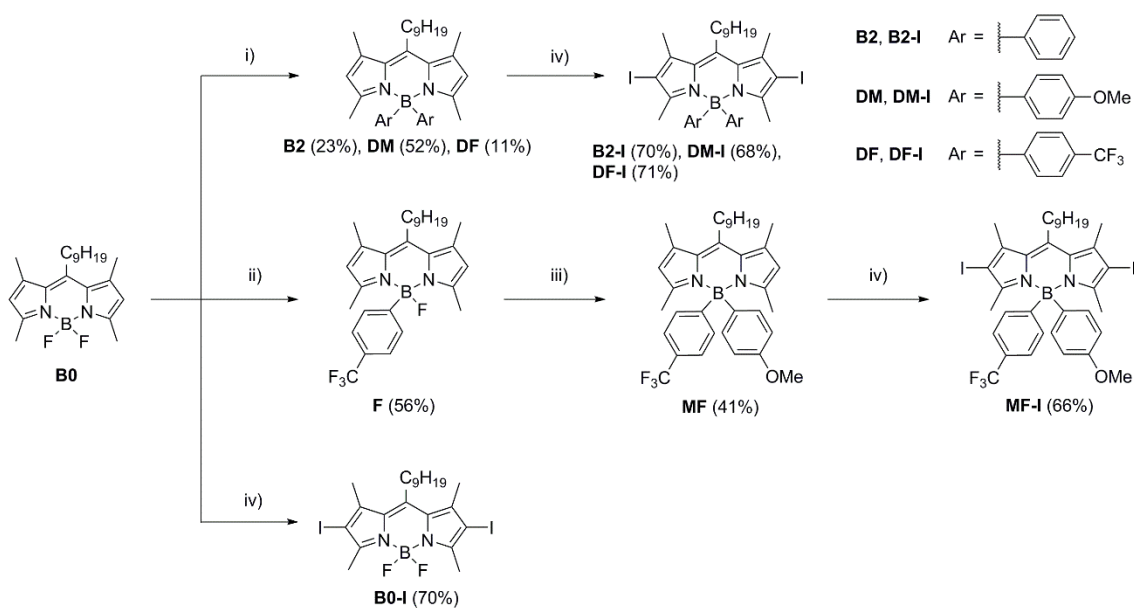


Figure 5. Frontier orbitals and energy diagrams of **PTB0'**, **PTB2'**, **PTDM'**, **PTDF'** and **PTMF'**.

Chapter 2

The modified BODIPYs containing the cardo structures with the dual EDGs, bis((4-methoxy)phenyl)-substituted BODIPY (**DM**), with the dual EWGs, bis((4-trifluoromethyl)phenyl)-substituted BODIPY (**DF**), and with the coexisting single EDG and EWG, (4-trifluoromethyl)phenyl-(4-methoxy)phenyl-substituted BODIPY (**MF**) were synthesized by employing the author's previous reports according to Scheme 1.^{15,17} By treating with the aryllithium reagents, the modification with EDGs and EWGs were achieved. The introduction of the heterogeneous types of the substituents for **MF** was accomplished by the tandem reactions with the Grignard reagents. Initially, by replacing from one of the fluorine groups to the EWG, the desired product was obtained. Then, the replacement of another fluorine group yielded to the desired molecule **MF**. The diiodo monomers **B0-I**, **B2-I**, **DM-I**, **DF-I** and **MF-I** were obtained from the corresponded compounds by treating with N-iodosuccinimide. All compounds were characterized by ¹H, ¹³C and ¹¹B NMR spectroscopies and mass measurements. Decomposition or photo-degradation was hardly observed under ambient conditions. Good solubilities were observed in common organic solvents owing to the alkyl chains.

Scheme 1. Synthetic routes for the monomers^a

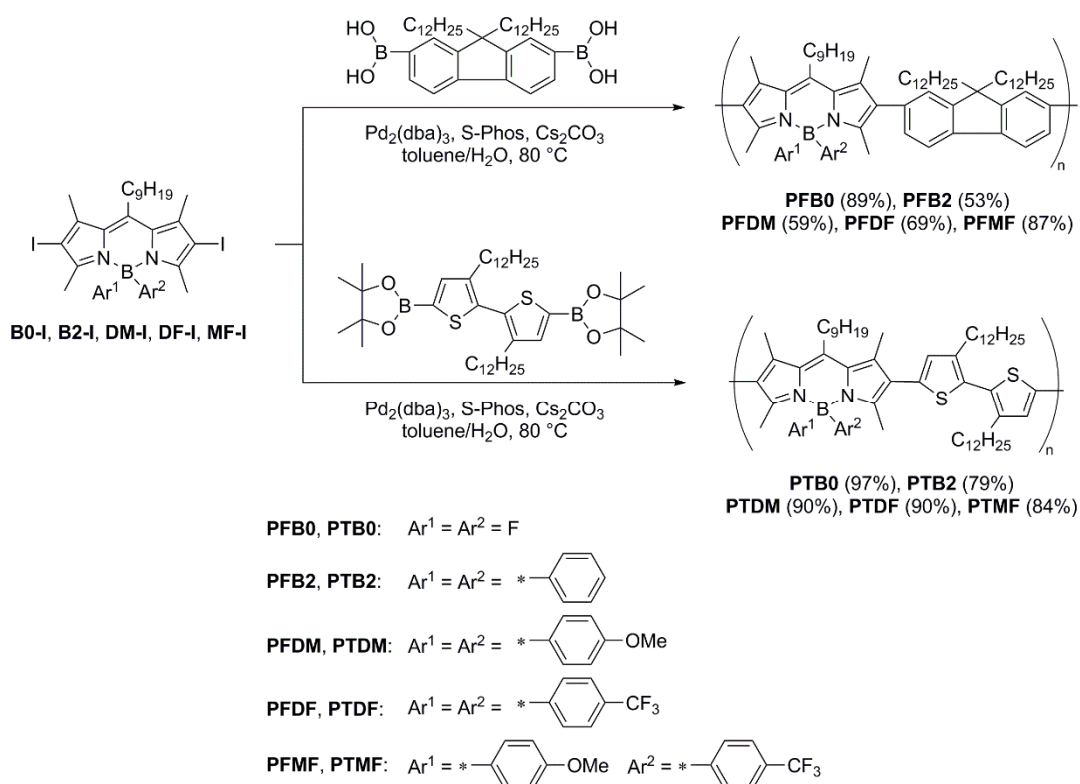
^aReagents and conditions: (i) Aryllithium (> 2 eq.), THF or diethyl ether, $-78\text{ }^{\circ}\text{C}$, 1 h; (ii) (4-(trifluoromethyl)phenyl)magnesium bromide (2.5 eq.), THF, reflux, 1 h; (iii) (4-methoxyphenyl)magnesium bromide (2.5 eq.), THF, $50\text{ }^{\circ}\text{C}$, 1 h; (iv) *N*-iodosuccinimide (2.5 eq.), dichloromethane, r.t., 30 min.

Chapter 2

Fluorene is one of typical comonomers for constructing main-chain conjugation through the alternating copolymer and can often present bright emission in the polymers. Bithiophene is known to work as a strong electron-donor. By the combination with electron-accepting units, strong electron coupling can be formed, leading to the bright emission in the red regions. By introducing EDGs and EWGs, the optical properties such as emission color can be modulated. To examine the roles of the cardo BODIPY-containing main-chain conjugation, the two series of copolymers were synthesized. The polymerizations with the diiodo monomers via the Suzuki–Miyaura coupling in the presence of Pd catalyst were executed as shown in Scheme 2. The polymers containing difluoroboron and diphenyl-substituted polymers were synthesized for comparing the electronic structures of the modified BODIPYs. The polymer properties determined from the GPC analysis are shown in Table 1. To remove the metal species originated from the catalyst thoroughly, the reprecipitation from methanol was repeated at least three times. The polymers were obtained as red or purple solids in good yields (59–97%). The number-average molecular weights (M_n) and the molecular weight distributions (M_w/M_n) of the polymers, measured by the size-exclusion chromatography (SEC) in chloroform toward polystyrene standards were from 6,200 to 11,500 with 1.7 to 2.5, respectively. Enough solubilities in common organic solvents such as chloroform, dichloromethane and tetrahydrofuran were observed for optical measurements by suppressing molecular weights of the polymers. The data for structural analysis by ^1H , ^{13}C and ^{11}B NMR measurements were corresponded to those of the single molecular units. Thus, the author concluded that the polymers possess the designed chemical structures. The synthesized polymers

hardly showed degradation by air, moisture and visible light exposure during the synthesis and optical measurements. Even after the UV (365 nm) irradiation for 30 min, significant changes were hardly observed in ^1H NMR spectra (Figure 6). These data represent high stabilities of the polymers.

Scheme 2. Synthetic routes for the polymers



Chapter 2

Table 1. Physical properties of the synthesized polymers^a

	M_n	M_w	M_w/M_n	n^b	Yield [%] ^c
PFB0	10,200	27,400	2.7	11.7	89
PFB2	6,600	14,300	2.2	6.7	53
PFDM	7,400	14,100	1.9	7.1	59
PFDF	6,000	10,200	1.7	5.3	69
PFMF	8,400	21,000	2.5	7.8	87
PTB0	9,500	16,500	1.7	10.9	97
PTB2	11,500	21,100	1.8	11.6	79
PTDM	7,800	13,300	1.7	7.4	90
PTDF	9,100	17,200	1.9	8.1	90
PTMF	11,400	20,400	1.8	10.4	84

^aEstimated from SEC with the polystyrene standards in chloroform. ^bAverage number of repeating units calculated from M_n and molecular weights of repeating units. ^cIsolated yields after reprecipitation.

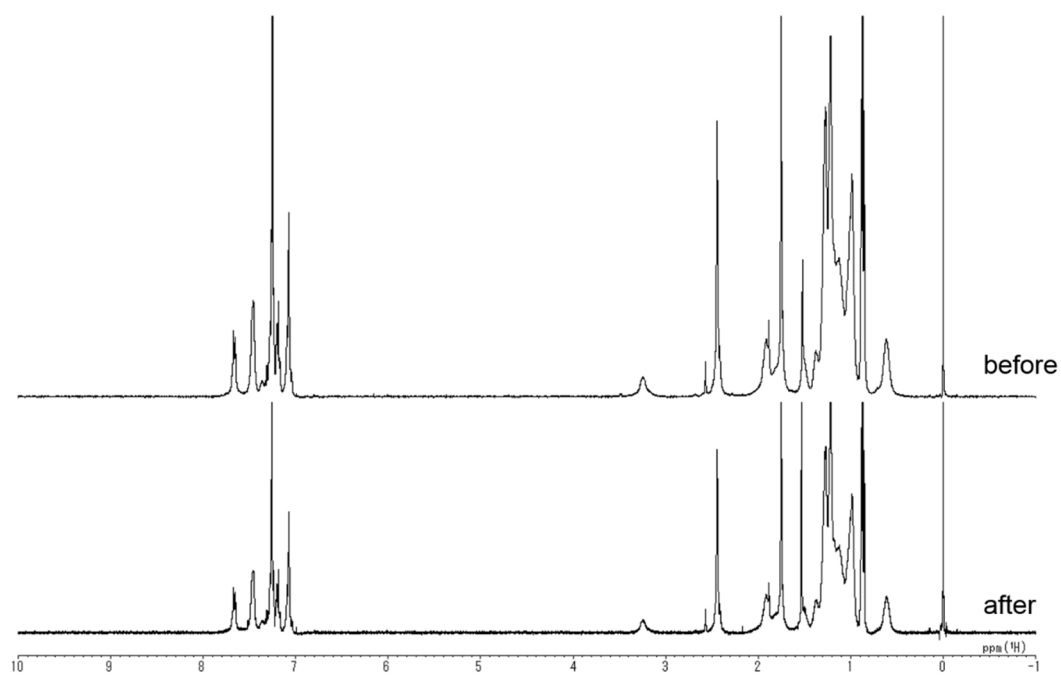


Figure 6. ^1H NMR spectra of **PFB2** in chloroform before and after UV (365 nm) irradiation for 30 min at ambient temperature.

Chapter 2

To survey the electronic structures of the polymers in the ground state, the UV–vis absorptions were measured with the chloroform solutions (Figure 7). The results from the absorption behaviors are summarized in Table 2. The characteristic absorption bands were observed from the modified BODIPYs with the peaks around 500 nm attributable to the π – π^* transition (Figure 7a).¹⁵ In addition, the magnitudes of the molar extinct coefficients were almost same. This result means that the electronic interaction should hardly influence on the conjugation in the ligand moiety. From the absorption spectra of the polymers composed of fluorene, the absorption bands were detected in the longer wavelength regions with the peaks around 540 nm than those of the corresponded BODIPYs (Figure 7b). These peak shifts represent the extension of the conjugation through the polymer main-chain. Interestingly, the degree of peak shift was independent from the side-chain substituents via the cardo boron. The peak positions of the modified polymers with EDGs and/or EWGs appeared at the same position to **PFB2** which has diphenyl substituents at the cardo boron. In addition, the absorption onsets of the polymers, which are often used to define the optical gap (E_g^{opt}), are in the range from 566 nm (2.18 eV) to 568 nm (2.18 eV) (Table 3). In particular, the differences in the HOMO–LUMO gaps of the polymers having EDGs, EWGs, or both groups were within 0.01 eV. Moreover, the HOMO and LUMO levels of the compounds were estimated from the cyclic voltammetry (CV) analyses as well as the band gaps (E_g^{CV}) (Figures 8 –11, Table 3). It was shown that all of the aryl substituted BODIPYs had similar HOMO and LUMO energy levels regardless of the substituents at the *para* position on their phenyl groups. The E_g^{CV} of the polymers bearing the cardo structures were comparable to their optical band gaps (E_g^{opt}). These data

significantly indicate that the electronic structures of the polymer main-chains should be isolated from the influences from the EDG and the EWG connected to the cardo boron, and the energy levels of the polymer main-chains were preserved in the ground states.

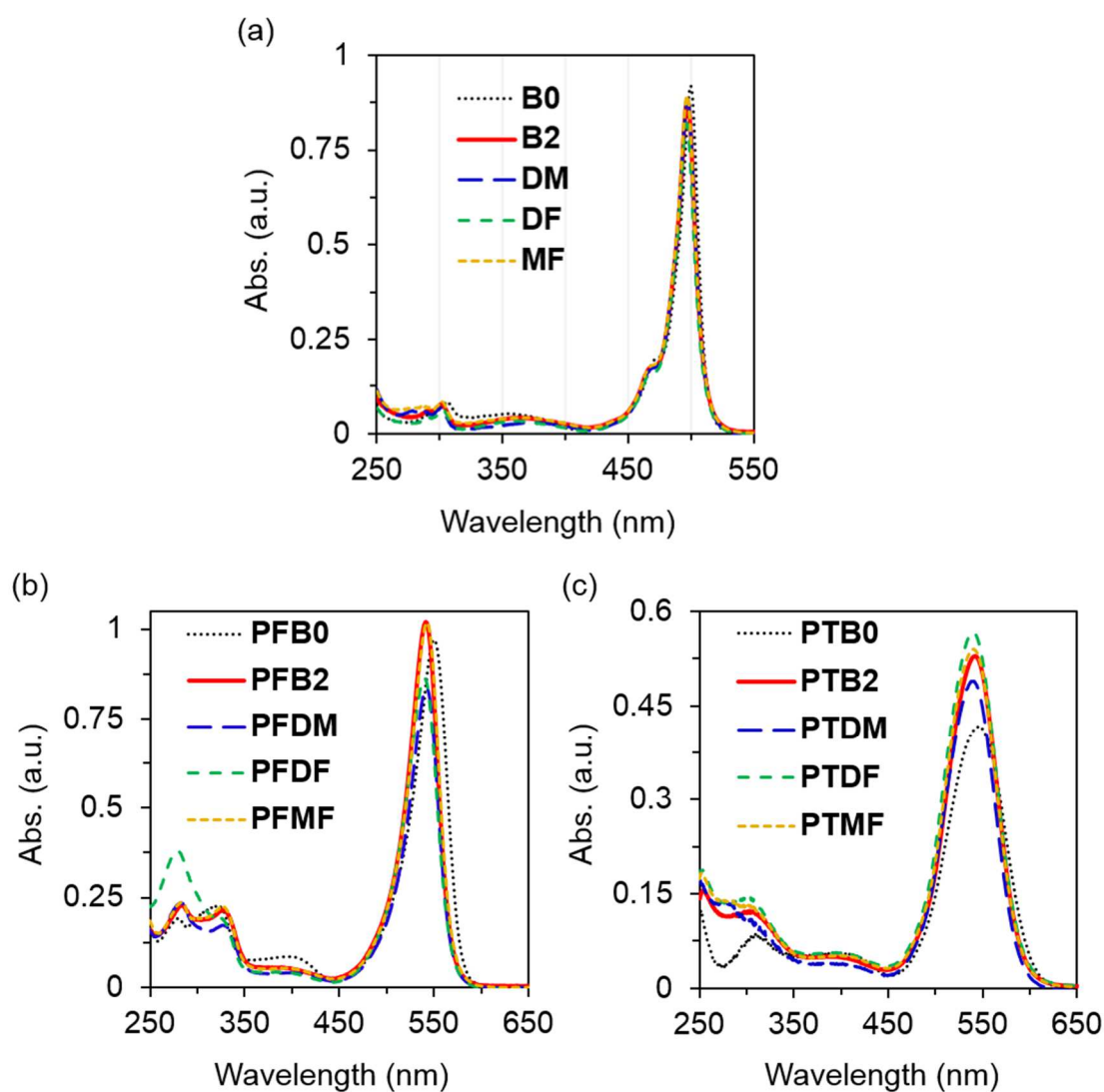


Figure 7. UV-vis absorption spectra of (a) **B0**, modified BODIPYs, (b) corresponding fluorene copolymers and (c) bithiophene copolymers in chloroform (1.0×10^{-5} M).

Chapter 2

Table 2. Optical properties of the compounds^a

	λ_{abs} [nm]	ε [$\text{M}^{-1} \text{cm}^{-1}$] ^b	λ_{PL} [nm]	Φ_{PL} ^c
B0	500	92,000	511 ^d	0.81 ^d
B2	497	88,000	539 ^d	0.34 ^d
DM	497	88,000	538 ^d	0.34 ^d
DF	496	82,000	537 ^d	0.32 ^d
MF	497	89,300	535 ^d	0.31 ^d
PFB0	550	96,900	579 ^e	0.75 ^e
PFB2	541	102,000	610 ^e	0.57 ^e
PFDM	542	83,800	597 ^e	0.49 ^e
PFDF	540	86,200	599 ^e	0.50 ^e
PFMF	542	102,000	599 ^e	0.51 ^e
PTB0	547	41,600	644 ^f	0.05 ^f
PTB2	541	52,900	649 ^f	0.07 ^f
PTDM	540	49,000	647 ^f	0.06 ^f
PTDF	540	56,700	648 ^f	0.05 ^f
PTMF	540	54,100	649 ^f	0.05 ^f

^aMeasured in chloroform (1.0×10^{-5} M). ^bMolar absorption coefficients of the absorption

maxima. ^cAbsolute fluorescence quantum yields determined using integrated sphere method.

^d**B0**, **B2**, **DM**, **DF** and **MF** were excited at 473, 469, 470, 469 and 469 nm, respectively. ^eExcited

at 500 nm. ^fExcited at 510 nm.

Table 3. Results of the electrochemical and optical measurement

	$E_{\text{onset, ox}}$	$E_{\text{onset, red}}$	E_{HOMO}	E_{LUMO}	E_{g}^{CV}	λ_{onset}	$E_{\text{g}}^{\text{opt}}$
	[V]	[V]	[eV]	[eV]	[eV]	[nm]	[eV]
B0	0.64	-1.71	-5.44	-3.09	2.35	512	2.42
B2	0.46	-1.98	-5.26	-2.82	2.44	510	2.43
DM	0.46	-1.91	-5.26	-2.89	2.37	510	2.43
DF	0.60	-1.83	-5.40	-2.97	2.43	510	2.43
MF	0.55	-1.88	-5.35	-2.92	2.43	510	2.43
PFB0	0.54	-1.67	-5.34	-3.13	2.21	576	2.15
PFB2	0.37	-1.92	-5.17	-2.88	2.29	566	2.19
PFDM	0.36	-1.86	-5.16	-2.94	2.23	567	2.19
PFDF	0.52	-1.76	-5.32	-3.04	2.28	566	2.19
PFMF	0.45	-1.81	-5.25	-2.99	2.26	568	2.18
PTB0	0.43	-1.49	-5.23	-3.31	1.92	600	2.07
PTB2	0.37	-1.78	-5.17	-3.02	2.14	587	2.11
PTDM	0.34	-1.80	-5.14	-3.00	2.14	586	2.12
PTDF	0.42	-1.68	-5.22	-3.12	2.10	589	2.11
PTMF	0.38	-1.71	-5.18	-3.08	2.10	588	2.11

^aThe onset wavelength of the UV-vis spectra in chloroform. ^bOptical band gaps were estimated from the corresponding λ_{onset} .

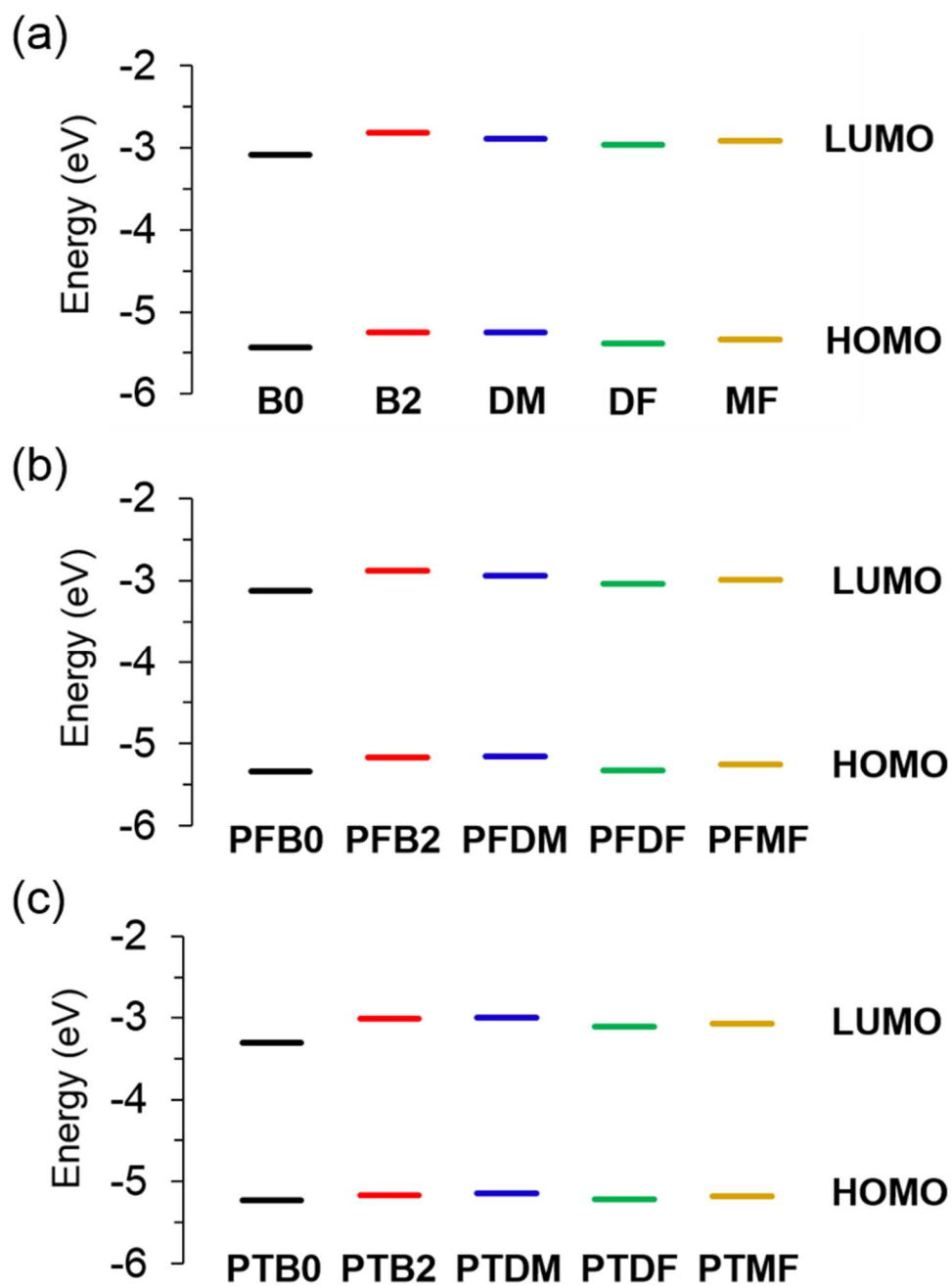


Figure 8. Energy diagrams of (a) **B0**, modified BODIPYs, (b) corresponding fluorene copolymers and (c) bithiophene copolymers calculated from the data of the cyclic voltammetry measurements.

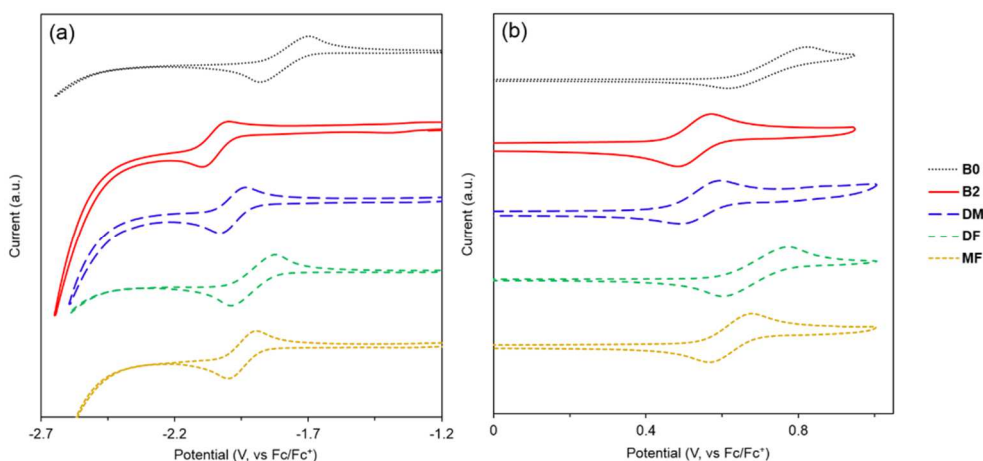


Figure 9. Cyclic voltammograms of the **B0**, **B2**, **DM**, **DF** and **MF** in (a) negative and (b) positive sweeps in dichloromethane (1.0×10^{-3} M) with 0.1 M tetrabutylammonium chloride as supporting electrolyte, Ag/AgCl as reference electrode, glassy carbon as working electrode, Pt as counter electrode, and scan rate at 0.05 V/s under argon.

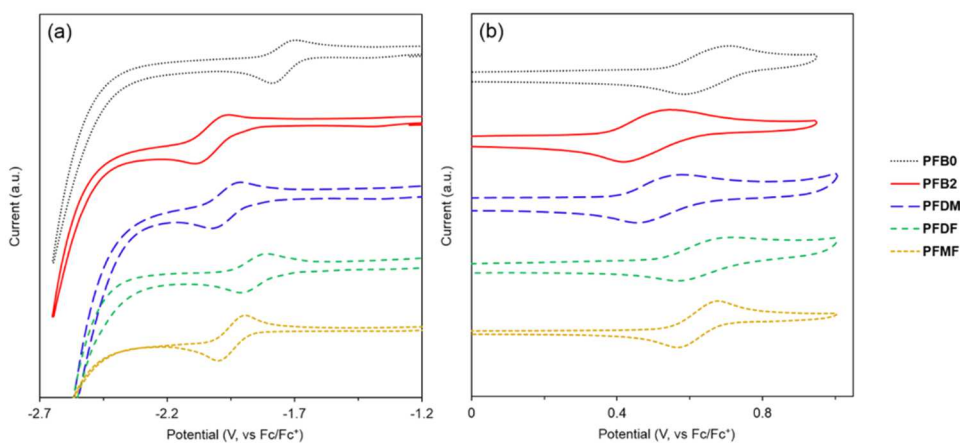


Figure 10. Cyclic voltammograms of the **PFB0**, **PFB2**, **PFDM**, **PFDF** and **PFMF** in (a) negative and (b) positive sweeps in dichloromethane (1.0×10^{-3} M) with 0.1 M tetrabutylammonium chloride as supporting electrolyte, Ag/AgCl as reference electrode, glassy carbon as working electrode, Pt as counter electrode, and scan rate at 0.05 V/s under argon.

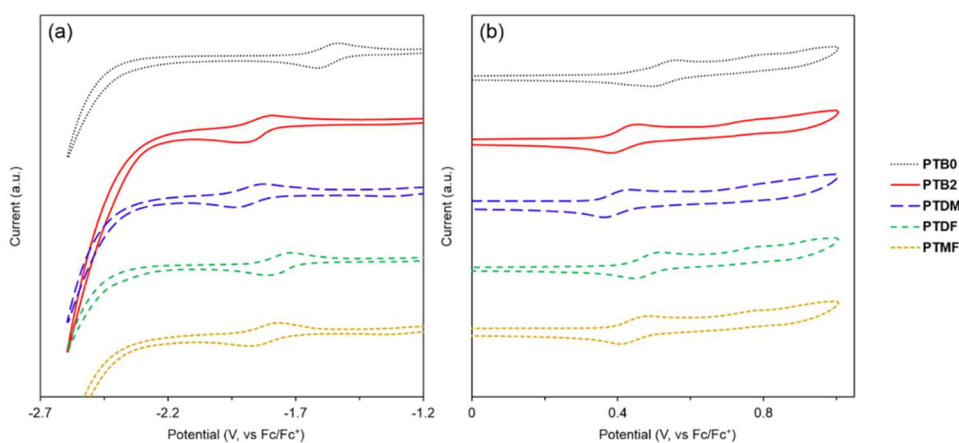


Figure 11. Cyclic voltammograms of the **PTB0**, **PTB2**, **PTDM**, **PTDF** and **PTMF** in (a) negative and (b) positive sweeps in dichloromethane (1.0×10^{-3} M) with 0.1 M tetrabutylammonium chloride as supporting electrolyte, Ag/AgCl as reference electrode, glassy carbon as working electrode, Pt as counter electrode, and scan rate at 0.05 V/s under argon.

To evaluate the electronic structures of the main-chain conjugation in the excited states, the emission properties were investigated in the solution state (Figure 12, Table 2). The polymers were dissolved in chloroform, and the photoluminescence spectra were obtained with the excitation light at 500 nm. All polymers composed of fluorene involving **PFB0** and **PFB2** showed the emission bands with the peaks around 570 nm attributable to the S_0 - S_1 transitions in BODIPYs. Comparing to the peak positions of the modified BODIPYs, the red-shifted emission bands were obtained. Similarly to the absorption data, the extension of the conjugation in the excited state should be indicated. **PFB2** showed the broader emission band than **PFB0**. It is known that the molecular motions at the substituents often induced the critical changes in the optical properties of BODIPYs.^{15a,18} From the X-ray structural analysis with the aryl-substituted BODIPY, it was found

that the position of the boron was out of the plane involving the dipyrromethene ligand.^{13a} In other words, the planarity of the complex was lowered by introducing the aryl group. In addition, it was demonstrated that the phenyl rings can rotate in the excited state from the TD-DFT calculation.¹⁵ From these results, it is suggested that the molecular motions at the phenyl groups should vigorously occur, leading to the peak broadening in the emission spectra. Significantly, **PFDM**, **PFDF** and **PFMF** presented almost same shapes of spectra and same absolute emission efficiencies (Table 2). This result means that the electronic states of the main-chain conjugation can be preserved from the introduction of the substituents at the cardo boron. The electronic interaction should hardly exist via the cardo boron. The emissions should be attributable to fluorescence of BODIPY. Moreover, as suggested above, the electronic environments were almost same in the solution states of the modified BODIPYs and polymers. The emission spectra of **PFDM**, **PFDF** and **PFMF** were, however, sharper than that of **PFB2** although these polymers provided the similar absorption spectra. These data mean that the substituent effects were exhibited only in the excited state. From the TD-DFT calculation for estimating the structure and the energy in the excited state, the rotation of the phenyl ring was presented.¹⁵ From this result, it is implied that the peak sharpening might be caused mainly by suppressing the molecular motions by the substitution at the para positions on the phenyl groups of these compounds.

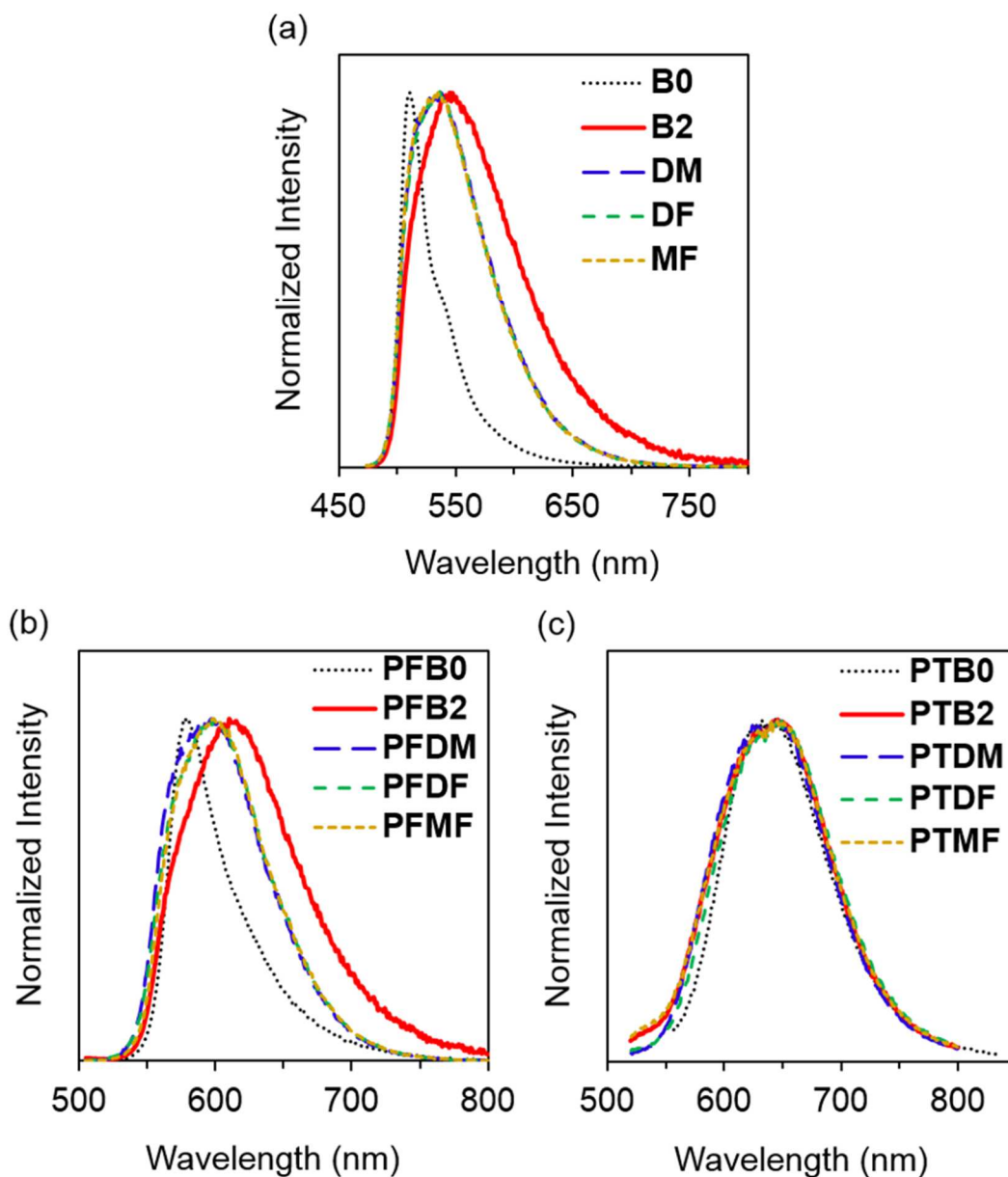


Figure 12. Photoluminescence spectra of (a) **B0**, modified BODIPYs, (b) corresponding fluorene copolymers and (c) bithiophene copolymers in chloroform (1.0×10^{-5} M).

To estimate the influence of the cardo boron on the formation of intermolecular interactions, the emission spectra with variable concentrations were monitored (Figures 13 and 14). The red-shifted emission bands were obtained from the concentrated solutions of **B0** and **PFB0**. On the other hand, the peak positions in the modified BODIPYs and polymers were hardly changed by increasing concentrations. This result clearly indicates that the cardo boron should also inhibit the intermolecular interactions. It is likely that the steric hindrance of the substituents suppress the accessibility of the molecules. The narrower emission bands were observed from the solutions with relatively-higher concentrations. The molecular tumbling at the phenyl ring in the cardo structure induces the broadening of the emission peaks.¹⁵ By inhibiting the molecular motions, the peak broadening should be inhibited in the higher concentrations, resulting in the sharp emission bands with good emission efficiencies.

Similar tendencies were obtained from the bithiophene-containing polymers in the optical properties. From the alternating polymers, the absorption bands with the peaks around 540 nm attributable to the π - π^* transition in BODIPY were obtained (Figure 7c). The red-shifted spectra of the polymers compared to those of the corresponding BODIPYs indicate the extension of the conjugation through the polymer main-chain. Comparing to the optical and electrochemical (Figure 8) properties of **PTB2**, the modified polymers with EDGs and/or EWGs presented the similar characteristics. These data indicate that the electronic structures can be preserved from the introduction of the side-chain substituents even through the polymer main-chain having strong electronic coupling in the ground state.

Chapter 2

In the series of the bithiophene copolymers, similar behaviors were also obtained about the emission spectra with the polymers composed of fluorene (Figure 12c and 15). The red-shifted emission bands from the strong electronic coupling were observed from the polymers compared to those of the corresponded BODIPYs. This result represents the extension of the conjugation through the polymer-main chains. Similar shapes and emission efficiencies were detected from the polymers. It should be mentioned that both of the bi-substituted EDGs and EWGs hardly cause the change in the intrinsic optical properties of the emission bands. These data clearly indicate that the main-chain conjugation can be preserved, and the cardo structure at the boron center should play a significant role in the electronic isolation of the main-chain conjugation from EDGs and/or EWGs in the side chains.

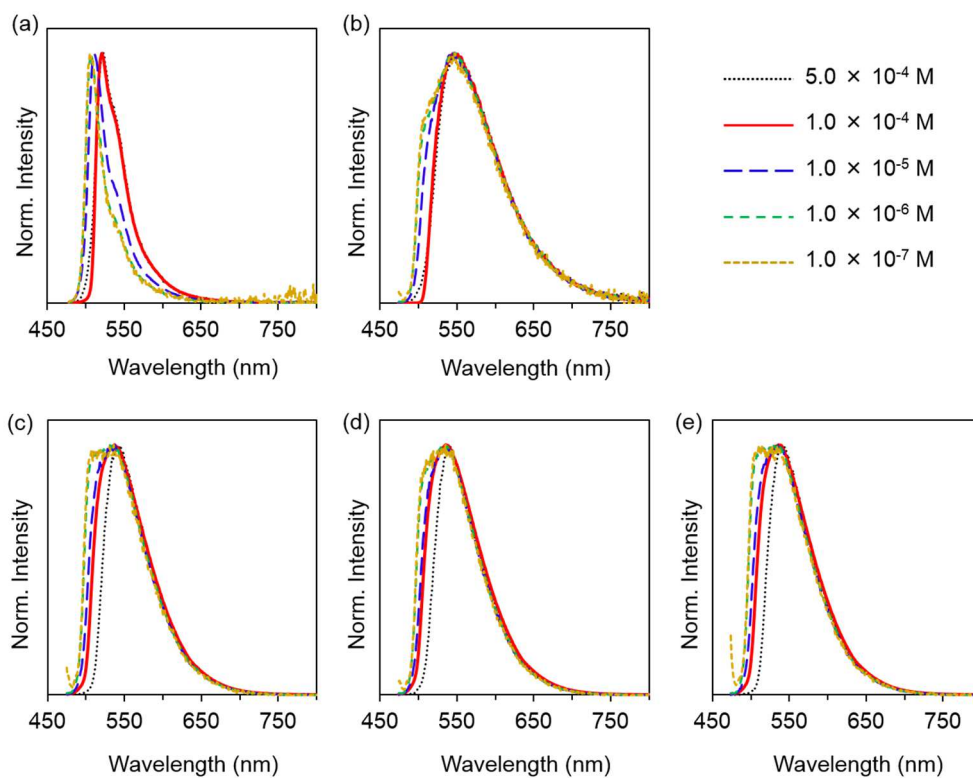


Figure 13. Photoluminescence spectra of (a) **B0**, (b) **B2**, (c) **DM**, (d) **DF** and (e) **MF** in chloroform with various concentrations.

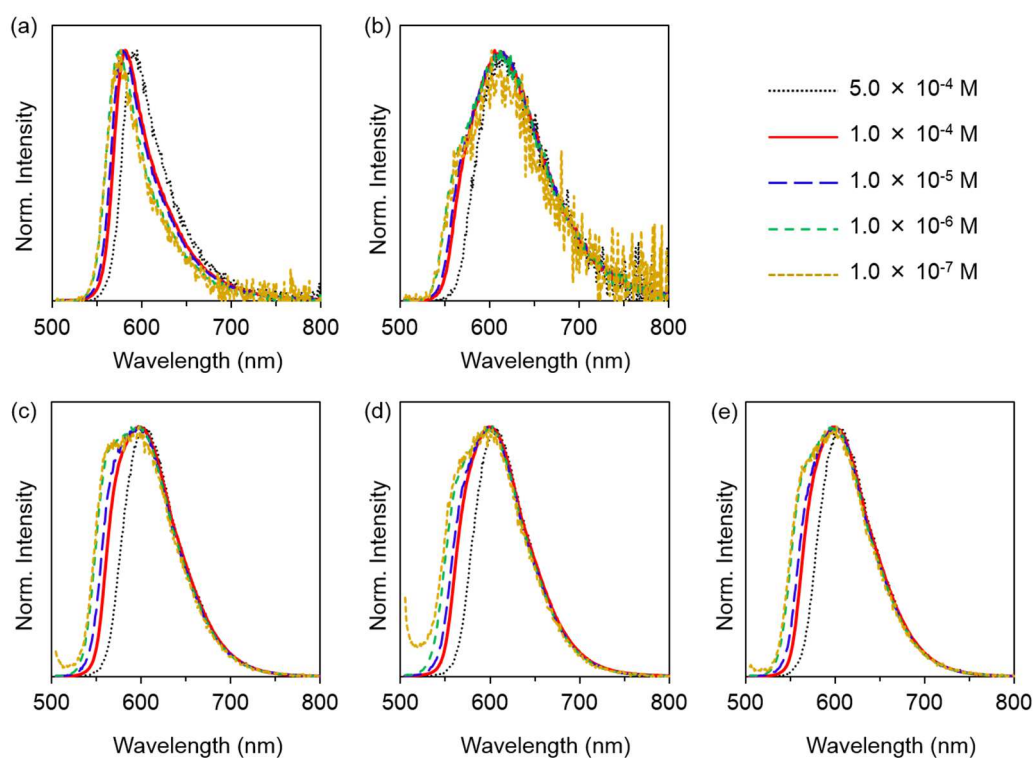


Figure 14. Photoluminescence spectra of (a) **PFB0**, (b) **PFB2**, (c) **PFDm**, (d) **PFDf** and (e) **PFMF** in chloroform with various concentrations.

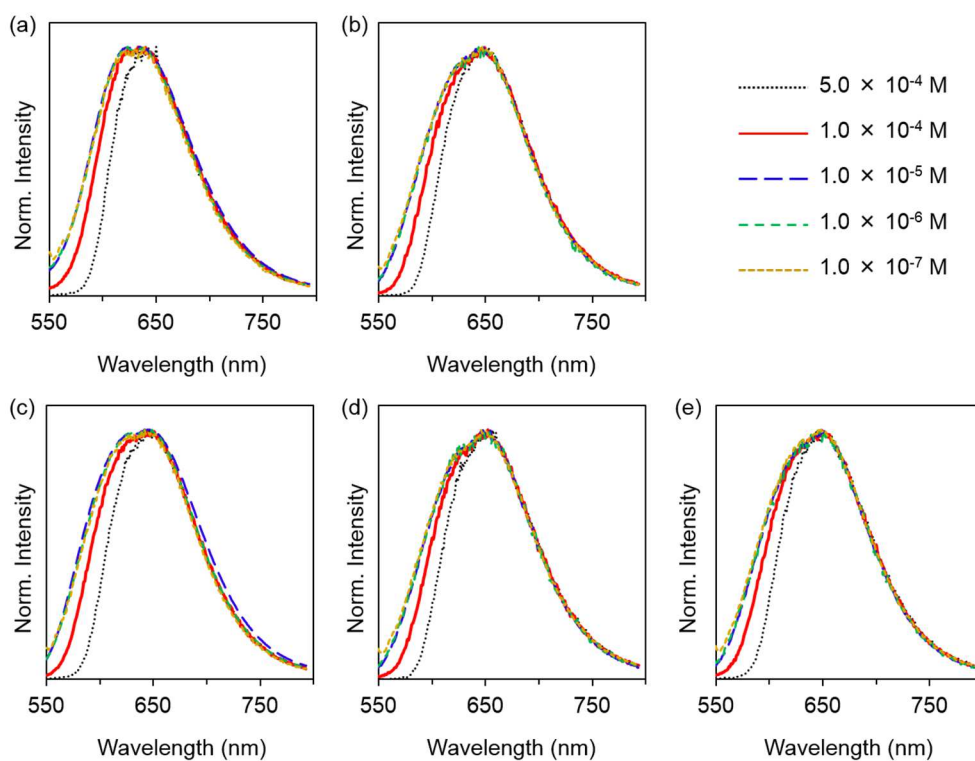


Figure 15. Photoluminescence spectra of (a) **PTB0**, (b) **PTB2**, (c) **PTDM**, (d) **PTDF** and (e) **PTMF** in chloroform with various concentrations.

Chapter 2

Conclusion

The series of the alternating polymers composed of the aryl-bearing BODIPYs with EDGs and/or EWGs were synthesized. From optical measurements, the isolation of the main-chain conjugation from the modification with EDGs and/or EWGs at the side chains via the cardo boron was presented in this manuscript. This result suggests that the BODIPY polymers with the cardo boron could be potential platforms for assembling the functional units with the suppression of non-specific interactions and for achieving multi-functional nanomaterials with preprogrammed designs. Advanced optical materials such as multi-emissive devices with the emissions not only from the polymer main-chains but also from the substituents at the cardo boron can be expected based on the author's strategy.

Experimental Sections

General: ^1H (400 MHz), ^{13}C (100 MHz), and ^{11}B (128 MHz) NMR spectra were recorded on JEOL JNM-EX400 spectrometers. In ^1H and ^{13}C NMR spectra, tetramethylsilane (TMS) was used as an internal standard in CDCl_3 . ^{11}B NMR spectra were referenced externally with $\text{BF}_3\cdot\text{OEt}_2$ (sealed capillary). Analytical thin-layer chromatography (TLC) was performed with silica gel 60 Merck F254 plates. Column chromatography was performed with a Wakogel C-300 silica gel. Number-average molecular weight (M_n) and molecular weight distribution (M_w/M_n) values of all polymers were estimated by size exclusion chromatography (SEC) with a TOSOH 8020 series [a dual pump system (DP-8020), a column oven (CO-8020), and a degasser (SD-8020)] equipped

with three consecutive polystyrene gel columns [TOSOH TSKgel: G2000H, G3000H and G4000H] and refractive-index (RI-8020) and ultraviolet detectors (UV-8020) at 40 °C. The system was operated at a flow rate of 1.0 mL/min with CHCl₃ as an eluent. Polystyrene standards were employed for calibration. UV-vis spectra were recorded on a SHIMADZU UV-3600 spectrophotometer. Fluorescence emission spectra were measured with a HORIBA JOBIN YVON Fluoromax-4P spectrofluorometer, and the absolute quantum yield was calculated by integrating sphere method on a HORIBA JOBIN YVON Fluoromax-P spectrofluorometer. Photoluminescence (PL) lifetime was measured by a Horiba FluoreCube spectrofluorometer system, and excitation was carried out at 375nm using UV diode laser (NanoLED 375 nm). Cyclic voltammetry (CV) was carried out on a BAS ALS-Electrochemical-Analyzer Model 600D with a glassy carbon (GC) working electrode, a Pt counter electrode, an Ag/Ag⁺ reference electrode, and the ferrocene/ferrocenium external reference at a scan rate of 50 mVs⁻¹. Ferrocene (Aldrich Chemical, Co.) was used as received. All reactions were performed under argon atmosphere.

Computational Details: The Gaussian 09 program package¹⁹ was used for computations of the compounds. The optimized structures was obtained by DFT calculation at the B3LYP/6-31G(d) level of theory. TD-DFT calculation was carried out at the B3LYP/6-31G(d) level for the electronic transitions.

Materials: 2,4-Dimethylpyrrole (Tokyo Kasei Kogyo, Co.), decanoyl chloride (Tokyo Kasei Kogyo, Co.), 4-bromoanisole (Tokyo Kasei Kogyo, Co.), 4-bromobenzotrifluoride (Tokyo Kasei Kogyo, Co.), *n*-butyllithium (*n*-BuLi, 1.6 mol/L in hexane, Kanto Chemical, Co., Inc.), boron

Chapter 2

trifluoride diethyl etherate ($\text{BF}_3 \cdot \text{OEt}_2$, Aldrich Chemical, Co.), *N*-iodosuccinimide (NIS, Tokyo Kasei Kogyo, Co.), [9,9-bis(2-dodecyl)-9H-fluorene-2,7-diyl]bisboronic acid (Aldrich Chemical, Co.), 2-dicyclohexylphosphino-2',6'-dimethoxybiphenyl (S-Phos, Wako Chemical, Co.), tris(dibenzylideneacetone dipalladium(0)) ($\text{Pd}_2(\text{dba})_3$, Wako Chemical, Co.), dichloromethane (Wako Chemical, Co.) and toluene (Wako Chemical, Co.) were used as received. Tetrahydrofuran (THF), diethyl ether and triethylamine were purified using a two-column solid-state purification system (Glasscouteur System, Joerg Meyer, Irvine, CA). **B0**¹⁷, **B2**¹⁵ and 2,2'-(3,3'-didodecyl-[2,2'-bithiophene]-5,5'-diyl)bis(4,4,5,5-tetramethyl-1,3,2-dioxaborolane)²⁰ were prepared according to the previous reports.

Synthesis of DM: *n*-BuLi (4.1 mL, 1.55 mol/L in hexane, 6.4 mmol) was added to the solution of 4-bromoanisole (0.80 mL, 6.4 mmol) in THF (120 mL) at -78°C . The reaction mixture was stirred for 1 h. Then, the solution of **B0** (0.60 g, 1.6 mmol, dissolved in 15 mL of THF) was added to the mixture via a cannula. After the reaction mixture was stirred for 30 min at 0°C , cooled saturated aqueous solution of ammonium chloride was added. The solution was extracted with dichloromethane, and the organic layer was washed with water and brine. After drying over MgSO_4 , the solvent was removed by a rotary evaporator. The product was purified by silica gel column chromatography with the mixed solvents of hexane/toluene (1/2) as an eluent. The product was obtained as an orange powder (0.46 g, 52%). $^1\text{H NMR}$ (CD_2Cl_2): $\delta = 7.17$ (4H, d, $J = 7.19$ Hz, Ar-*H*), 6.76 (4H, d, $J = 8.22$ Hz, Ar-*H*), 5.97 (2H, s, Ar-*H*), 3.76 (6H, s, $-\text{OCH}_3$), 3.02 (2H, t, $J = 7.80$ Hz, Ar- CH_2), 2.45 (6H, s, Ar- CH_3), 1.80–1.60 (8H, m, Ar- CH_3 , $-\text{CH}_2-$), 1.49–1.20 (12H, br, -

CH_2 -), 0.89 (3H, t, $J = 6.70$ Hz, $-CH_3$) ppm. ^{13}C NMR ($CDCl_3$): $\delta = 158.00, 153.02, 147.34, 137.50, 134.87, 132.05, 122.52, 112.85, 55.06, 32.51, 32.03, 30.33, 29.72, 29.70, 29.44, 28.86, 22.81, 17.10, 17.03, 14.21$ ppm. ^{11}B NMR (CD_2Cl_2): $\delta = -0.39$ ppm. HRMS (ESI) m/z calcd. $[M+H]^+$: 551.3803, found: 551.3798.

Synthesis of DF: *n*-BuLi (0.92 mL, 1.55 mol/L in hexane, 6.7 mmol) was added to the solution of 4-bromobenzotrifluoride (0.92 mL, 6.7 mmol) in diethyl ether (12.5 mL) at -78 °C. The reaction mixture was stirred for 1.5 h. Then, the solution of **B0** (1.0 g, 2.7 mmol in 25 mL of diethyl ether) was added to the mixture via a cannula. After the reaction mixture was stirred for 1.5 h at -78 °C, methanol was added. The solution was extracted with dichloromethane, and the organic layer was washed with water and brine. After drying over $MgSO_4$, the solvent was removed by a rotary evaporator. The product was purified by silica gel column chromatography with the mixed solvents of hexane/ethyl acetate (50/1) as an eluent. The isolated product was dissolved in a small amount of THF, and the product was reprecipitated from cold methanol to give pure **DF** as a candy-like orange paste (0.19 g, 11%). 1H NMR (CD_2Cl_2): $\delta = 7.44$ (4H, d, $J = 7.98$ Hz, Ar-*H*), 7.35 (4H, br s, Ar-*H*), 6.02 (2H, s, Ar-*H*), 3.06 (2H, t, $J = 8.22$ Hz, Ar- CH_2 -), 2.47 (6H, s, Ar- CH_3), 1.70–1.60 (8H, br, Ar- CH_3 , $-CH_2$ -), 1.42 (2H, quint, $-CH_2$ -), 1.36–1.20 (10H, br, $-CH_2$ -), 0.88 (3H, t, $J = 6.94$ Hz, $-CH_3$) ppm. ^{13}C NMR ($CDCl_3$): $\delta = 152.81, 147.96, 138.40, 133.65, 131.98, 128.31, 128.00, 126.16, 124.02, 123.99, 123.95, 123.91, 122.83, 32.36, 31.88, 30.12, 29.56, 29.27, 28.82, 22.67, 17.05, 16.90, 14.06$ ppm. ^{11}B NMR (CD_2Cl_2): $\delta = -1.37$ ppm. HRMS (APCI) m/z calcd. $[M+H]^+$: 627.3340, found: 627.3336.

Chapter 2

Synthesis of F: 4-Bromobenzotrifluoride (1.48 mL, 10.7 mmol) in THF (70 mL) was added to magnesium (0.38 g, 16 mmol) at r.t. under argon atmosphere. The reaction solution was stirred at 60 °C for 30 min. The resulting solution was cooled to r.t. and transferred via a cannula to a solution of **B0** (1.0 g, 2.7 mmol) in THF (50 mL). After the mixture solution was stirred at reflux temperature for 1 h, water was added to the reaction mixture to quench the reaction. The solution was extracted with dichloromethane, and the organic layer was washed with water and brine. After drying over MgSO₄, the solvent was removed by a rotary evaporator. The product was purified by column chromatography with hexane/ethyl acetate (24/1). The isolated product was dissolved in a small amount of THF, and the product was reprecipitated from methanol to give pure **F** as an orange powder (0.75 g, 56%). ¹H NMR (CD₂Cl₂): δ = 7.41 (4H, br, Ar-*H*), 6.01 (2H, s, Ar-*H*), 3.09 (2H, br, Ar-CH₂-), 2.47 (6H, s, Ar-CH₃), 2.12 (6H, s, Ar-CH₃), 1.74 (2H, br, -CH₂-), 1.56–1.52 (2H, m, -CH₂-), 1.40–1.32 (10H, br, -CH₂-), 0.89 (3H, t, *J* = 6.94 Hz, -CH₃) ppm. ¹¹B NMR (CD₂Cl₂): δ = 2.15 ppm. HRMS (ESI) *m/z* calcd. [M-H]⁻: 499.2913, found: 499.2918.

Synthesis of MF: 4-Bromoanisole (0.10 mL, 0.80 mmol) in THF (5.5 mL) was added to magnesium (29 mg, 1.2 mmol) at r.t. under argon atmosphere. The reaction solution was stirred at 50 °C for 1.5 h. The resulting solution was cooled to r.t. and transferred via a cannula to a solution of **F** (0.2 g, 0.4 mmol) in THF (7.6 mL). After the mixture solution was refluxed for 3 h, water was added to the reaction mixture to quench the reaction. The solution was extracted with dichloromethane, and the organic layer was washed with water and brine. After drying over MgSO₄, the solvent was removed by a rotary evaporator. The product was purified by column

chromatography with hexane/toluene (3/1). The isolated product was dissolved in a small amount of THF, and pure **MF** was obtained from the reprecipitation with cold methanol as a candy-like orange paste (96 mg, 41%). ^1H NMR (CD_2Cl_2): $\delta = 7.41$ (2H, d, $J = 7.74$ Hz, Ar-*H*), 7.28 (2H, br, Ar-*H*), 7.19 (2H, d, $J = 7.80$ Hz, Ar-*H*), 6.77 (2H, dt, $J = 8.65, 2.07$ Hz, Ar-*H*), 6.00 (2H, s, Ar-*H*), 3.77 (3H, s, - OCH_3), 3.04 (2H, t, $J = 8.10$ Hz, Ar- CH_2 -), 2.46 (6H, s, Ar- CH_3), 1.71–1.54 (8H, m, CH_2 , Ar- CH_3), 1.49–1.20 (12H, br, - CH_2 -), 0.88 (3H, t, $J = 6.58$ Hz, - CH_3) ppm. ^{13}C NMR (CDCl_3): $\delta = 158.21, 152.94, 147.59, 137.91, 134.98, 133.36, 132.36, 132.01, 127.86, 127.54, 126.29, 123.80, 123.77, 123.73, 123.69, 122.62, 112.96, 54.96, 32.37, 31.88, 30.12, 29.56, 29.28, 28.71, 22.67, 17.00, 16.89, 14.05$ ppm. ^{11}B NMR (CD_2Cl_2): $\delta = -0.98$ ppm. HRMS (ESI) m/z calcd. $[\text{M}+\text{H}]^+$: 589.3572, found: 589.3564.

Synthesis of the Iodized Monomers (**B0-I**, **B2-I**, **DM-I**, **DF-I** and **MF-I**)

General procedure: **B0** (1.00 g, 2.67 mmol) and *N*-iodosuccinimide (2.40 g, 10.7 mmol) were dissolved in dichloromethane (120 mL) under argon atmosphere. After stirred at r.t. for 0.5 h, the solvent was removed by a rotary evaporator. The mixture was purified with flash column chromatography with dichloromethane as an eluent. The product **B0-I** was dissolved in a small amount of THF and precipitated from methanol as an orange solid (1.22 g, 73%). ^1H NMR (CDCl_3): $\delta = 3.00$ (2H, t, $J = 8.45$ Hz, Ar- CH_2 -), 2.61 (6H, s, Ar- CH_3), 2.48 (6H, s, Ar- CH_3), 1.70–1.42 (4H, br, - CH_2 -), 1.40–1.20 (10H, br, - CH_2 -), 0.89 (3H, t, $J = 6.83$ Hz, - CH_3) ppm. ^{13}C NMR (CDCl_3): $\delta = 155.31, 146.48, 142.24, 131.50, 86.32, 31.84, 31.79, 30.33, 29.50, 29.43, 29.23, 22.64, 18.98, 16.11, 14.05$ ppm. ^{11}B NMR (CDCl_3): $\delta = 0.29$ ppm. HRMS (ESI) m/z calcd.

Chapter 2

[M+H]⁺: 625.0565; found, m/z 625.0566.

B2-I: An orange solid, 86% yield. ¹H NMR (CDCl₃): δ = 7.33–7.12(8H, br, Ar-*H*), 3.13 (2H, t, *J* = 8.35 Hz, Ar-CH₂-), 2.54 (6H, s, Ar-CH₃), 1.88 (6H, s, Ar-CH₃), 1.66 (2H, quint, *J* = 7.98 Hz, -CH₂-), 1.46 (2H, quint, *J* = 7.43 Hz, -CH₂-), 1.39–1.20 (10H, br, -CH₂-), 0.89 (3H, t, *J* = 6.70 Hz, -CH₃) ppm. ¹³C NMR (CDCl₃): δ = 153.78, 146.83, 139.71, 133.64, 131.69, 127.42, 126.04, 87.79, 32.22, 31.84, 30.10, 29.65, 29.51, 29.25, 22.65, 19.72, 18.61, 14.05 ppm. ¹¹B NMR (CDCl₃): δ = 0.39 ppm. HRMS (ESI) m/z calcd. [M+H]⁺: 743.1525; found, m/z 743.1518.

DM-I: A red solid, 68% yield. ¹H NMR (CD₂Cl₂): δ = 7.17 (4H, br, Ar-*H*), 6.77 (4H, dt, *J* = 8.34 Hz, 2.18 Hz, Ar-*H*), 3.77 (6H, s, -OCH₃), 3.12 (2H, t, *J* = 8.35 Hz, Ar-CH₂-), 2.54 (6H, s, Ar-CH₃), 1.89 (6H, s, Ar-CH₃), 1.66 (2H, quint, *J* = 7.89 Hz, -CH₂-), 1.46 (2H, quint, *J* = 7.39 Hz, -CH₂-), 1.39–1.22 (10H, br, -CH₂-), 0.89 (3H, t, *J* = 6.83 Hz, -CH₃) ppm. ¹³C NMR (CDCl₃): δ = 158.14, 153.73, 146.67, 139.56, 134.70, 131.63, 112.99, 87.75, 54.94, 32.22, 31.84, 30.11, 29.64, 29.54, 29.26, 22.65, 19.69, 18.57, 14.04 ppm. ¹¹B NMR (CDCl₃): δ = 0.88 ppm. HRMS (APCI) m/z calcd. [M+H]⁺: 803.1736, found: 803.1726.

DF-I: A red solid, 71% yield. ¹H NMR (CD₂Cl₂): δ = 7.47 (4H, d, *J* = 7.98 Hz, Ar-*H*), 7.36 (4H, br, Ar-*H*), 3.15 (2H, t, *J* = 8.26 Hz, Ar-CH₂-), 2.56 (6H, s, Ar-CH₃), 1.83 (6H, s, Ar-CH₃), 1.66 (2H, quint, *J* = 7.84 Hz, -CH₂-), 1.46 (2H, quint, *J* = 7.25 Hz, -CH₂-), 1.39–1.20 (10H, br, -CH₂-), 0.89 (3H, t, *J* = 6.55 Hz, -CH₃) ppm. ¹³C NMR (CDCl₃): δ = 153.73, 147.44, 140.64, 133.57, 131.73, 128.81, 128.49, 125.99, 124.35, 124.31, 124.27, 124.24, 123.28, 88.15, 32.25, 31.84, 30.10, 29.71, 29.52, 29.25, 22.66, 19.80, 18.81, 14.05 ppm. ¹¹B NMR (CDCl₃): δ = -0.59 ppm.

HRMS (APCI) m/z calcd. $[M+H]^+$: 627.3340, found: 627.3336.

MF-I: A red solid, 66% yield. ^1H NMR (CD_2Cl_2): δ = 7.45 (2H, d, J = 7.74 Hz, Ar-*H*), 7.38–7.23 (2H, br, Ar-*H*), 7.18 (2H, br, Ar-*H*), 6.79 (2H, dt, J = 8.65, 2.17 Hz, Ar-*H*), 3.78 (3H, s, - OCH_3), 3.13 (2H, t, J = 7.55 Hz, Ar- CH_2 -), 2.55 (6H, s, Ar- CH_3), 1.87 (6H, s, Ar- CH_3), 1.64 (2H, br, - CH_2 -), 1.53–1.20 (12H, br, - CH_2 -), 0.89 (3H, t, J = 6.73 Hz, - CH_3) ppm. ^{13}C NMR (CDCl_3): δ = 158.36, 153.73, 147.05, 140.08, 134.84, 133.40, 131.59, 128.25, 127.91, 126.05, 124.06, 124.03, 123.99, 123.95, 123.35, 113.17, 87.96, 54.95, 32.19, 31.83, 30.10, 29.63, 29.50, 29.25, 22.65, 19.74, 18.67, 14.06 ppm. ^{11}B NMR (CD_2Cl_2): δ = -0.29 ppm. HRMS (ESI) m/z calcd. $[M-H]^-$: 839.1359, found: 839.1372.

Synthesis of the Polymers:

Synthesis of PFB0: Water (2.0 mL) was added to the solution of **B0-I** (0.15 g, 0.24 mmol), [9,9-bis(dodecyl)-9H-fluorene-2,7-diyl]bisboronic acid (0.14 g, 0.24 mmol), $\text{Pd}_2(\text{dba})_3$ (2.2 mg, 2.4 μmol), S-Phos (3.9 mg, 9.6 μmol) and cesium carbonate (0.78 g, 2.4 mmol) in toluene (2.0 mL). The reaction mixture was stirred at 80 °C for 72 h (**PFB0**, **PFB2**) or 48 h (**PFDM**, **PFDE**, **PFMF**) under argon atmosphere, and poured into a large amount of methanol to collect the polymer by filtration. The precipitate was dissolved in a small amount of THF, and then the product was reprecipitated from ethanol. The polymer collected by filtration was dried in vacuum to give **PFB0** as a red solid (0.19 g, 89%). M_n = 10,200, M_w/M_n = 2.7. ^1H NMR (CDCl_3): δ = 7.90–7.60 (2H, br, Ar-*H*), 7.40–7.10 (4H, br, Ar-*H*), 3.14 (2H, Ar- CH_2 -), 2.66–2.30 (12H, Ar- CH_3), 2.01 (4H, $>\text{C}(\text{CH}_2)_2$), 1.77 (2H, - CH_2 -), 1.47–0.95 (52H, - C_6H_{12} - and - $\text{C}_{10}\text{H}_{20}$ -), 0.93–0.51 (9H, - CH_3) ppm.

Chapter 2

^{13}C NMR (CDCl_3): $\delta = 152.71, 151.10, 146.88, 139.89, 136.25, 134.44, 132.64, 131.63, 129.21, 125.12, 119.64, 55.22, 40.38, 31.94, 31.88, 30.46, 30.08, 29.66, 29.58, 29.52, 29.39, 29.36, 29.28$ ppm. ^{11}B NMR (CDCl_3): $\delta = 8.14$ ppm.

PFB2: A red solid, 53% yield. $M_n = 6,200, M_w/M_n = 2.2$. ^1H NMR (CDCl_3): $\delta = 7.90\text{--}7.00$ (14H, br, Ar-*H*), 3.24 (2H, Ar- CH_2 -), 2.44 (6H, Ar- CH_3), 2.01–1.64 (12H, $>\text{C}(\text{CH}_2)_2$, $-\text{CH}_2$ -, and Ar- CH_3), 1.59–0.78 (55H, $-\text{C}_7\text{H}_{15}$ and $-\text{C}_{10}\text{H}_{20}$ -), 0.61 (6H, br, $-\text{CH}_3$) ppm. ^{13}C NMR (CDCl_3): $\delta = 151.93, 150.79, 147.30, 140.97, 139.58, 134.79, 134.03, 133.42, 132.08, 129.55, 127.31, 127.21, 125.62, 125.22, 119.19, 55.15, 55.10, 40.33, 32.49, 31.94, 31.90, 30.30, 29.99, 29.63, 29.53, 29.35, 29.31, 23.92, 22.70, 22.67, 15.75, 15.06, 14.11, 14.08$ ppm. ^{11}B NMR (CDCl_3): $\delta = -2.25$ ppm.

PFDM: A red solid, 59% yield. $M_n = 7,400, M_w/M_n = 1.9$. ^1H NMR (CDCl_3): $\delta = 7.66$ (2H, m, Ar-*H*), 7.51–7.20 (4H, br, Ar-*H*), 7.08 (4H, m, Ar-*H*), 6.83 (4H, m, Ar-*H*), 3.80 (6H, $-\text{OCH}_3$), 3.24 (2H, Ar- CH_2 -), 2.44 (6H, Ar- CH_3), 2.90–1.64 (12H, $>\text{C}(\text{CH}_2)_2$, $-\text{CH}_2$ -, and Ar- CH_3), 1.62–0.78 (55H, $-\text{C}_7\text{H}_{15}$ and $-\text{C}_{10}\text{H}_{20}$ -), 0.62 (6H, br, $-\text{CH}_3$) ppm. ^{13}C NMR (CDCl_3): $\delta = 157.77, 151.85, 150.73, 147.14, 139.52, 135.06, 134.66, 133.41, 133.24, 131.94, 129.53, 125.18, 119.15, 112.68, 55.13, 54.91, 40.36, 32.47, 31.94, 31.90, 30.32, 30.30, 29.62, 29.53, 29.36, 29.32, 23.93, 22.70, 22.67, 15.73, 15.04, 14.12, 14.10$ ppm. ^{11}B NMR (CDCl_3): $\delta = 0.88$ ppm.

PFDF: A red solid, 89% yield. $M_n = 6,000, M_w/M_n = 1.7$. ^1H NMR (CDCl_3): $\delta = 7.79$ (2H, m, Ar-*H*), 7.62–7.39 (6H, br, Ar-*H*), 7.32 (2H, m, Ar-*H*), 7.07 (4H, m, Ar-*H*), 3.26 (2H, Ar- CH_2 -), 2.45 (6H, Ar- CH_3), 2.13–1.60 (12H, $>\text{C}(\text{CH}_2)_2$, $-\text{CH}_2$ -, and Ar- CH_3), 1.58–0.78 (55H, $-\text{C}_7\text{H}_{15}$ and $-\text{C}_{10}\text{H}_{20}$ -), 0.62 (6H, br, $-\text{CH}_3$) ppm. ^{13}C NMR (CDCl_3): $\delta = 150.94, 150.82, 147.93, 139.75, 135.19,$

134.34, 133.86, 132.98, 132.09, 129.52, 126.12, 125.07, 124.03, 123.42, 119.15, 55.22, 40.24, 32.46, 31.90, 31.85, 30.22, 29.97, 29.92, 29.56, 29.50, 29.47, 29.44, 29.31, 29.27, 23.82, 22.65, 15.58, 15.06, 14.06 ppm. ^{11}B NMR (CDCl_3): $\delta = -3.03$ ppm.

PFMF: A red solid, 87% yield. $M_n = 8,400$, $M_w/M_n = 2.5$. ^1H NMR (CDCl_3): $\delta = 7.68$ (2H, m, Ar-*H*), 7.59–7.42 (4H, br, Ar-*H*), 7.41–7.27 (2H, m, Ar-*H*), 7.08 (4H, m, Ar-*H*), 6.84 (2H, m, Ar-*H*), 3.80 (6H, - OCH_3), 3.24 (2H, Ar- CH_2 -), 2.44 (6H, Ar- CH_3), 2.12–1.59 (12H, $>\text{C}(\text{CH}_2)_2$, - CH_2 -, and Ar- CH_3), 1.58–0.76 (55H, - C_7H_{15} and - $\text{C}_{10}\text{H}_{20}$ -), 0.62 (6H, br, - CH_3) ppm. ^{13}C NMR (CDCl_3): $\delta = 158.07$, 151.83, 150.82, 147.51, 139.64, 135.14, 134.92, 133.80, 133.20, 132.02, 129.54, 126.25, 125.11, 123.80, 123.55, 119.30, 112.91, 55.17, 54.93, 40.32, 33.95, 32.47, 31.93, 31.88, 30.27, 29.96, 29.60, 29.51, 29.34, 29.30, 23.91, 22.68, 22.66, 15.80, 15.06, 14.10, 14.08 ppm. ^{11}B NMR (CDCl_3): $\delta = 5.30$ ppm.

PTB0: A metallic purple solid, 97% yield. $M_n = 9,500$, $M_w/M_n = 1.7$. ^1H NMR (CDCl_3): $\delta = 6.79$ (2H, br, Ar-*H*), 3.11 (2H, Ar- CH_2 -), 2.74–2.36 (16H, Ar- CH_3 , Ar- CH_2 -), 1.81–0.96 (54H, - C_7H_{14} - and - $\text{C}_{10}\text{H}_{20}$ -), 0.93–0.71 (9H, - CH_3) ppm. ^{13}C NMR (CDCl_3): $\delta = 153.71$, 147.49, 142.42, 137.84, 134.20, 131.61, 129.87, 129.41, 126.53, 31.94, 31.84, 30.78, 30.42, 29.72, 29.69, 29.68, 29.64, 29.55, 29.49, 29.37, 29.25, 29.08, 28.94, 22.69, 22.64, 14.67, 14.08, 14.05, 13.49 ppm. ^{11}B NMR (CDCl_3): $\delta = 0.59$ ppm.

PTB2: A metallic purple solid, 79% yield. $M_n = 11,500$, $M_w/M_n = 1.8$. ^1H NMR (CDCl_3): $\delta = 7.45$ –7.07 (10H, br, Ar-*H*), 6.64 (2H, br, Ar-*H*), 3.20 (2H, Ar- CH_2 -), 2.60–2.32 (10H, Ar- CH_3 , Ar- CH_2 -), 1.93–0.93 (54H, - C_7H_{14} - and - $\text{C}_{10}\text{H}_{20}$ -), 0.92–0.73 (9H, - CH_3) ppm. ^{13}C NMR (CDCl_3): $\delta = 152.79$,

Chapter 2

147.89, 142.19, 141.98, 135.14, 135.06, 133.85, 132.06, 129.76, 129.10, 128.71, 128.61, 127.23, 126.62, 125.70, 32.37, 31.94, 31.87, 30.70, 30.25, 29.69, 29.65, 29.60, 29.58, 29.44, 29.38, 29.30, 28.98, 22.71, 22.67, 15.90, 15.20, 14.12, 14.10 ppm. ^{11}B NMR (CDCl_3): $\delta = 5.20$ ppm.

PTDM: A metallic purple solid, 90% yield. $M_n = 7,800$, $M_w/M_n = 1.7$. ^1H NMR (CDCl_3): $\delta = 7.45$ – 7.10 (4H, br, Ar-*H*), 6.86 – 6.71 (4H, br, Ar-*H*), 6.64 (2H, br, Ar-*H*), 3.78 (6H, $-\text{OCH}_3$), 3.20 (2H, Ar- CH_2 -), 2.72 – 2.30 (10H, Ar- CH_3 , Ar- CH_2 -), 1.99 – 1.00 (54H, $-\text{C}_7\text{H}_{14}$ - and $-\text{C}_{10}\text{H}_{20}$ -), 0.98 – 0.74 (9H, $-\text{CH}_3$) ppm. ^{13}C NMR (CDCl_3): $\delta = 157.89$, 152.78 , 147.67 , 141.96 , 135.17 , 135.01 , 134.87 , 132.03 , 129.73 , 129.11 , 128.76 , 128.61 , 126.58 , 125.10 , 112.77 , 54.88 , 32.39 , 31.93 , 31.86 , 30.68 , 30.25 , 29.67 , 29.64 , 29.59 , 29.44 , 29.36 , 29.29 , 28.99 , 22.69 , 22.65 , 15.85 , 15.17 , 14.09 , 14.06 ppm. ^{11}B NMR (CDCl_3): $\delta = -2.44$ ppm.

PTDF: A metallic purple solid, 90% yield. $M_n = 9,100$, $M_w/M_n = 1.9$. ^1H NMR (CDCl_3): $\delta = 7.56$ – 7.30 (8H, br, Ar-*H*), 6.66 (2H, br, Ar-*H*), 3.22 (2H, Ar- CH_2 -), 2.72 – 2.22 (10H, Ar- CH_3 , Ar- CH_2 -), 1.93 – 0.95 (54H, $-\text{C}_7\text{H}_{14}$ - and $-\text{C}_{10}\text{H}_{20}$ -), 0.93 – 0.75 (9H, $-\text{CH}_3$) ppm. ^{13}C NMR (CDCl_3): $\delta = 152.61$, 148.53 , 142.22 , 136.03 , 134.56 , 133.74 , 132.05 , 129.94 , 129.27 , 128.75 , 128.41 , 128.10 , 127.07 , 126.04 , 124.09 , 123.33 , 32.39 , 31.91 , 31.84 , 30.66 , 30.19 , 29.64 , 29.63 , 29.57 , 29.54 , 29.42 , 29.40 , 29.34 , 29.26 , 29.14 , 28.97 , 22.68 , 22.65 , 16.00 , 15.21 , 14.07 , 14.06 ppm. ^{11}B NMR (CDCl_3): $\delta = -2.44$ ppm.

PTMF: A metallic purple solid, 84% yield. $M_n = 11,400$, $M_w/M_n = 1.8$. ^1H NMR (CDCl_3): $\delta = 7.55$ – 7.17 (6H, br, Ar-*H*), 6.87 – 6.75 (2H, br, Ar-*H*), 6.65 (2H, br, Ar-*H*), 3.79 (3H, $-\text{OCH}_3$), 3.21 (2H, Ar- CH_2 -), 2.76 – 2.29 (10H, Ar- CH_3 , Ar- CH_2 -), 2.02 – 1.01 (54H, $-\text{C}_7\text{H}_{14}$ - and $-\text{C}_{10}\text{H}_{20}$ -), 0.98 –

0.78 (9H, $-CH_3$) ppm. ^{13}C NMR ($CDCl_3$): $\delta = 158.16, 152.75, 148.15, 142.27, 142.21, 142.09, 135.53, 134.87, 133.54, 132.08, 129.84, 129.19, 128.62, 127.97, 127.65, 126.82, 126.17, 125.18, 123.86, 123.47, 112.99, 54.92, 32.38, 31.92, 31.84, 30.67, 30.20, 29.66, 29.64, 29.58, 29.42, 29.35, 29.27, 28.98, 22.68, 22.65, 15.93, 15.19, 14.08, 14.06$ ppm. ^{11}B NMR ($CDCl_3$): $\delta = -2.25$ ppm.

References

- (a) Bolognesi, A.; Betti, P.; Botta, C.; Destri, S.; Giovanella, U.; Moreau, J.; Pasini, M.; Porzio, W. *Macromolecules* **2009**, *42*, 1107–1113. (b) Xiong, M. J.; Li, Z. H.; Wong, M. S. *Aust. J. Chem.* **2007**, *60*, 608–614. (c) Giovanella, U.; Betti, P.; Botta, C.; Destri, S.; Moreau, J.; Pasini, M.; Porzio, W.; Vercelli, B.; Bolognesi, A. *Chem. Mater.* **2011**, *23*, 810–816. (d) Wu, F.-I.; Shih, P.-I.; Shu, C.-F. *Macromolecules* **2005**, *38*, 9028–9036. (e) Matsumoto, N.; Miyazaki, T.; Nishiyama, M.; Adachi, C. *J. Phys. Chem. C* **2009**, *113*, 6261–6266. (f) Li, Z. H.; Wong, M. S. *Org. Lett.* **2006**, *8*, 1499–1502. (g) McFarlane, S. L.; Piercey, D. G.; Coumont, L. S.; Tucker, R. T.; Fleischauer, M. D.; Brett, M. J.; Veinot, J. G. C. *Macromolecules* **2009**, *42*, 591–598. (h) Wu, F.-I.; Reddy, D. S.; Shu, C.-F. *Chem. Mater.* **2003**, *15*, 269–274. (i) Bian, C.; Jiang, G.; Tong, H.; Cheng, Y.; Xie, Z.; Wang, L.; Jing, X.; Wang, F. *J. Polym. Sci. Part A: Polym. Chem.* **2011**, *49*, 3911–3919. (j) Zhang, B.; Chen, Y.; Liu, G.; Xu, L.-Q.; Chen, J.; Zhu, C.-X.; Neoh, K.-G.; Kang, E.-T. *J. Polym. Sci. Part A: Polym. Chem.* **2012**, *50*, 378–387. (k) Concilio, S.; Pfister, P. M.; Tirelli, N.; Kocher, C.; Suter, U. W. *Macromolecules* **2001**, *34*, 3607–3614. (l) Tonzola, C. J.; Alam, M. M.; Jenekhe, S. A. *Macromol. Chem. Phys.* **2005**,

Chapter 2

206, 1271–1279.

2. (a) Yeo, H.; Tanaka, K.; Chujo, Y. *J. Polym. Sci. Part A: Polym. Chem.* **2012**, *50*, 4433–4442.
(b) Yeo, H.; Tanaka, K.; Chujo, Y. *Macromolecules* **2013**, *46*, 2599–2605.
3. Yeo, H.; Tanaka, K.; Chujo, Y. *Polymer* **2015**, *60*, 228–233.
4. Yeo, H.; Tanaka, K.; Chujo, Y. *J. Polym. Sci. A: Polym. Chem.* **2015**, *53*, 2026–2035.
5. Chujo, Y.; Tanaka, K. *Bull. Chem. Soc. Jpn.* **2015**, *88*, 633–643.
6. (a) Tanaka, K.; Yanagida, T.; Hirose, A.; Yamane, H.; Yoshii, R.; Chujo, Y. *RSC Adv.* **2015**, *5*, 96653–96659. (b) Hirose, A.; Tanaka, K.; Yoshii, R.; Chujo, Y. *Polym. Chem.* **2015**, *6*, 5590–5595. (c) Yoshii, R.; Suenaga, K.; Tanaka, K.; Chujo, Y. *Chem. Eur. J.* **2015**, *21*, 7231–7237. (d) Suenaga, K.; Yoshii, R.; Tanaka, K.; Chujo, Y. *Macromol. Chem. Phys.* **2016**, *217*, 414–421. (e) Yoshii, R.; Hirose, A.; Tanaka, K.; Chujo, Y. *J. Am. Chem. Soc.* **2014**, *136*, 18131–18139. (f) Yoshii, R.; Nagai, A.; Tanaka, K.; Chujo, Y. *Macromol. Rapid Commun.* **2014**, *35*, 1315–1319. (g) Yoshii, R.; Tanaka, K.; Chujo, Y. *Macromolecules* **2014**, *47*, 2268–2278. (h) Tanaka, K.; Chujo, Y. *NPG Asia Mater.* **2015**, *7*, e223. (i) Hirose, A.; Tanaka, K.; Tamashima, K.; Chujo, Y. *Tetrahedron Lett.* **2014**, *55*, 6477–6481. (j) Yoshii, R.; Hirose, A.; Tanaka, K.; Chujo, Y. *Chem. Eur. J.* **2014**, *20*, 8320–8324. (k) Yoshii, R.; Nagai, A.; Tanaka, K.; Chujo, Y. *Chem. Eur. J.* **2013**, *19*, 4506–4512.
7. (a) Ulrich, G.; Ziesel, R.; Harriman, A. *Angew. Chem. Int. Ed.* **2008**, *47*, 1184–1201. (b) Ziesel, R.; Ulrich, G.; Harriman, A. *New J. Chem.* **2007**, *31*, 496–501. (c) Bones, N.; Leen, V.; Dehaen, W. *Chem. Soc. Rev.* **2012**, *41*, 1130–1172.

8. (a) Yoshii, R.; Yamane, H.; Nagai, A.; Tanaka, K.; Taka, H.; Kita, H.; Chujo, Y. *Macromolecules* **2014**, *47*, 2316–2323. (b) Kajiwara, Y.; Nagai, A.; Tanaka, K.; Chujo, Y. *J. Mater. Chem. C* **2013**, *1*, 4437–4444. (c) Tanaka, K.; Yanagida, T.; Yamane, H.; Hirose, A.; Yoshii, R.; Chujo, Y. *Bioorg. Med. Chem. Lett.* **2015**, *25*, 5331–5334. (d) Tanaka, K.; Yamane, H.; Yoshii, R.; Chujo, Y. *Bioorg. Med. Chem.* **2013**, *21*, 2715–2719. (e) Ni, Y.; Lee, S.; Son, M.; Aratani, N.; Ishida, M.; Yamada, H.; Furuta, H.; Kim, D.; Wu, J. *Angew. Chem. Int. Ed.* **2016**, *55*, 2815–2819. (f) Shimizu, S.; Murayama, A.; Haruyama, T.; Iino, T.; Mori, S.; Furuta, H.; Kobayashi, N. *Chem. Eur. J.* **2015**, *21*, 12996–13003. (g) Saikawa, M.; Daicho, M.; Nakamura, T.; Uchida, J.; Yamamura, M.; Nabeshima, T. *Chem. Commun.* **2016**, *52*, 4014–4017. (h) Ooyama, Y.; Hagiwara, Y.; Oda, Y.; Fukuoka, H.; Ohshita, J. *RSC Adv.* **2014**, *4*, 1163–1167.
9. (a) Kobayashi, T.; Komatsu, T.; Kamiya, M.; Campos, C.; Gonzalez-Gaitan, M.; Terai, T.; Hanaoka, K.; Nagano, T.; Urano, Y. *J. Am. Chem. Soc.* **2012**, *134*, 11153–11160. (b) Komatsu, T.; Oushiki, D.; Takeda, A.; Miyamura, M.; Ueno, T.; Terai, T.; Hanaoka, K.; Urano, Y.; Mineno, T.; Nagano, T. *Chem. Commun.* **2011**, *47*, 10055–10057. (c) Komatsu, T.; Urano, Y.; Fujikawa, Y.; Kobayashi, T.; Kojima, H.; Terai, T.; Hanaoka, K.; Nagano, T. *Chem. Commun.* **2009**, 7015–7017.
10. (a) Spies, C.; Huynh, A.-M.; Huch, V.; Jung, G. *J. Phys. Chem. C* **2013**, *117*, 18163–18169. (b) Bergström, F.; Mikhalyov, I.; Hägglöf, P.; Wortmann, R.; Ny, T.; Johansson, L. B.-Å. *J. Am. Chem. Soc.* **2002**, *124*, 196–204. (c) Kajiwara, Y.; Nagai, A.; Chujo, Y. *Bull. Chem. Soc.*

Chapter 2

- Jpn* **2011**, *84*, 471–481. (d) Kajiwarara, Y.; Nagai, A.; Chujo, Y. *J. Mater. Chem.* **2010**, *20*, 2985–2992.
11. (a) Zhang, D.; Wen, Y.; Xiao, Y.; Yu, G.; Liu, Y.; Qian, X. *Chem. Commun.* **2008**, *44*, 4777–4779. (b) Ozdemir, T.; Atilgan, S.; Kutuk, I.; Yildirim, L. T.; Tulek, A.; Bayindir, M.; Akkaya, E. U. *Org. Lett.* **2009**, *11*, 2105–2107. (c) Gai, L.; Lu, H.; Zou, B.; Lai, G.; Shen, Z.; Li, Z. *RSC Adv.* **2012**, *2*, 8840–8846. (d) Lu, H.; Wang, Q.; Gai, L.; Li, Z.; Deng, Y.; Xiao, X.; Lai, G.; Shen, Z. *Chem. Eur. J.* **2012**, *18*, 7852–7861. (e) Liu, C.-L.; Chen, Y.; Shelar, D. P.; Li, C.; Cheng, G.; Fu, W.-F. *J. Mater. Chem. C* **2014**, *2*, 5471–5478.
12. (a) Hundnall, T. W.; Lin, T.-P.; Gabbai, F. P. *J. Fluor. Chem.* **2010**, *131*, 1182–1186. (b) Li, Z.; Lin, T.-P.; Liu, S.; Huang, C.-W.; Hundnall, T. W.; Gabbai, F. P.; Conti, P. S. *Chem. Commun.* **2011**, *47*, 9324–9326. (c) Haefele, A.; Zedde, C.; Retaillieu, P.; Ulrich, G.; Ziessel, R. *Org. Lett.* **2010**, *12*, 1672–1675. (d) Bonnier, C.; Piers, W. E.; Ali, A. A.-S.; Thompson, A.; Parvez, M. *Organometallics* **2009**, *28*, 4845–4851. (e) Ulrich, G.; Goze, C.; Goeb, S.; Retaillieu, P.; Ziessel, R. *New J. Chem.* **2006**, *30*, 982–986. (f) Landrum, M.; Smertenko, A.; Edwards, R.; Hussey, P. J.; Steel, P. G. *Plant J.* **2010**, *62*, 529–538.
13. (a) Goze, C.; Ulrich, G.; Mallon, L. J.; Allen, B. P.; Harriman, A.; Ziessel, R. *J. Am. Chem. Soc.* **2006**, *128*, 10231–10239. (b) Yamamura, M.; Yazaki, S.; Seki, M.; Matsui, Y.; Ikeda, H.; Nabeshima, T.; *Org. Biomol. Chem.* **2015**, *13*, 2574–2581.
14. Kubota, Y.; Uehara, J.; Funabiki, K.; Ebihara, M.; Matsui, M. *Tetrahedron Lett.* **2010**, *51*, 6195–6198.

15. Yamane, H.; Tanaka, K.; Chujo, Y. *Tetrahedron Lett.* **2015**, *56*, 6786–6790.
16. (a) Yoshii, R.; Yamane, H.; Tanaka, K.; Chujo, Y. *Macromolecules* **2014**, *47*, 3755–3760. (b) Yoshii, R.; Nagai, A.; Tanaka, K.; Chujo, Y. *J. Polym. Sci. Part A: Polym. Chem.* **2013**, *51*, 1726–1733. (c) Alemdaroglu, F. E.; Alexander, S. C.; Ji, D.; Prusty, D. K.; Boersch, M.; Herrmann, A. *Macromolecules* **2009**, *42*, 6529–6536. (d) Cortizo-Lacalle, D.; Howells, C. T.; Gambino, S.; Vilela, F.; Vobecka, Z.; Findlay, N. J.; Inigo, A. R.; Thomson, S. A. J.; Skabara, P. J.; Samuel, I. D. W. *J. Mater. Chem.* **2012**, *22*, 14119–14126. (e) Economopoulos, S. P.; Chochos, C. L.; Ioannidou, H. A.; Neophytou, M.; Charilaou, C.; Zissimou, G. A.; Frost, J. M.; Sachetan, T.; Shahid, M.; Nelson, J.; Heeney, M.; Bradley, D. D. C.; Itskos, G.; Koutentis, P. A.; Choulis, S. A. *RSC Adv.* **2013**, *3*, 10221–10229. (f) Ma, X.; Azeem, E. A.; Liu, X.; Cheng, Y.; Zhu, C. *J. Mater. Chem. C* **2014**, *2*, 1076–1084. (g) Ma, X.; Jiang, X.; Zhang, S.; Huang, X.; Cheng, Y.; Zhu, C. *Polym. Chem.* **2013**, *4*, 4396–4404. (h) Ma, X.; Mao, X.; Zhang, S.; Huang, X.; Cheng, Y.; Zhu, C. *Polym. Chem.* **2013**, *4*, 520–527. (i) Maeda H.; Nishimura, Y.; Hiroto, S.; Shinokubo, H. *Dalton Trans.* **2013**, *42*, 15885–15888. (j) Meng, G.; Velayudham, S.; Smith, A.; Luck, R.; Liu, H. *Macromolecules* **2009**, *42*, 1995–2001. (k) Nepomnyashchii, A. B.; Broering, M.; Ahrens, J.; Bard, A. J. *J. Am. Chem. Soc.* **2011**, *133*, 8633–8645. (l) Popere, B. C.; Della Pelle, A. M.; Poe, A.; Balaji, G.; Thayumanavan, S. *Chem. Sci.* **2012**, *3*, 3093–3102. (m) Popere, B. C.; Della Pelle, A. M.; Thayumanavan, S. *Macromolecules* **2011**, *44*, 4767–4776. (n) Rong, Y.; Wu, C. F.; Yu, J. B.; Zhang, X. J.; Ye, F. M.; Zeigler, M.; Gallina, M. E.; Wu, I. C.; Zhang, Y.; Chan, Y. H.; Sun, W.; Uvdal, K.; Chiu,

Chapter 2

- D. T. *ACS Nano* **2013**, *7*, 376–384. (o) Sen, C. P.; Shrestha, R. G.; Shrestha, L. K.; Ariga, K.; Valiyaveetil, S. *Chem. Eur. J.* **2015**, *21*, 17344–17354. (p) Squeo, B. M.; Gasparini, N.; Ameri, T.; Palma-Cando, A.; Allard, S.; Gregoriou, V. G.; Brabec, C. J.; Scherf, U.; Chochos, C. L. *J. Mater. Chem. A* **2015**, *3*, 16279–16286. (q) Thivierge, C.; Loudet, A.; Burgess, K.; *Macromolecules* **2011**, *44*, 4012–4015. (r) Usta, H.; Yilmaz, M. D.; Avestro, A.-J.; Boudinet, D.; Denti, M.; Zhao, W.; Stoddart, J. F.; Facchetti, A. *Adv. Mater.* **2013**, *25*, 4327–4334.
17. Vincent, M.; Beabout, E.; Benett, R.; Hewavitharanage, P. *Tetrahedron Lett.* **2013**, *54*, 2050–2054.
18. (a) Qin, W.; Baruah, M.; Van der Auweraer, M.; De Schryver, F. C.; Boens, N. *J. Phys. Chem. A* **2005**, *109*, 7371–7384. (b) Qin, W.; Rohand, T.; Baruah, M.; Stefan, A.; Van der Auweraer, M.; Dehaen, W.; Boens, N. *Chem. Phys. Lett.* **2006**, *420*, 562–568. (c) Qin, W.; Baruah, M.; Stefan, A.; Van der Auweraer, M.; Boens, N. *ChemPhysChem* **2005**, *6*, 2343–2351.
19. Gaussian 09, Revision A.1, Frisch, M. J.; Trucks, G. W.; Schlegel, H. B.; Scuseria, G. E.; Robb, M. A.; Cheeseman, J. R.; Scalmani, G.; Barone, V.; Mennucci, B.; Petersson, G. A.; Nakatsuji, H.; Caricato, M.; Li, X.; Hratchian, H. P.; Izmaylov, A. F.; Bloino, J.; Zheng, G.; Sonnenberg, J. L.; Hada, M.; Ehara, M.; Toyota, K.; Fukuda, R.; Hasegawa, J.; Ishida, M.; Nakajima, T.; Honda, Y.; Kitao, O.; Nakai, H.; Vreven, T.; Montgomery, Jr., J. A.; Peralta, J. E.; Ogliaro, F.; Bearpark, M.; Heyd, J. J.; Brothers, E.; Kudin, K. N.; Staroverov, V. N.; Kobayashi, R.; Normand, J.; Raghavachari, K.; Rendell, A.; Burant, J. C.; Iyengar, S. S.; Tomasi, J.; Cossi, M.; Rega, N.; Millam, J. M.; Klene, M.; Knox, J. E.; Cross, J. B.; Bakken,

V.; Adamo, C.; Jaramillo, J.; Gomperts, R.; Stratmann, R. E.; Yazyev, O.; Austin, A. J.; Cammi, R.; Pomelli, C.; Ochterski, J. W.; Martin, R. L.; Morokuma, K.; Zakrzewski, V. G.; Voth, G. A.; Salvador, P.; Dannenberg, J. J.; Dapprich, S.; Daniels, A. D.; Farkas, Ö.; Foresman, J. B.; Ortiz, J. V.; Cioslowski, J.; Fox, D. J. Gaussian, Inc., Wallingford CT, **2009**.

20. Yoshii, R.; Tanaka, K.; Chujo, Y. *Macromolecules* **2014**, *47*, 2268–2278.

Chapter 2

Chapter 3

The Dual-Emissive Polymer Based on BODIPY Homopolymer

Bearing Anthracene on Cardo Boron

ABSTRACT: The dual-emissive polymer based on cardo BODIPYs was synthesized. Cardo BODIPY having anthracene as a cardo unit was constructed via organometallic reagents and polymerized by oxidative coupling for obtaining homopolymer. The synthetic polymer showed various emission color derived from the polymer main chain and anthracene moieties.

Chapter 3

Introduction

Dual-emissive polymers show the two different color emissions from a single polymer chain, and they are expected to be versatile materials.¹ The colors of emission materials, especially white, are composed of the combination of multiple colors, involving red, green and blue. When different color emitters are connected, energy transfer often occurs between dyes. Therefore, it is challenging to obtain dual emission and to tune the emission color.

Chujo *et al.* reported dual-emissive conjugated polymers based on cardo fluorenes.² These polymers had emissive dyes on the cardo carbon. These dyes were isolated from the polymer main chain, and energy transfer between the cardo moieties and the polymer chain was suppressed. Therefore, the cardo fluorene polymers showed dual emission.

Cardo structures can be also constructed on a hetero atom, such as boron. Boron dipyromethenes (BODIPYs) were used as a scaffold for constructing the cardo structure by the introduction of aromatic groups to boron atoms. In chapter 2, the author reported that the electronic states of polymer main chain were preserved from modification with electron-withdrawing and/or donating groups on the *para*-position of phenyl groups tethered to the cardo-borons of BODIPYs.³ From these results, it is proposed that when light emitting dyes are substituted on the phenyl groups in the cardo BODIPYs instead of electron-withdrawing and/or donating groups, the main chain of polymers and dyes on cardo side chain can individually show their intrinsic emissions. Therefore, dual-color emission can be expected to be observed from a single polymer.

Herein, the author designed the cardo BODIPY bearing 9,10-diphenylanthracene on the cardo

boron. Anthracene was chosen for a blue color emitter. In contrast, the polymer main chain was supposed to show different emission color from anthracene because expanded conjugation should show emission in longer wavelength region. Anthracene bearing cardo BODIPY, **B2A**, was synthesized via organometallic reagents and a Pd-catalyzed coupling reaction. Then, several homopolymers composed of cardo BODIPYs were synthesized. From the optical measurements of synthetic products, it was revealed that the BODIPY homopolymer showed dual emission properties originated from both the polymer main chain and anthracene moieties.

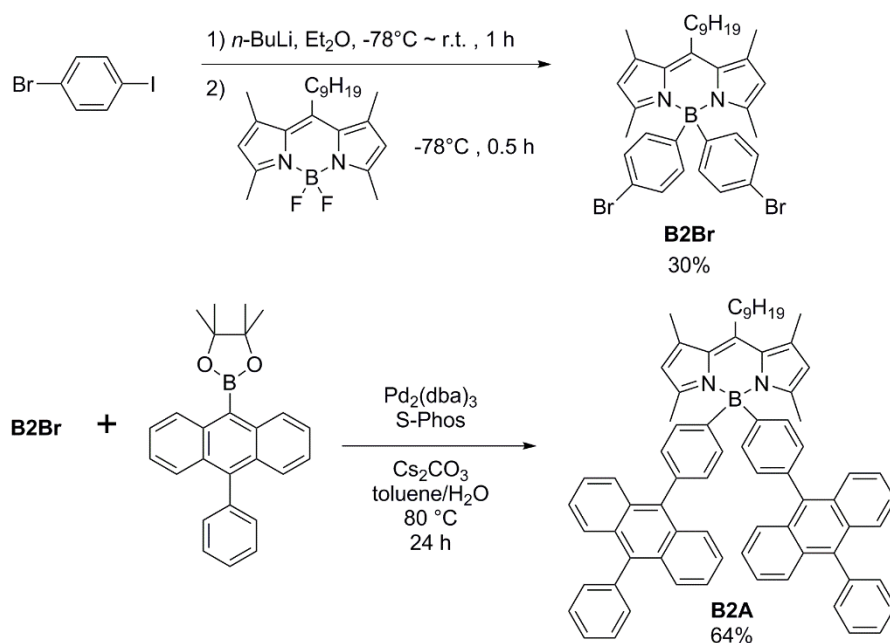
Chapter 3

Results and Discussion

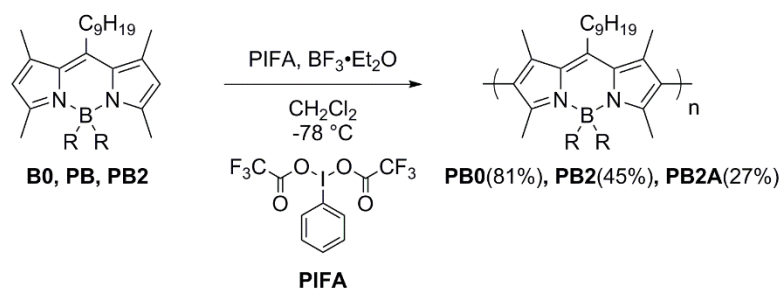
To obtain the dual emission, anthracene was chosen for the blue emitter. **B2A** was designed as the anthracene bearing cardo BODIPY and synthesized according to scheme 1. The author used the difluorinated compound **B0** as a starting material.⁴ To synthesize **B2Br** which has bromine atom at the *para*-position of cardo boron, 1-bromo-4-iodobenzene was transformed to the Grignard reagent and introduced into boron atom instead of fluorine atom. Next, the anthracene moiety was introduced via the Suzuki–Miyaura coupling in the presence of Pd catalyst. Then, **B2Br** was converted to **B2A**. The products showed good solubility in the common organic solvents such as chloroform, THF, and ethanol. The structures of all compounds were confirmed by ¹H, ¹¹B, ¹³C NMR spectroscopies and ionization mass measurements.

Next, the cardo BODIPYs (**B2** and **B2A**) and **B0** were used as a monomer. **B0** and **B2** were prepared according to the previous reports.^{4,5} The polymerization was accomplished by oxidative coupling with the BODIPY monomers in the presence of [bis(trifluoroacetoxy)iodo]benzene (PIFA) and BF₃·OEt₂ in CH₂Cl₂ (Scheme 2). The products showed good solubility in common organic solvents such as chloroform, THF, and DMF. The polymer properties determined from the GPC analysis are shown in Table 1.

Scheme 1. Synthetic routes for the cardo BODIPYs

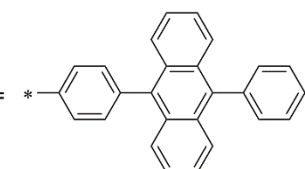


Scheme 2. Synthetic routes for the polymers



B0, PB0 : $\text{R} = \text{F}$

B2, PB2 : $\text{R} =$ *—

B2A, PB2A : $\text{R} =$ *—

Chapter 3

Table 1. Physical properties of the synthesized polymers^a

	reaction time [h]	M_n	M_w/M_n	n^b	Yield [%] ^c
PB0	1	14,000	4.1	36.2	81
PB2	20	11,000	2.6	22.4	45
PB2A	6	6,600	2.5	6.04	27

^aEstimated from SEC with the polystyrene standards in chloroform. ^bAverage number of repeating units calculated from M_n and molecular weights of repeating units. ^cIsolated yields after reprecipitation.

The UV–vis absorption spectra of the products (both monomers and polymers) were measured to discuss about the electronic states in the ground state (Figure 1). All monomers showed strong and sharp absorption bands around 500 nm. As the optical properties of **B0** and **B2** were clarified in the previous report⁵, those absorption peaks can be attributed to $S_0 \rightarrow S_1$ ($\pi \rightarrow \pi^*$) transition. Moreover, **B2A** showed other absorption bands below 450nm derived from the anthracene moieties.

Polymers also showed strong and sharp absorption bands similarly to those of the monomers. **PB0** and **PB2** showed $S_0 \rightarrow S_1$ ($\pi \rightarrow \pi^*$) transition bands around 590 nm. On the other hand, **PB2A** based on anthracene-bearing cardo BODIPY showed the $S_0 \rightarrow S_1$ ($\pi \rightarrow \pi^*$) transition band with the peak at 560 nm. **PB2A** showed the absorption band attributable to anthracene similarly to its monomer **B2A**.

Figure 2 shows the photoluminescence spectra of the monomers and polymers in chloroform (1.0×10^{-5} mol/L). As the author mentioned in the previous report⁵, **B2** which has a cardo structure on its boron atom showed the broad and red-shifted emission band with a smaller quantum yield compared to **B0**. This difference in emission was derived from the molecular motion at the phenyl group. **B2A** showed almost same emission properties to **B2**. From this results, the anthracene moiety should rotate in the solution like as the phenyl groups in **B2**.

The emission properties of polymers were different from those of their monomers. The difluorinated compound **B0** showed a sharp and strong emission band, and this properties are typical for BODIPYs. **PB0** synthesized by **B0** as a monomer also showed sharp emission band

Chapter 3

similarly to the monomer. On the other hand, the emission properties of **PB2** and **PB2A** were different from their monomers. Although cardo BODIPY monomers showed the broad emission spectra, their polymers (**PB2** and **PB2A**) showed sharp emission spectra like **PB0**. From these results, the author suggests that these sharp emission spectra should be derived from suppression of molecular motion at polymers.

Figure 3 shows the **PB2A** photoluminescence spectra which were excited at different wavelength in chloroform (1.0×10^{-7} mol/L). When **PB2A** was excited at the absorption region of the main-chain (500 nm), the emission band was observed around 600 nm. This emission was could be derived from the polymer main chain. On the other hand, when the excitation was performed at the absorption region of the anthracene moieties (377 nm), **PB2A** showed dual emission. The emission band in the region from 400 nm to 500 nm was also observed with the main-chain emission band. This blue emission should be derived from the anthracene moieties. From these data, it is supposed that energy transfer from the anthracene units to the polymer main chain should be suppressed via the cardo structure. Additionally, emission colors were varied by excitation wavelength, then coordination of CIE diagram changed (Figure 4).

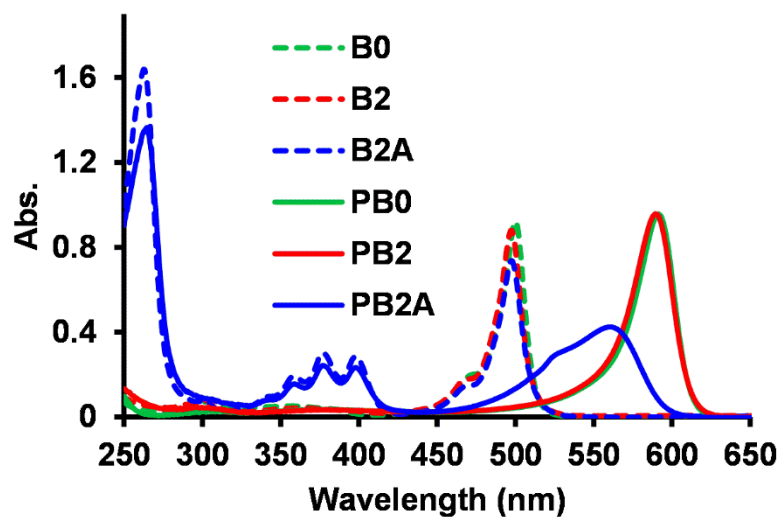


Figure 1. UV-vis-NIR absorption spectra of the products in CHCl_3 (1×10^{-5} M).

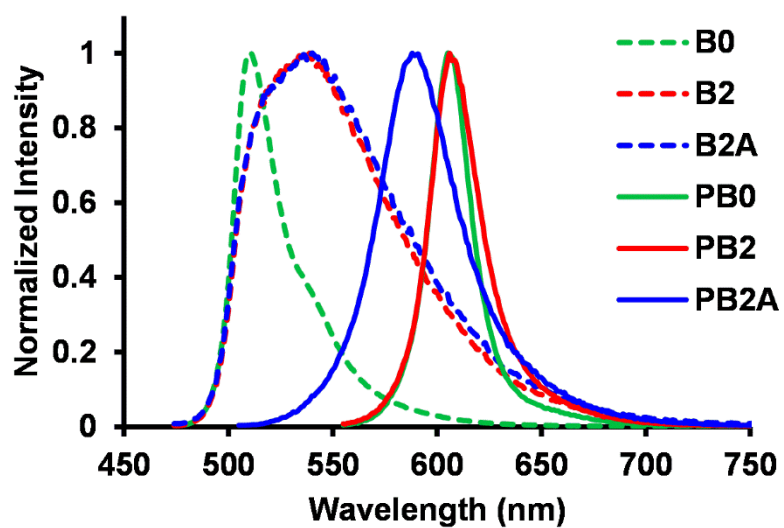


Figure 2. Photoluminescence spectra of the products in chloroform (1.0×10^{-5} M).

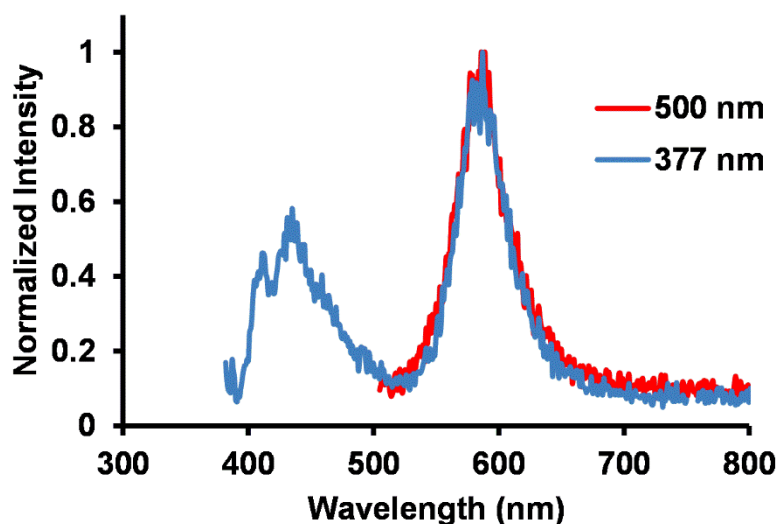


Figure 3. Photoluminescence spectra of **PB2A** in chloroform (1.0×10^{-7} M) excited at 500 nm (red line) and 377 nm (blue line).

Table 2. Optical properties of the compounds^a

	λ_{abs} (nm)	ε ($\text{M}^{-1}\text{cm}^{-1}$) ^b	λ_{PL} (nm)	Φ_{PL} ^c
B0	500	92,000	511 ^d	0.81 ^d
B2	497	88,000	539 ^e	0.34 ^e
B2A	497	74,000	540 ^e	0.29 ^e
PB0	591	96,000	605 ^f	0.35 ^f
PB2	589	96,000	606 ^f	0.38 ^f
PB2A	560	43,000	588 ^g	0.43 ^g

^aMeasured in chloroform (1.0×10^{-5} M). ^bMolar absorption coefficients of the absorption maxima.

^cAbsolute fluorescence quantum yields determined using integrated sphere method. ^dExcited at

473 nm. ^eExcited at 469 nm. ^fExcited at 550 nm. ^gExcited at 500 nm.

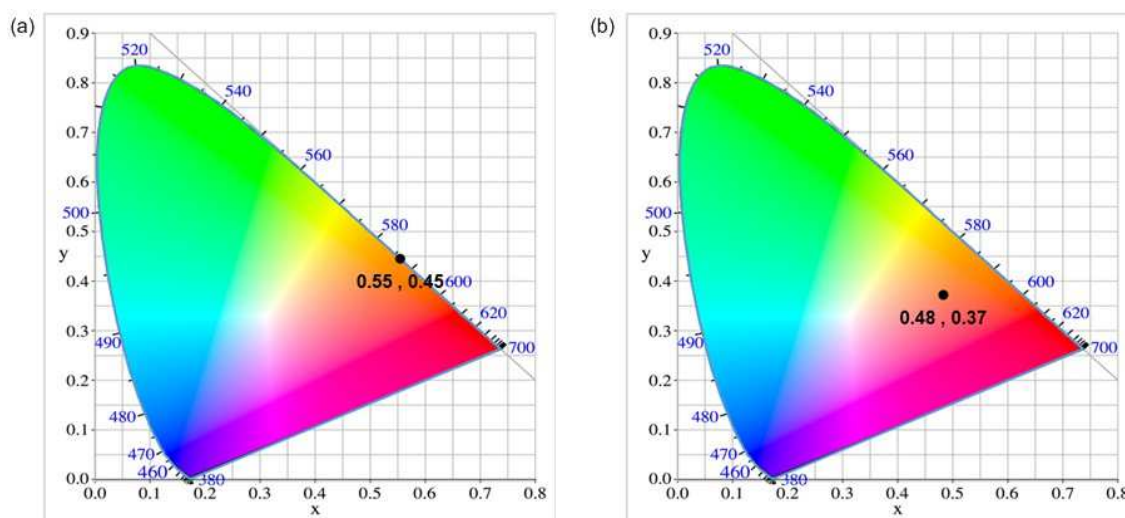


Figure 4. CIE diagram of **PB2A** excited at (a) 500 nm, (b) 377 nm.

Conclusion

The dual-emissive materials based on a cardo structure were presented in this chapter. BODIPYs can be used as a scaffold for constructing cardo structures on their boron atoms. As the author reported that the electronic states of the polymer main chain composed of cardo BODIPYs were preserved from the cardo unit in the chapter 2, the conjugated polymers based on cardo BODIPYs can show emission from main chain without influence of side chains. Actually, the BODIPY conjugated polymer bearing anthracene as the cardo unit showed two distinct emissions derived from both polymer main chains and side chains. From these results, the homopolymer based on cardo BODIPYs should be a promising structure to realize multi-color emissions.

Chapter 3

Experimental Section

General: ^1H (400 MHz), ^{13}C (100 MHz) and ^{11}B (128 MHz) NMR spectra were recorded on a JEOL JNM EX400 spectrometer. ^{11}B NMR spectra were referenced externally to $\text{BF}_3\cdot\text{OEt}_2$ (sealed capillary). Analytical thin-layer chromatography (TLC) was performed with silica gel 60 Merck F254 plates. Column chromatography was performed with Wakogel C-300 silica gel. UV-vis spectra were recorded on a Shimadzu UV-3600 spectrophotometer. Fluorescence emission spectra were recorded on a HORIBA JOBIN YVON Fluoromax-4 spectrofluorometer, and the absolute quantum yield was calculated by integrating sphere method on the HORIBA JOBIN YVON Fluoromax-4 spectrofluorometer in chloroform.

Synthesis of B2Br: *n*-BuLi (5.2 mL, 1.63 mol/L in hexane) was added to the solution of 1-bromo-4-iodobenzene (2.4 g, 8.5 mmol) in diethyl ether (16 mL) at $-78\text{ }^\circ\text{C}$ under argon atmosphere. The reaction mixture was stirred for 0.5 h at $-78\text{ }^\circ\text{C}$ and for 0.5 h at room temperature. Then, the solution of **B0**⁴ (0.8 g, 2.1 mmol in 18 mL of diethyl ether) was added to the reaction mixture via cannula at $-78\text{ }^\circ\text{C}$. After the reaction mixture was stirred for 0.5 h at $-78\text{ }^\circ\text{C}$, methanol was added. The solution was extracted with dichloromethane and washed with water and brine. After the organic phase was dried over MgSO_4 , the solvent was removed by a rotary evaporator. The silica gel column chromatography with hexane/dichloromethane (9:1) gave **B2Br** as a orange solid (0.41 g, 0.63 mmol, 30 %). ^1H NMR (CDCl_3): $\delta = 7.31$ (4H, d, $J = 8.3$ Hz), 7.08 (4H, br), 6.00 (2H, s), 3.03 (2H, d, $J = 8.3$ Hz), 2.45 (6H, s), 1.70 (6H, s), 1.67 – 1.59 (2H, m), 1.42 – 1.39 (2H, m), 1.30 – 1.27 (10H, m), 0.88 (3H, t, $J = 6.8$ Hz) ^{13}C NMR (CDCl_3): $\delta = 152.7$, 147.7 , 138.0 , 135.3 ,

131.9, 130.3, 122.7, 122.6, 120.2, 32.3, 31.9, 30.1, 29.5, 29.3, 28.6, 22.6, 17.1, 16.9, 16.9, 14.1 ppm. ^{11}B NMR (CDCl_3): $\delta = -0.98$ (br) ppm. HRMS (ESI): Calcd. for $[\text{M}+\text{H}]^+$, 647.1802; found, m/z 647.1786.

Synthesis of B2A: Water (8.0 mL) was added to the solution of **B2B2** (0.50 g, 0.77 mmol), 10-phenyl-9-anthraceneboronic acid (1.9 g, 3.5 mmol), $\text{Pd}_2(\text{dba})_3$ (14 mg, 15 μmol), S-Phos (56 mg, 0.14 mmol) and cesium carbonate (5.0 g, 15 mmol) in toluene (8.0 mL). The reaction mixture was stirred at 80 °C for 24 h under argon atmosphere. The solution was extracted with toluene and washed with water and brine. After the organic phase was dried over MgSO_4 , the solvent was removed by a rotary evaporator. The product was purified by column chromatography with hexane/dichloromethane (4:1). The isolated product was dissolved in a small amount of CH_2Cl_2 , and the product was precipitated from methanol to give pure **B2A** as a orange solid (0.49 g, 64%).

^1H NMR (CDCl_3): $\delta = 7.81$ (4H, dd, $J = 7.2, 3.1$ Hz), 7.69–7.48 (18H, m), 7.37 (4H, d, $J = 7.8$ Hz), 7.32–7.31 (8H, m), 6.18 (2H, s), 3.19 (2H, t, $J = 8.3$ Hz), 2.59 (6H, s), 2.15 (6H, s), 1.79–1.77 (2H, m), 1.54–1.51 (2H, m), 1.36–1.28 (10H, m), 0.86 (3H, t, $J = 6.96$ Hz) ppm. ^{13}C NMR (CDCl_3): $\delta = 158.1, 149.2, 147.7, 139.4, 138.4, 137.8, 136.5, 136.0, 133.7, 132.2, 131.4, 130.2, 130.0, 130.0, 128.4, 127.4, 127.3, 126.8, 124.9, 124.6, 122.6, 32.4, 31.8, 30.8, 30.3, 29.6, 29.3, 28.8, 22.6, 17.4, 17.0, 14.0$ ppm. ^{11}B NMR (CDCl_3): $\delta = -0.20$ (br) ppm. HRMS (APCI): Calcd. for $[\text{M}+\text{H}]^+$, 995.5470; found, m/z 995.5465.

Synthesis of PB0: $\text{BF}_3 \cdot \text{OEt}_2$ (0.33 mL, 0.38 g, 2.7 mmol) was added to a solution of **B0** (0.10 g, 0.27 mmol) and PIFA (0.23 g, 0.53 mmol) in CH_2Cl_2 (2.0 mL) at -78 °C, and the solution was

Chapter 3

stirred at $-78\text{ }^{\circ}\text{C}$ for 1 h. The solution was poured into MeOH (25 mL) and triethylamine (3 mL) to collect desired polymer by filtration. The precipitate was dissolved in a small amount of THF, and further reprecipitated from a large excess of EtOH twice to give **PB0** as a metallic red solid (81 mg, 81%). $M_n = 14,000$, $M_w/M_n = 4.1$. $^1\text{H NMR}$ (CDCl_3): $\delta = 3.68\text{--}1.06$ (28H, m), $0.96\text{--}0.82$ (3H, m) ppm. $^{11}\text{B NMR}$ (CDCl_3): $\delta = 0.59$ (br) ppm.

Synthesis of PB2: $\text{BF}_3\cdot\text{OEt}_2$ (0.35 mL, 0.41 g, 2.9 mmol) was added to a solution of **B2** (0.14 g, 0.29 mmol) and PIFA (0.25 g, 0.57 mmol) in CH_2Cl_2 (2.1 mL) at $-78\text{ }^{\circ}\text{C}$, and the solution was stirred at $-78\text{ }^{\circ}\text{C}$ for 20 h. The solution was poured into MeOH (30 mL) and triethylamine (3 mL) to collect desired polymer by filtration. The precipitate was dissolved in a small amount of THF, and further reprecipitated from a large excess of EtOH twice to give **PB2** as a purplish red solid (62 mg, 45%). $M_n = 11,000$, $M_w/M_n = 2.6$. $^1\text{H NMR}$ (CDCl_3): $\delta = 7.48\text{--}6.92$ (10H, m), $3.35\text{--}0.95$ (28H, m), $0.93\text{--}0.79$ (3H, m) ppm. $^{11}\text{B NMR}$ (CDCl_3): $\delta = -1.17$ (br) ppm.

Synthesis of PB2A: $\text{BF}_3\cdot\text{OEt}_2$ (0.20 mL, 0.23 g, 1.6 mmol) was added to a solution of **B2A** (0.16 g, 0.16 mmol) and PIFA (0.14 g, 0.32 mmol) in CH_2Cl_2 (1.2 mL) at $-78\text{ }^{\circ}\text{C}$, and the solution was stirred at $-78\text{ }^{\circ}\text{C}$ for 6 h. The solution was poured into MeOH (20 mL) and triethylamine (2 mL) to collect desired polymer by filtration. The precipitate was dissolved in a small amount of THF, and the polymeric products were reprecipitated in a large excess of EtOH. To remove monomer and dimers, this procedure was repeated several times, and then **PB2A** was collected as a purplish red solid (43 mg, 27%). $M_n = 6,000$, $M_w/M_n = 2.5$. $^1\text{H NMR}$ (CDCl_3): $\delta = 7.97\text{--}6.60$ (34H, m), $3.44\text{--}0.36$ (31H, m) ppm. $^{11}\text{B NMR}$ (CDCl_3): $\delta = -3.13$ (br) ppm.

References

1. (a) Wu, H.; Ying, L.; Yang, W.; Cao, Y. *Chem. Soc. Rev.* **2009**, *38*, 3391–3400. (b) Bu, J.; Watanabe, K.; Hayasaka, H.; Akagi, K. *Nat. Commun.* **2014**, *5*, 3799 (1-7). (c) Kuo, C.-P.; Chuang, C.-N.; Chang, C.-L.; Leung, M.; Lian, H.-Y.; Chia-Wen Wu, K. *J. Mater. Chem. C* **2013**, *1*, 2121–2130. (d) Takamizu, K.; Inagaki, A.; Nomura, K. *ACS Macro Lett.* **2013**, *2*, 980–984. (e) Lin, J.-Y.; Wong, J.; Xie, L.-H.; Dong, X.-C.; Yang, H. Y.; Huang, W. *Macromol. Rapid Commun.* **2014**, *35*, 895–900. (f) Osken, I.; Gundogan, A. S.; Tekin, E.; Eroglu, M. S.; Ozturk, T. *Macromolecules* **2013**, *46*, 9202–9210. (g) Chong, H.; Nie, C.; Zhu, C.; Yang, Q.; Liu, L.; Lv, F.; Wang, S. *Langmuir* **2012**, *28*, 2091–2098. (h) Luo, J.; Li, X.; Chen, J.; Huang, F.; Cao, Y. *Synth. Met.* **2011**, *161*, 1982–1986. (i) Wang, H.-Y.; Qian, Q.; Lin, K.-H.; Peng, B.; Huang, W.; Liu, F.; Wei, W. *J. Polym. Sci. B; Polym. Phys.* **2012**, *50*, 180–188.
2. (a) Yeo, H.; Tanaka, K.; Chujo, Y. *Polymer* **2015**, *60*, 228–233. (b) Yeo, H.; Tanaka, K.; Chujo, Y. *J. Polym. Sci. A: Polym. Chem.* **2015**, *53*, 2026–2035.
3. Yamane, H.; Ito, S.; Tanaka, K.; Chujo, Y. *Polym. Chem.* **2016**, *7*, 2799–2807.
4. Vincent, M.; Beabout, E.; Benett, R.; Hewavitharanage, P. *Tetrahedron Lett.* **2013**, *54*, 2050–2054.
5. Yamane, H.; Tanaka, K.; Chujo, Y. *Tetrahedron Lett.* **2015**, *56*, 6786–6790.

Chapter 3

Chapter 4

Efficient Light Absorbers Based on Thiophene-Fused Boron

Dipyrromethene (BODIPY) Dyes

ABSTRACT: The author presents the development of the thiophene-fused boron dipyrromethene derivatives as efficient light absorbers. The two strategies for the evolution of the optical properties such as the peak positions of absorption wavelengths and molar extinct coefficients were established by the substituent effects: By introducing iodine groups, the bathochromic shifts of the peak positions (+15 nm) and the enhancement of molar extinct coefficients were simultaneously received owing to the heavy atom effect. Next, it was found that the modification with the trifluoromethyl group contributed to the large bathochromic shift (+60 nm) because of the lowering effect on the lowest unoccupied molecular orbital of the dye by the substituent. Finally, the author obtained the dyes with large molar extinct coefficients ($184,140 \text{ M}^{-1} \text{ cm}^{-1}$ at 592 nm, $72,180 \text{ M}^{-1} \text{ cm}^{-1}$ at 623 nm), sharp absorption bands, and low emissions.

Chapter 4

Introduction

Efficient light-absorbers are useful for the applications as a wide variety of optical materials in biochemistry and biology. For example, for the construction of artificial photosynthesis systems, the light-absorbing molecules which have a large molar extinct coefficient are a key material as an energy receiver to improve conversion efficiency from light energy to the driving force of chemical reactions.¹ As another instance, the light-absorbing ability with the specific wavelength region is feasible for the regulation of photosynthesis. It is known as the Emerson enhancement effect that the photosynthesis in several types of algae can be enhanced by the light irradiation in the wavelength range around 650 nm.^{2,3} In contrast, the light over 690 nm can suppress the efficiency. These phenomena were observed in other plants.⁴ This fact suggests the scenario that by loading the efficient light absorbers to the light around 650 nm on the wall of green houses, the sunlight can be transformed to the light which has the suppression effect on weed growths. Thus, the lights with the specific wavelength region around 650 nm or over 690 nm are a valid tool for precisely controlling the plant growth.

Boron dipyrromethene (BODIPY) is well known as a fluorophore for biochemical and biotechnological usages.⁵ Because of strong emission intensity, low environmental dependency of optical properties and high stability to photo-degradation, BODIPY can be used as a conventional fluorophore for a marker or a labeling reagent under various situations. Nagano and Urano *et al.* reported the bioprobes based on the photochemistry of BODIPY.⁶ By regulating energy transfer involving the BODIPYs, they can monitor the bioreactions with the changes of emission intensity

from the probe with high sensitivity and specificity. Moreover, hetero ring-fused BODIPYs have been synthesized.⁷⁻⁹ In particular, thiophene-fused BODIPYs (Figure 1) were reported as a photosensitizer to generate singlet oxygen.¹⁰ By the modification with sulfur or iodine elements for receiving the heavy atom effect, the intersystem crossing after photo-excitation to these BODIPYs can be readily induced. Accordingly, the triplet-excited states of the BODIPYs efficiently generate the singlet oxygen via a sensitizing reaction. The superior ability of light absorbing contributes to enhancing the sensitizing efficiency. It should be mentioned that these BODIPYs have sharp spectra of light-absorption and emission from the red-light to the near-infrared region. Based on these optical properties of thiophene-fused BODIPYs, the author was inspired to develop an efficient light absorber without emission. In particular, the author aimed to develop new series of thiophene-fused BODIPYs to improve the light-absorption ability in the red-light region.

Herein, the author reports the synthesis and the efficient light-absorbing ability of the new series of thiophene-fused BODIPYs. The substituent effects of two distinct groups on the optical properties were examined to improve molar extinct coefficients and the peak position of absorption wavelengths. By employing the heavy atom effect of iodine, the evolution of the optical properties such as the position of absorption bands, the enhancement of absorption ability, and the suppression of the emission can be simultaneously achieved. Next, according to the data of the molecular orbital of the dye calculated by computer simulation, the author was inspired the introduction of the trifluoromethyl group into the thiophene-fused BODIPY. Finally, the selective

Chapter 4

light absorption in the red-light region was accomplished.

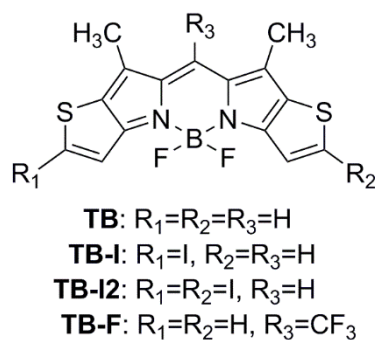
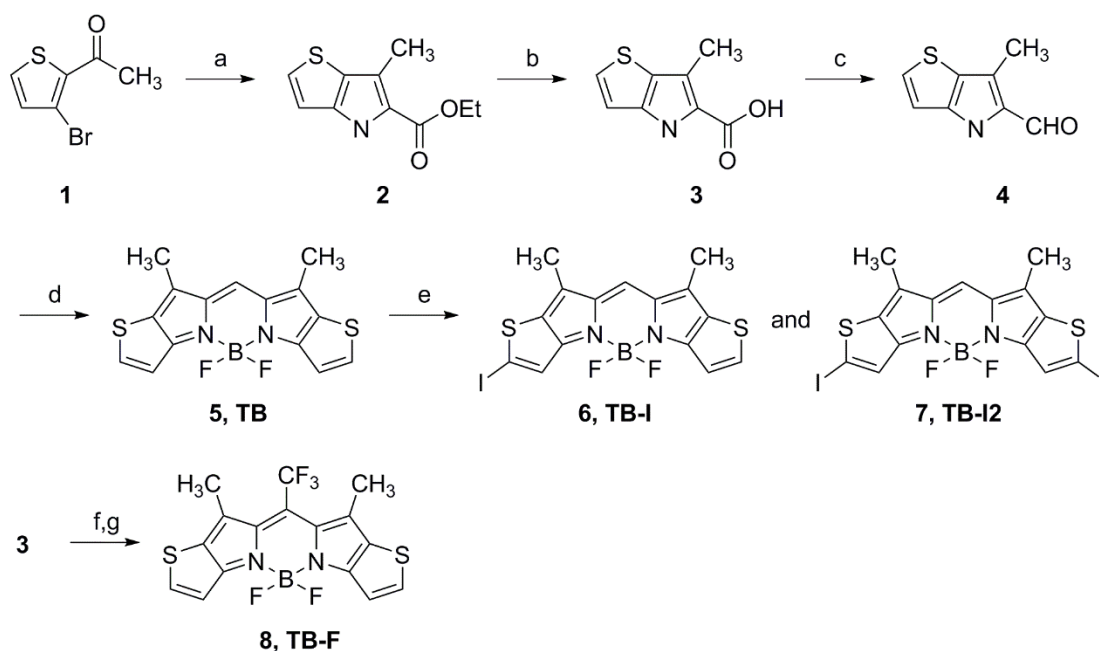


Figure 1. Chemical structures of the thiophene-fused BODIPYs used in this study.

Scheme 1. Synthetic outlines for thiophene-fused BODIPYs^a



^aReagents and conditions: (a) Ethyl cyanoacetate, CuI, Cs₂CO₃, DMSO, 50 °C, 4 h, 61%; (b) NaOH, H₂O, ethanol, reflux, 1 h, 95%; (c) i) trifluoroacetic acid, 50 °C, 20 min, ii) CH(OEt)₃ 50 °C, 30 min, 70%; (d) i) POCl₃, dichloromethane, r.t., 3 d, ii) triethylamine, BF₃·Et₂O, r.t., 2 d, 10%; (e) *N*-iodosuccinimide, acetic acid, chloroform, r.t., 24 h, 32% for **TB-I**, 23% for **TB-I2**; (f) i) trifluoroacetic acid, 40 °C, 40 min, ii) trifluoroacetic anhydride, 80 °C, 1 h; (g) BF₃·Et₂O, triethylamine, toluene, 80 °C, 2 h, 0.7% (in 2 steps).

Results and Discussion

The author designed the thiophene-fused BODIPYs as shown in Figure 1. The synthesis of **TB** derivatives is outlined in Scheme 1. Until the preparation of the precursors before the ligand formation, all reactions proceeded in good yields. Because of the instability of the aldehyde **4** and the ligand moiety before the introduction of boron, the reaction yields in the formation of boron complexes were relatively low. From the characterization with ^1H and ^{11}B NMR spectroscopies and mass measurements, the products have the expected structures. The dyes were obtained as colored solids with the solubility in conventional organic solvents such as chloroform and THF. During the measurements, the decomposition and photo-degradation were subtly observed.

The optical properties of **TB** were investigated. The absorption band was observed with the peak at 562 nm from UV-vis absorption measurement (Figure 2). The molar extinct coefficient exceeded $10^5 \text{ M}^{-1} \text{ cm}^{-1}$ (Table 1). These data mean that **TB** possesses the sharp and large absorption in the visible region. From the photoluminescence spectrum, although the emission band was obtained with the peak at 571 nm, the quantum yield of **TB** can be efficiently suppressed ($\Phi_{\text{F}} = 0.04$). The low emission intensity of **TB** should be originated from the fact that the decay of the excited state of **TB** should proceed via the triplet-excited state. Indeed, new emission bands with long lifetimes at the similar peak position and in the longer wavelength region than that of the emission at room temperature at 77 K assigned as a delayed fluorescence and phosphorescence, respectively. These data clearly indicate that **TB** is a promising seed compound for realizing expected optical properties such as sharp spectra, large molar extinct coefficients and low

emissions.

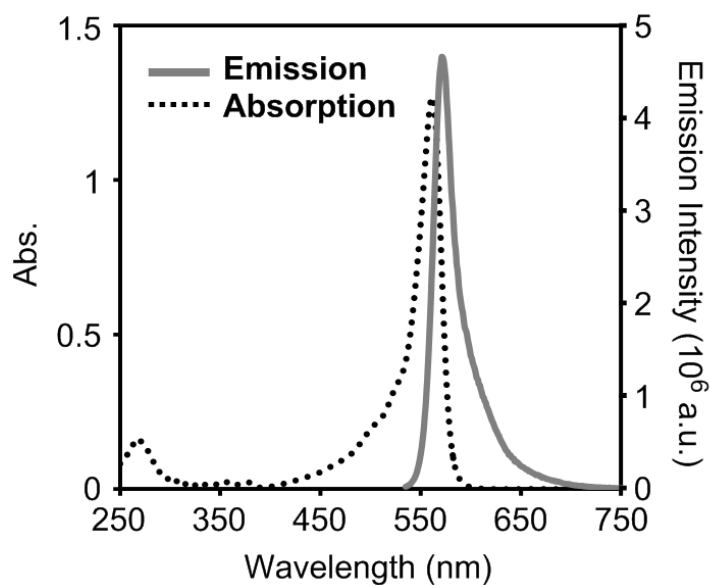


Figure 2. UV–vis absorption (10 μM) and photoluminescence spectra (1 μM) of **TB** in THF. The wavelength of the excitation light was at 530 nm.

Table 1. Optical properties of thiophene-fused BODIPYs

	$\lambda_{\text{max,abs}}$ [nm]	ϵ [$\text{M}^{-1}\text{cm}^{-1}$]	Φ_{F}^a
TB	562	127,000	0.04
TB-I	577	170,000	<0.01
TB-I2	592	184,000	<0.01
TB-F	623	72,200	<0.01

^aDetermined as an absolute value.

Next, for tuning the optical properties of **TB**, an iodide group was introduced via the heavy atom effect. To maximize the expression of the heavy atom effect, iodide groups were directly attached to the thiophene rings.¹¹ Figure 3 clearly represents that the absorption bands of **TB-I**s showed the bathochromic shifts than that of **TB**. By introducing a single iodide group, the peak positions were moved by 15 nm to the red-light region. These data can be supported by the results from computer calculations. The gap widths of the energy levels between the frontier orbitals were narrowed by increasing the number of the iodine substituents (Figure 4). Moreover, the molar extinct coefficients were enhanced by increasing the number of iodide groups. According to the previous report on the photophysical properties of iodinated BODIPY derivatives, these changes could be owing to the heavy atom effect.¹² Indeed, the iodinated **TB** derivatives hardly showed emissions ($\Phi_F < 0.01$). The heavy atom effect of iodine could contribute to inhibiting the fluorescence emission. In summary, the introduction of iodine into BODIPYs is valid for regulating the peak positions of absorption.

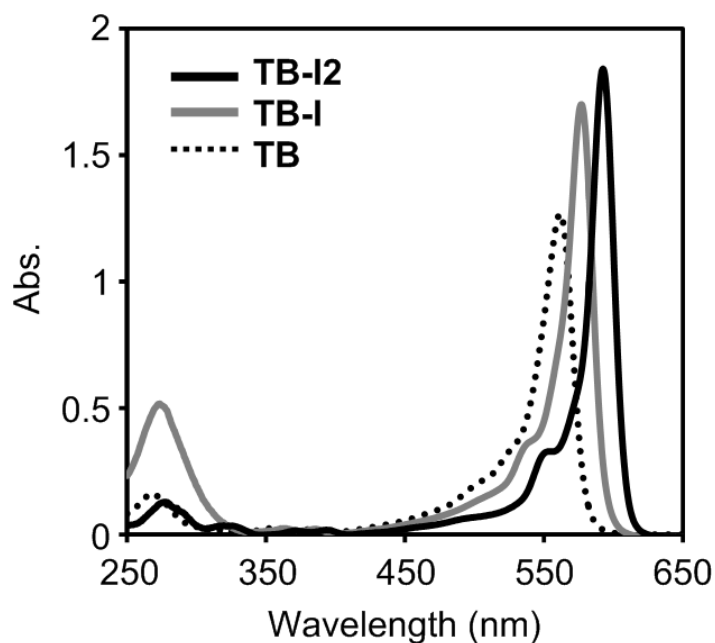


Figure 3. Absorption changes of **TB** by introducing iodine groups. The spectra were obtained from the solutions containing the dyes ($10 \mu\text{M}$) in THF.

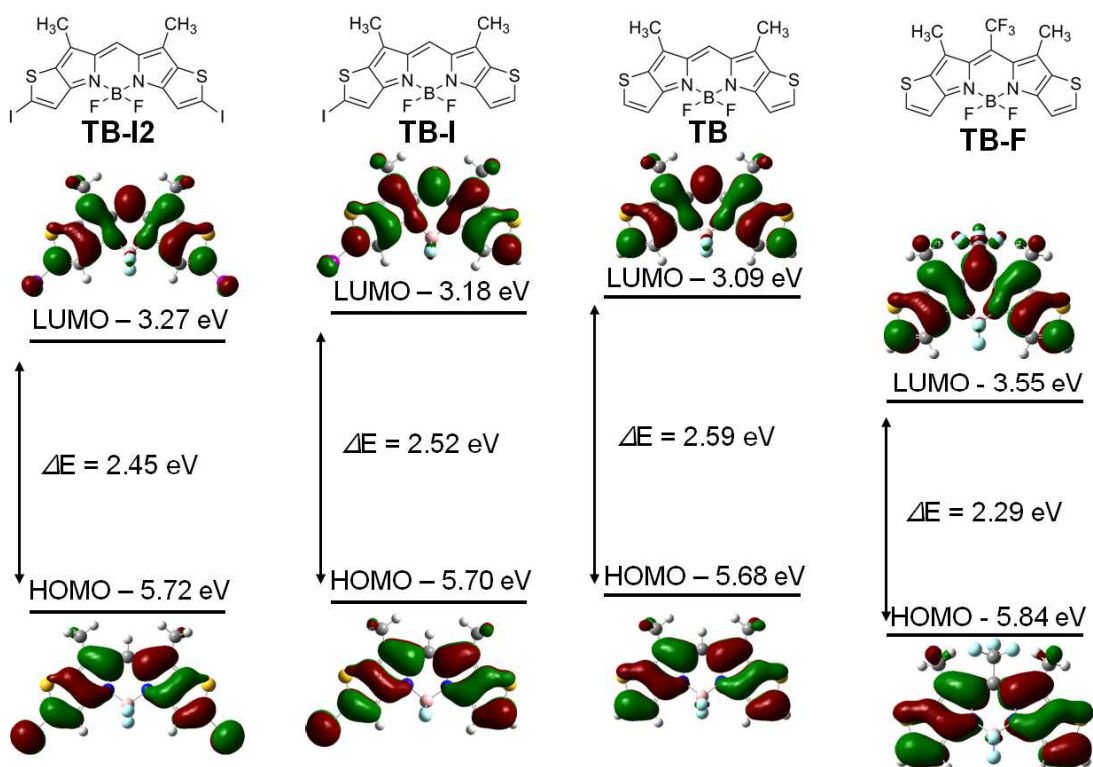


Figure 4. The changes in energy levels and shapes of frontier orbitals by introducing a trifluoromethyl group into the *meso*-position in **TB**. The DFT calculations were performed with a B3LYP/SVP method.

To explore another method for the modulation of the peak position of absorption wavelength, initially I carried out the density functional theory (DFT) calculation of **TB** with a B3LYP/SVP method. According to the computer modeling on the shape of the lowest unoccupied molecular orbital (LUMO) of **TB**, the localization of the orbital was found at the *meso*-position (Figure 4). Based on this result, the author designed the new dye, **TB-F**, having a trifluoromethyl group. The strong ability of electron withdrawing can lower the energy level of LUMO and decrease the gap width of the energy level between the frontier orbitals. Thus, it can be expected that drastic bathochromic shift of the absorption band should be received. The synthesis of **TB-F** was executed with similar procedures as other **TB** derivatives. Because of low stability of the intermediate before boron complexation, the reaction yield in the formation of the BODIPY ring was low. The desired compound was obtained as a solid, and it was confirmed that **TB-F** has enough solubility in conventional organic solvents such as chloroform and THF for the optical measurements. During the measurements, less decomposition and photo-degradation were also observed with **TB-F**.

Figure 5 presents the absorption spectrum of **TB-F**. As the author expected, **TB-F** showed the large absorption band at longer wavelength region by +60 nm than that of **TB** ($\lambda_{\max} = 623$ nm). Similarly as **TB**, the emission band was mainly obtained between 550 nm and 650 nm. This absorption wavelength is adequate for generating the light which can inhibit the photosynthesis.³ Furthermore, the emission was subtly obtained from **TB-F** ($\Phi_{\text{F}} < 0.01$). These data suggest that the efficient light absorbers for the red light can be prepared based on the thiophene-fused BODIPYs. In addition, these optical properties suggest another possibility for using the thiophene-

Chapter 4

fused BODIPYs as a quencher. Comparing to the conventional efficient absorbers called as QSY ($\epsilon_{\max} = 90,000 \text{ cm}^{-1}\text{M}^{-1}$)¹⁵ and BHQ ($\epsilon_{\max} = 35,600 \text{ cm}^{-1}\text{M}^{-1}$)¹⁶, the thiophene-fused BODIPYs have several advantages as a quencher besides of the intrinsic merits of BODIPY dyes. It should be emphasized that the molar extinct coefficients of the thiophene-fused BODIPYs are two or three times larger than those of the conventional absorbers.^{13,14} Thus, it can be said that the thiophene-fused BODIPYs are promised to be an efficient quencher on the biotechnological assays.¹⁵

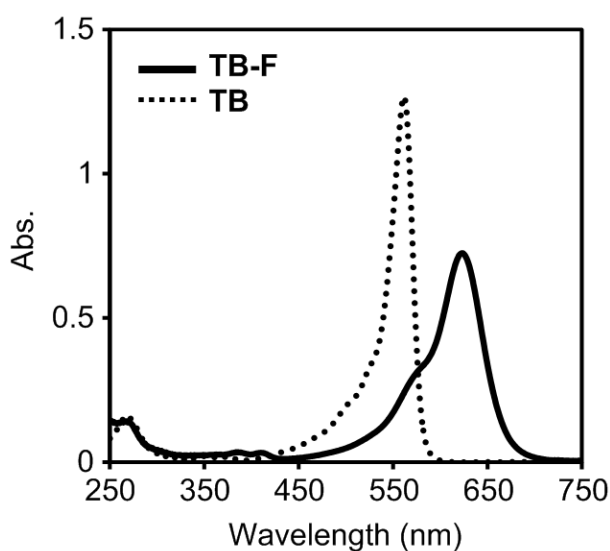


Figure 5. Absorption changes of **TB** by introducing a trifluoromethyl group. The spectra were obtained from the solutions containing the dyes ($10 \mu\text{M}$) in THF.

Conclusion

The author demonstrates the validity of the **TB** skeleton for the design of an efficient light absorber. The author established two manners for evolving the optical properties of **TB**: By employing the heavy atom effect, the peak positions can be shifted to the red-light region. The enhancement of molar extinct coefficients was also obtained. It was found that the introduction of the strong electron-withdrawing group at the *meso*-position in the BODIPY skeleton was responsible for the drastic bathochromic shift in the absorption spectrum. Finally, the author obtained the series of efficient light absorbers for the red light. These compounds have suitable optical properties for generating the light to control photosynthesis and plant growth. Furthermore, thiophene-fused BODIPYs with the efficient light-absorbing ability are promised to be applicable for efficient sensitizers. These materials and chemical modification methods for modulating the optical properties presented here could be versatile for developing efficient photo-responsive bio-related materials to control the biological activities and efficient quenchers on the biotechnological assays with labelled biomolecules.

Chapter 4

Experimental Section

General: ^1H (400 MHz), ^{13}C (100 MHz), and ^{11}B (128 MHz) NMR spectra were recorded on JEOL JNM-EX400 spectrometers. In the ^1H NMR and ^{13}C NMR spectra was used tetramethylsilane (TMS) as an internal standard in CDCl_3 , and ^{11}B NMR spectra were referenced externally to $\text{BF}_3\cdot\text{OEt}_2$ (sealed capillary). UV-vis absorption spectra were recorded on a SHIMADZU UV-3600 spectrophotometer. Fluorescence emission spectra and absolute quantum yields were recorded on a HORIBA JOBIN YVON Fluoromax-4P spectrofluorometer equipped with the integrating sphere. 2-Acetyl-3-bromothiophene (**1**) was purchased from Aldrich and used without further purification. Computations were performed using the Gaussian 03 suite of programs.¹⁶

Synthesis of 2: The synthesis was performed according to the previous report¹⁷: To the mixture containing **1** (8.62 g, 42.0 mmol), CuI (0.80 g, 4.20 mmol l), and CsCO_3 (34.2 g, 105 mmol) in DMSO (42 mL), ethyl isocyanoacetate (5.23 g, 46.2 mmol) was added dropwise at room temperature. After stirring at 50 °C for 4 h, the products were extracted with dichloromethane. The organic layer was washed with brine twice, dried over MgSO_4 and filtrated. The filtrate was condensed with evaporation, and the silica gel column chromatography with hexane as a mixture eluent (hexane : ethyl acetate = 7 : 1) gave **2** as a pale yellow solid (5.35 g, 25.6 mmol, 61 %). ^1H NMR (CDCl_3) δ : 8.88 (1H, s), 7.30 (1H, d, $J = 10.51$ Hz), 6.91 (1H, d, $J = 10.02$ Hz), 4.37 (2H, q, $J = 28.10$ Hz), 2.53 (3H, s), 1.40 (3H, t, $J = 24.19$ Hz). ^{13}C NMR (CDCl_3) δ : 162.3, 139.6, 129.1, 126.6, 123.2, 120.3, 111.42, 60.5, 14.7, 12.3. HRMS (ESI) m/z calcd. $[\text{M}+\text{H}]^+$: 210.0583, found:

210.0582.

Synthesis of 3: The mixture containing **2** (6.00 g, 28.7 mmol) and NaOH_{aq.} (17.2 g, 430 mmol in 120 mL) in 225 mL of ethanol was refluxed for 1 h. After cooling to room temperature, conc. HCl (10%) was added dropwise to acidify. The products were extracted with dichloromethane, and the organic layer was washed with brine, dried over MgSO₄ and filtrated. Evaporation of the filtrate yielded **3** as a dark purple solid (4.96 g, 27.3 mmol, 95 %). ¹H NMR (DMSO-*d*₆) δ: 12.44 (1H, s), 11.51 (1H, s), 7.46 (1H, d, *J* = 10.72 Hz), 6.92 (1H, d, *J* = 11.21 Hz), 2.40 (3H, s). ¹³C NMR (DMSO-*d*₃) δ: 162.8, 139.8, 128.5, 124.6, 123.1, 118.0, 112.0, 11.8. HRMS (ESI) *m/z* calcd [M-H]⁻: 180.0125, found: 180.0118.

Synthesis of 4: The solution of **3** (11.1 g, 61.2 mmol) dissolved in trifluoroacetic acid (200 mL) was stirred at 50 °C for 20 min, and then triethyl orthoformate (36.3 g, 245 mmol) was added. After stirring at 50 °C for 30 min, excess amounts of cyclopentyl methyl ether (CPME) and sat. NaHCO_{3aq.} were poured into the reaction solution. The organic layer was washed with brine and water, dried over MgSO₄, filtrated and condensed by evaporation. The silica gel column chromatography with the mixture eluent (hexane : ethyl acetate = 2 : 1) afforded **4** as a brown solid (7.11 g, 43.0 mmol, 70 %). Because of low stability, the compound **4** was used for the next step immediately after checking the spectrum of ¹H NMR. ¹H NMR (CDCl₃) δ: 9.75 (1H, s), 9.10 (1H, s), 7.44 (1H, d, *J* = 12.43 Hz), 6.94 (1H, d, *J* = 11.70 Hz), 2.54 (3H, s). HRMS (EI⁺) *m/z* calcd. [M]⁺: 165.0248, found: 165.0244.

Synthesis of 5 (TB): To the solution of **4** (7.11g, 43.0 mmol) in dichloromethane (215 mL), POCl₃

Chapter 4

(7.92 g, 51.7 mmol) was added dropwise at 0 °C. After stirring at room temperature for 3 days in the dark, triethylamine (30.0 mL, 215 mmol) was added dropwise at 0 °C. After stirring at 0 °C for 15 min, BF₃·Et₂O (38 mL, 308 mmol) was added dropwise, and then the mixture was stirred at room temperature for 2 days. The reaction was quenched by adding 100 mL of water, and the products were extracted with dichloromethane. The organic layer was washed with water twice and brine, dried over MgSO₄, filtrated, and condensed by evaporation. The residue was passed through the silica gel column with the mixture eluent (hexane : ethyl acetate = 3 : 1). The resulting product was dissolved in THF, and **5** was obtained as a red purple solid (0.684 g, 2.07 mmol, 10%) from the reprecipitation in methanol. ¹H NMR (CDCl₃) δ: 7.64 (2H, d, *J* = 10.26 Hz), 7.40 (1H, s), 7.11 (2H, d, *J* = 9.53 Hz), 2.47 (6H, s). ¹³C NMR (CDCl₃) δ: 158.5, 140.9, 139.9, 132.1, 131.8, 123.6, 114.0, 11.0. ¹¹B NMR (CDCl₃) δ: 0.39. HRMS (EI+) *m/z* calcd. [M]⁺: 332.0425, found: 332.0425.

Synthesis of 6(TB-I) and 7(TB-I): The mixture containing **5** (0.312 g, 0.934 mmol) and *N*-iodosuccinimide (0.210 g, 0.934 mmol) in chloroform (140 mL) and acetic acid (14 mL) was stirred at room temperature for 24 h in the dark under Ar atmosphere. Then, the reaction solution was washed with NaOH_{aq.} (2.5 M, 200 mL) twice, water, and brine, dried over MgSO₄, and filtrated. After evaporation, the products were suspended onto silica gel. **TB-I** (0.137 g, 32%) and **TB-I2** (0.129 g, 23%) were purified with the silica gel column chromatography with toluene as an eluent as a green silver and a black powder, respectively. Because of poor solubility of **TB-I** in conventional organic solvents, the clear spectrum of ¹³C NMR was not obtained. **TB-I**: ¹H NMR

(CDCl₃) δ : 7.68 (1H, d, J = 12.70 Hz), 7.42 (1H, s), 7.40 (1H, s), 7.09 (1H, d, J = 14.16 Hz), 2.43 (3H, s), 2.41 (3H, s). ¹¹B NMR (CDCl₃) δ : 0.293. HRMS (EI+) m/z calcd. [M]⁺: 457.9391, found: 457.9404. **TB-I2**: ¹H NMR (THF-*d*₈) δ : 7.85 (1H, s), 7.39 (2H, s), 2.42 (6H, s). ¹³C NMR (CDCl₃) δ : 157.3, 139.7, 135.6, 130.7, 125.6, 123.6, 95.4, 9.7. ¹¹B NMR (CDCl₃) δ : 0.195. HRMS (ESI) m/z calcd [M-H]⁻: 582.8285, found: 582.8292.

Synthesis of 8(TB-F): The mixture of **3** (1.0 g, 5.52 mmol) in trifluoroacetic acid (50 mL) was stirred at 40 °C for 40 min under Ar atmosphere, and then trifluoroacetic anhydride (2.29 mL, 16.6 mmol) was added dropwise to the reaction solution. After stirring at 80 °C for 1 h and cooling to room temperature, the deep blue solution was poured into the mixture with water (100 mL) and toluene (100 mL). After neutralization by adding NaHCO₃, the products were extracted with toluene. The organic layer was washed with sat. NaHCO₃aq., water, and brine, dried over MgSO₄, and filtrated. After evaporation, the crude products containing the aldehyde were used for the next step without further purification because of low stability. The residue was dissolved in 50 mL of toluene, and triethylamine (1.54 mL, 22.07 mmol) was added dropwise to the solution. After stirring at room temperature for 15 min, BF₃·Et₂O (2.72 mL, 22.1 mmol) was added dropwise. After stirring at room temperature for 10 min, the mixture was heated at 80 °C and stirred for 2 h. After quenching the reaction by adding water, the product was extracted with toluene. The organic layer was washed with brine twice, dried over MgSO₄, and filtrated. After evaporation, the silica gel column chromatography with the mixture eluent (toluene : ethyl acetate = 9 : 1) was performed. The resulting solid was dissolved in THF, and **TB-F** was obtained from the precipitation in

Chapter 4

methanol as a glossy green solid (7.2 mg, 0.7%). ^1H NMR (CDCl_3) δ : 7.67 (2H, d, $J = 16.57$ Hz), 7.05 (2H, d, $J = 16.32$ Hz). ^{13}C NMR (CDCl_3) δ : 159.1, 143.8, 138.1, 136.5, 133.4, 128.6, 122.3 (q, $J = 275$ Hz), 114.5, 15.4. ^{11}B NMR (CDCl_3) δ : 0.195. HRMS (EI+) m/z calcd. $[\text{M}]^+$: 400.0299, found: 400.0282.

References

1. Hagfeldt, A.; Boschloo, G.; Sun, L.; Kloo, L.; Pettersson, H. *Chem. Rev.* **2010**, *110*, 6595–6663.
2. Emerson, R.; Chalmers, R. V.; Cederstrand, C. N. *Proc. Natl. Acad. Sci. USA* **1957**, *43*, 133–143.
3. Dring, M. J.; Lüning, K. *Mar. Biol.* **1985**, *87*, 109–117.
4. Canaani, O.; Cahen, D.; Malkin, S. *FEBS Lett.* **1982**, *150*, 142–146.
5. (a) Ulrich, G.; Ziessel, R.; Harriman, A. *Angew. Chem. Int. Ed.* **2008**, *47*, 1184–1201. (b) Ziessel, R.; Ulrich, G.; Harriman, A. *New J. Chem.* **2007**, *31*, 496–501. (c) Bones, N.; Leen, V.; Dehaen, W. *Chem. Soc. Rev.* **2012**, *41*, 1130–1172.
6. (a) Kobayashi, T.; Komatsu, T.; Kamiya, M.; Campos, C.; González-Gaitán, M.; Terai, T.; Hanaoka, K.; Nagano, T.; Urano, Y. *J. Am. Chem. Soc.* **2012**, *134*, 11153–11160. (b) Komatsu, T.; Oshiki, D.; Takeda, A.; Miyamura, M.; Ueno, T.; Terai, T.; Hanaoka, K.; Urano, Y.; Mineno, T.; Nagano, T. *Chem. Commun.* **2011**, *47*, 10055–10057. (c) Komatsu, T.; Urano, Y.; Fujikawa, Y.; Kobayashi, T.; Kojima, H.; Terai, T.; Hanaoka, K.; Nagano, T. *Chem. Commun.*

- 2009, 7015–7017.
7. Umezawa, K.; Nakamura, Y.; Makino, H.; Citterio, D.; Suzuki, J. *J. Am. Chem. Soc.* **2008**, *130*, 1550–1551.
 8. Umezawa, K.; Matsui, A.; Nakamura, Y.; Citterio, D.; Suzuki, K. *Chem. Eur. J.* **2009**, *15*, 1096–1106.
 9. (a) Banfi, S.; Caruso, E.; Zaza, S.; Mancini, M.; Gariboldi, M. B.; Monti, E. *J. Photochem. Photobiol. B* **2012**, *114*, 52–60. (b) Chen, Y.; Zhao, J.; Xie, L.; Guo, H.; Li, Q. *RSC Adv.* **2012**, *2*, 3942–3953. (c) Bellier, Q.; Dailier, F.; Jeanneau, E.; Maury, O.; Andraud, C. *New J. Chem.* **2012**, *36*, 768–773. (d) Caruso, E.; Banfi, S.; Barbieri, P. Leva, B.; Orlandi, V. T. *J. Photochem. Photobiol. B* **2012**, *114*, 44–51. (e) Jiang, X.-D.; Zhang, H.; Zhang, Y.; Zhao, W. *Tetrahedron* **2012**, *68*, 9795–9801.
 10. Awuah, S. G.; Polreis, J.; Biradar, V.; You, Y. *Org. Lett.* **2011**, *13*, 3884–3887.
 11. Lim, S. H.; Thivierge, C.; Nowak-Sliwinska, P.; Han, J.; van den Bergh, H.; Wagnières, G.; Burgess, K.; Lee, H. B. *J. Med. Chem.* **2010**, *53*, 2865–2874.
 12. Adarsh, N.; Shanmugasundaram, M.; Avirah, R. R.; Ramaiah, D. *Chem. Eur. J.* **2012**, *18*, 12655–12662.
 13. Kabeláč, M.; Zimandl, F.; Fessler, T.; Chval, Z.; Lankaš, F. *Phys. Chem. Chem. Phys.* **2010**, *12*, 9677–90684.
 14. Johansson, H. E.; Johansson, M. K.; Wong, A. C.; Armstrong, E. S.; Peterson, E. J.; Grant, R. E.; Roy, M. A.; Reddington, M. V.; Cook, R. M. *Appl. Environ. Microbiol.* **2011**, *77*, 4223–

Chapter 4

4225.

15. Tyagi, S.; Kramer, F. R. *Nat. Biotechnol.* **1996**, *14*, 303–308.
16. Frisch, M. J.; Trucks, G. W.; Schlegel, H. B.; Scuseria, G. E.; Robb, M. A.; Cheeseman, J. R. ; Montgomery, J. A., Jr.; Vreven, T.; Kudin, K. N.; Burant, J. C.; Millam, J. M.; Iyengar, S. S.; Tomasi, J.; Barone, V.; Mennucci, B.; Cossi, M.; Scalmani, G.; Rega, N.; Petersson, G. A.; Nakatsuji, H.; Hada, M.; Ehara, M.; Toyota, K.; Fukuda, R.; Hasegawa, J.; Ishida, M.; Nakajima, T.; Honda, Y. ; Kitao, O.; Nakai, H.; Klene, M.; Li, X.; Knox, J. E.; Hratchian, H. P.; Cross, J. B.; Adamo, C.; Jaramillo, J.; Gomperts, R.; Stratmann, R. E.; Yazyev, O.; Austin, A. J.; Cammi, R.; Pomelli, C.; Ochterski, J. W.; Ayala, P. Y.; Morokuma, K.; Voth, G. A.; Salvador, P.; Dannenberg, J. J.; Zakrzewski, V. G.; Dapprich, S.; Daniels, A. D.; Strain, M. C.; Farkas, O.; Malick, D. K.; Rabuck, A. D.; Raghavachari, K.; Foresman, J. B.; Ortiz, J. V.; Cui, Q.; Baboul, A. G.; Clifford, S.; Cioslowski, J.; Stefanov, B. B.; Liu, G.; Liashenko, A.; Piskorz, P.; Komaromi, I.; Martin, R. L.; Fox, D. J.; Keith, T.; Al-Laham, M. A.; Peng, C. Y.; Nanayakkara, A.; Challacombe, M.; Gill, P. M. W.; Johnson, B.; Chen, W.; Wong, M. W.; Gonzalez, C.; Pople, J. A. Gaussian 03, revision D.01; Gaussian, Inc.: Wallingford CT, **2004**.
17. Cai, Q.; Li, Z.; Wei, J.; Ha, C.; Pei, D.; Ding, K. *Chem. Commun.* **2009**, 7581–7583.

Chapter 5

Synthesis of Furan-Substituted Aza-BODIPYs

Having Strong Near-Infrared Emission

ABSTRACT: Near-infrared (NIR) emissive aza-boron dipyrromethene (aza-BODIPY) was synthesized. To realize strong NIR emission, the furanyl groups were introduced into the aza-BODIPY structure. The synthesized compound showed the emission band with the peak at 735 nm. Comparing to the well-known aza-BODIPY, the emission band was found in the longer wavelength region by 70 nm. The quantum yield of the product was similar to the conventional aza-BODIPY.

Chapter 5

Introduction

NIR-emissive materials are attractive for various applications such as telecommunication, laser, organic light emitting diodes, biological systems, etc.¹ Therefore, the development of highly emissive NIR materials have been strongly required.

Boron dipyrromethenes (BODIPYs) are well known to be one of beneficial light-emitting dyes because they have various advantages such as large absorption and luminescent abilities in the narrow wavelength regions, high photo-stability, and environment-resistant emissive properties.² It is easy to modify BODIPYs by the introduction of substituents to its core structure. The emission color of BODIPYs can be tuned by modification. It was reported that aza-BODIPYs having nitrogen atoms on the *meso*-position instead of methylene bridge showed emission in longer wavelength region than common BODIPYs because of low-lying LUMO energy level.³ One of the most famous aza-BODIPYs is tetraphenyl aza-BODIPY (**TPAB**) which show emission in the red region with high quantum yield (Figure 1). Recently, thiophene-substituted aza-BODIPYs were reported (Figure 1).⁴ These BODIPYs showed emission in much longer wavelength regions than **TPAB**. These results could be derived from less steric hindrance and electron-donating properties. However, the quantum yields of these thiophene-substituted aza-BODIPYs were low. These results were supposed to be derived from heavy atom effect of sulfur atoms.

Herein, the author designed the new aza-BODIPY to obtain NIR emission with high quantum yields. To avoid heavy atom effect, furan was chosen as the substituents instead of the thiophene or phenyl groups. Furan has five-membered ring and works as a donor unit. Therefore, introducing

of furan should be effective to realize strong NIR emission. For this purpose, two furanyl groups having aza-BODIPY **5** (Figure 2) was synthesized.

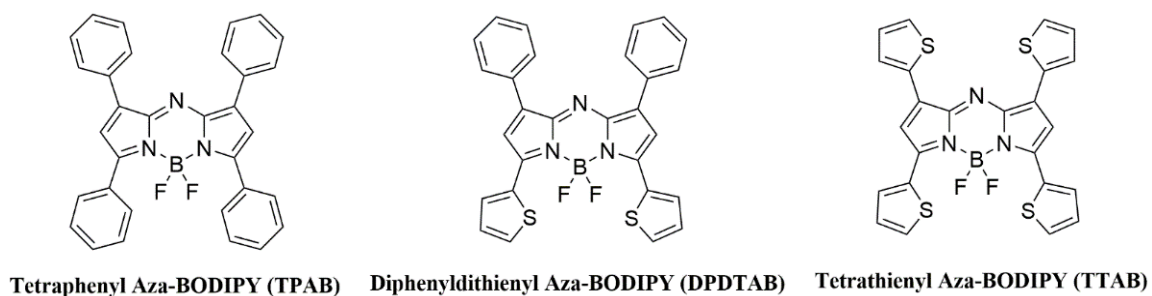


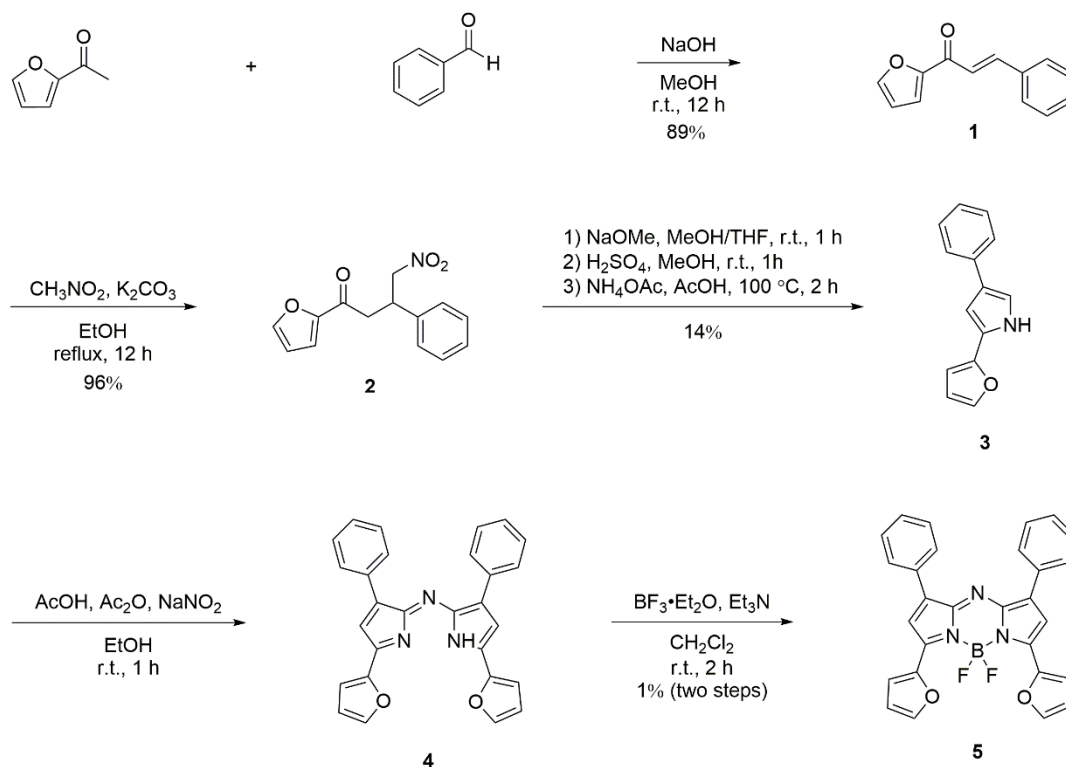
Figure 1. Structures of tetraphenyl Aza-BODIPY, diphenyldithienyl Aza-BODIPY and tetrathienyl Aza-BODIPY.



Figure 2. Structure of Aza-BODIPY **5**

Results and Discussion

The synthetic route of furan-substituted aza-BODIPY is outlined in Scheme 1. The products showed good solubility in the common organic solvents such as chloroform, THF, and ethanol. The structures of all compounds were confirmed by ^1H and ^{11}B NMR spectroscopies and ionization mass measurements (Figures 3 and 4).

Scheme 1. Synthetic routes for **5**

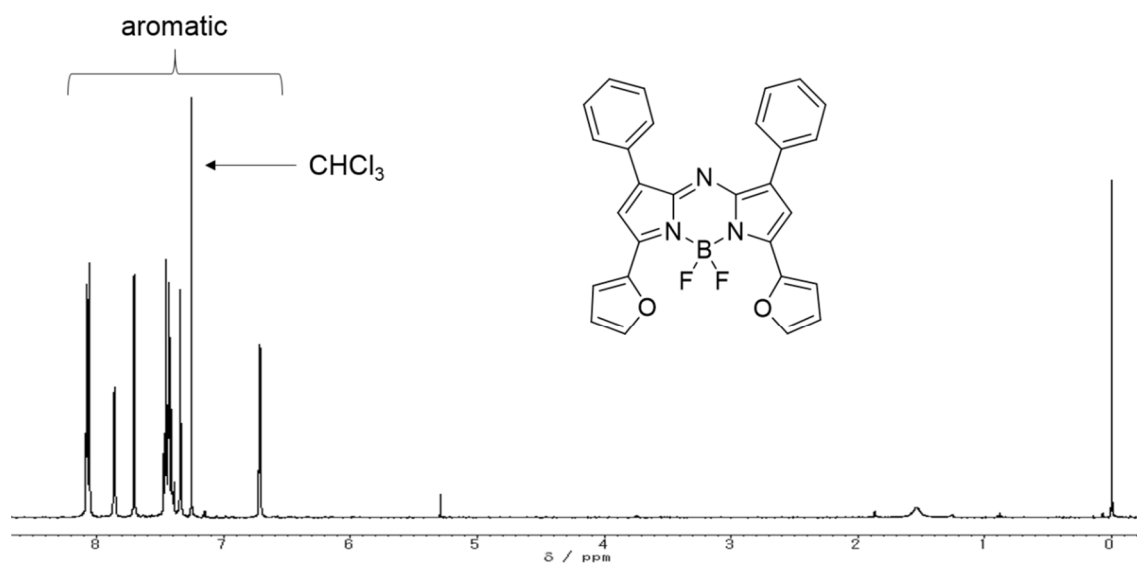


Figure 3. ^1H NMR spectrum of **5** in CDCl_3 .

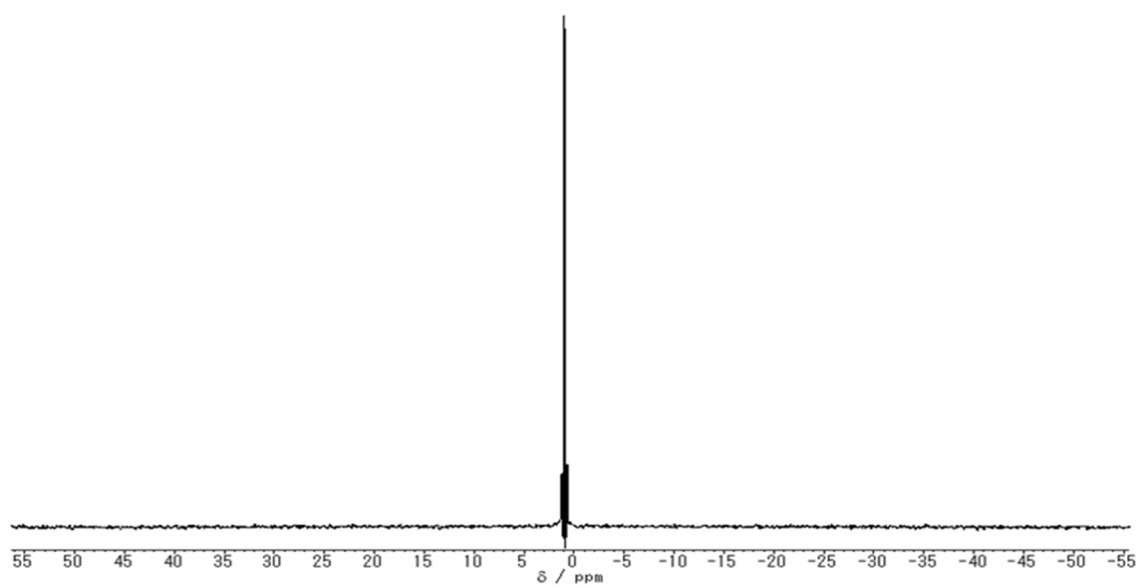


Figure 4. ^{11}B NMR spectrum of **5** in CDCl_3 .

Chapter 5

To receive information on the electronic states of the synthesized compounds, the computer calculations were performed (Figure 5). The author optimized the geometries of aza-BODIPYs by the density functional theory (DFT). Compared to **TPAB** which has four phenyl groups on its aza-BODIPY core, the steric hindrance was reduced in **5** which has two furanyl groups at the lower side of aza-BODIPY core. Accordingly, the expansion of conjugation with the decrease of band gap energy was proposed. Therefore, **5** was expected to show absorption and emission bands in longer wavelength regions than **TPAB**.

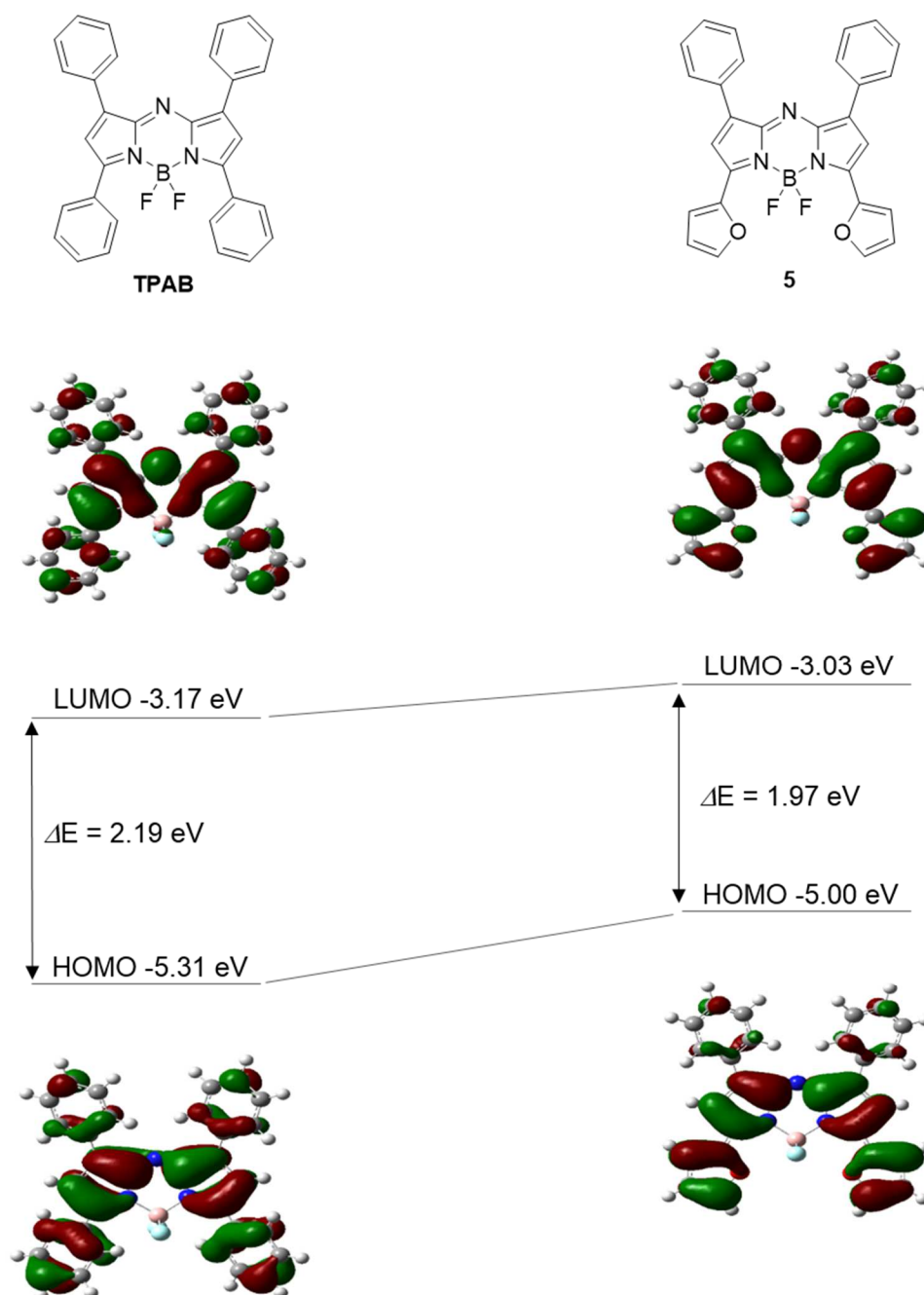


Figure 5. Structures and molecular orbital diagrams for LUMO and HOMO of **5** and **TPAB** calculated with DFT (B3LYP/6-31G(d)//B3LYP/6-31G(d)).

Chapter 5

The UV–vis absorption and photoluminescence (PL) properties of **5** and **TPAB** are presented in Table 1. Figure 6 shows the absorption spectra of aza-BODIPYs in chloroform solution (1.0×10^{-5} mol/L). **5** showed sharp absorption band with the peak at 722 nm, and molar extinction coefficient was very large ($\epsilon = 130,000 \text{ M}^{-1}\text{cm}^{-1}$). The absorption of **5** was in the NIR region. On the other hand, the absorption band of **TPAB** was observed in shorter wavelength region than **5**. These data indicate that more effective expansion of conjugation can occur in **5** than **TPAB**. It is implied that the furanyl groups could have less steric hindrance compared with 6-membered rings such as phenyl groups. Therefore, the bandgap energy of **5** decreased from **TPAB**, and red-shifted absorption band was observed.

Figure 7 shows the emission spectra of **5** and **TPAB** in chloroform solution (1.0×10^{-6} mol/L). **5** showed red-shifted emission band compared with **TPAB**. Although the emission band of **TPAB** was still in the visible region, the emission band of **5** was observed in the NIR region with the peak at 735 nm. Moreover, the quantum yields of both aza-BODIPYs were similar value. In the previous reports⁴, thiophene-substituted aza-BODIPYs have much lower quantum yields than **TPAB** because sulfur atoms of thiophene caused heavy atom effect. Furan-substituted aza-BODIPY **5** is composed without heavy atoms. Therefore, the quantum yield of **5** should be maintained.

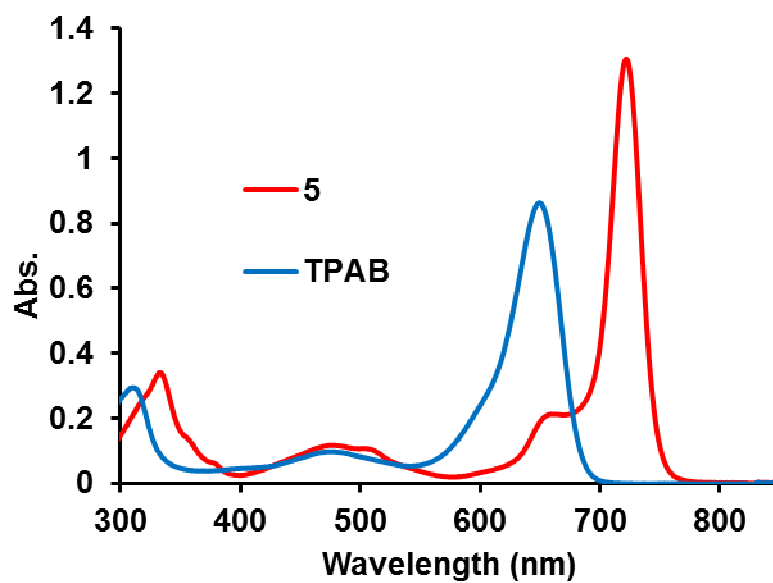


Figure 6. UV-vis-NIR absorption spectra of **5** and **TPAB** in CHCl_3 (1×10^{-5} M).

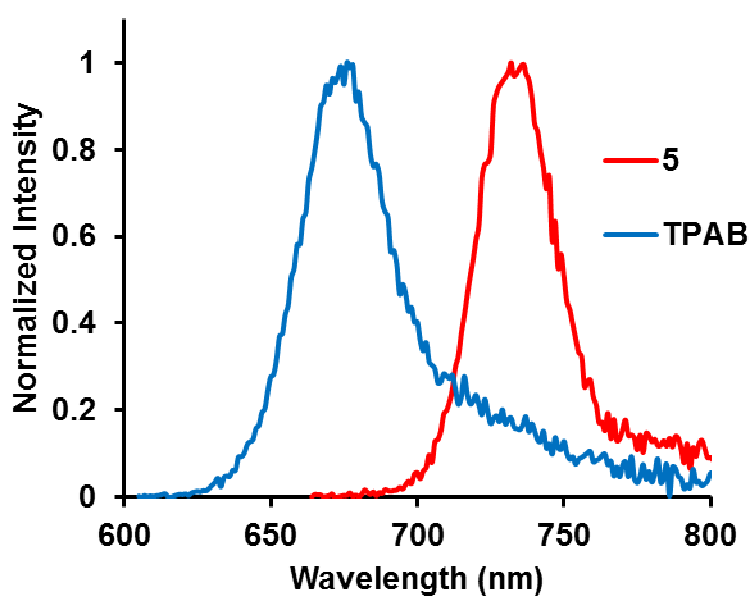


Figure 7. Photoluminescence spectra of **5** and **TPAB** in CHCl_3 (1×10^{-6} M).

Table 1. UV–vis–NIR absorption and photoluminescence data for **5** and **TPAB** in CHCl₃.

	$\lambda_{\text{abs.}}$ (nm) ^a	ϵ (M ⁻¹ cm ⁻¹)	λ_{PL} (nm) ^{b, c}	Φ_{PL} ^d
5	722	130,000	735	0.87
TPAB	649	86,000	676	0.77

^a Measured in CHCl₃ (1.0 × 10⁻⁵ M). ^b Measured in CHCl₃ (1.0 × 10⁻⁶ M). ^c **5** and **TPAB** were excited at 659 nm, 600 nm, respectively. ^d Reported **TPAB** ($\Phi_{\text{PL}} = 0.77$, in ortho-xylene) was used as a standard.³

Conclusion

Furan-substituted aza-BODIPY with strong and sharp NIR emission was developed. Compound **5** showed strong emission band in near-infrared region with the peak at 735 nm and similar quantum yield with **TPAB**. These results were derived from introducing furanyl groups which have a heavy-atom free structure and less steric hindrance. From these results, introduction of furanyl groups could be an effective strategy to obtain strong emission in the NIR region with aza-BODIPYs.

Experimental Section

General: ^1H (400 MHz) and ^{11}B (128 MHz) NMR spectra were recorded on a JEOL JNM EX400 spectrometer. ^1H NMR used tetramethylsilane (TMS) as an internal standard in CDCl_3 , and ^{11}B NMR spectra were referenced externally to $\text{BF}_3 \cdot \text{OEt}_2$ (sealed capillary). Analytical thin-layer chromatography (TLC) was performed with silica gel 60 Merck F254 plates. Column chromatography was performed with Wakogel C-300 silica gel. UV–vis–NIR absorption spectra were recorded on a SHIMADZU UV-3600 spectrophotometer, fluorescence emission spectra were measured on a HORIBA JOBIN YVON Fluoromax-4P spectrofluorometer.

Computational Details: The Gaussian 09 program package⁵ was used for computations of the compounds. The optimized structures was obtained by DFT calculation at the B3LYP/6-31G(d) level of theory.

Synthesis of 1: **1** was prepared according to the previous report.⁶ 2-Acetylfuran (4.6 mL, 45 mmol) was dissolved in methanol (300 mL). To the solution, benzaldehyde (4.6 mL, 45 mmol) followed by 5% aqueous NaOH solution (45 mL) was added. The reaction mixture was kept in stirred condition at room temperature for 12 h. Water (200 mL) was poured into the reaction mixture and the precipitated solid was filtered and washed with water (200 mL) to yield a white solid (7.8 g, 89%). ^1H NMR (CDCl_3) : 7.89 (1H, d, $J = 15.9$ Hz), 7.67–7.64 (3H, m), 7.48–7.40 (4H, m), 7.36–7.31 (1H, m), 6.60 (1H, dd, $J = 3.7, 1.72$ Hz).

Synthesis of 2: A mixture of **1** (1 g, 5 mmol), nitromethane (14 mL, 25 mmol), and K_2CO_3 (14 mg, 1.1 mmol) in ethanol (10 mL) was heated to reflux for 12 h. After cooling to room temperature,

Chapter 5

the solvent was removed by a rotary evaporator, and the oily residue was dissolved in CH_2Cl_2 and washed with water. The combined organic layers were washed with brine, dried over magnesium sulfate and concentrated to give the target compounds as a dark brown oily residue (1.3 g, 96%).

The obtained **2** was used for the next reaction without purification. ^1H NMR (CDCl_3) : 7.57–7.55 (1H, m), 7.34–7.24 (5H, m), 7.18 (1H, dd, $J = 3.6, 0.7$ Hz), 6.52 (1H, m), 4.80 (1H, dd, $J = 13.0, 6.6$ Hz), 4.69 (1H, dd, $J = 13.0, 8.0$ Hz), 4.22–4.14 (1H, m), 3.38–3.24 (2H, m)

Synthesis of 3: **2** (1.3 g, 4.9 mmol) was dissolved in THF (25 mL) and methanol (50 mL) at room temperature, and NaOMe (1.3 g, 24 mmol) was added into the mixture. After 1 h the mixture was added dropwise to a solution of H_2SO_4 (15 mL) in methanol (50 mL) at 0 °C, following the solution was allowed to warm to room temperature and stirred for further 1 h. The resulting mixture was poured into water and ice (350 mL), and the solution was neutralized with aqueous 4 M NaOH. Then, the products were extracted with CH_2Cl_2 . The combined extracts were washed with water and brine and dried over magnesium sulfate. The solvent was removed by a rotary evaporator to provide acetal compound as an oil, which was used in the next stage without further purification. The oil was treated with acetic acid (24 mL) and NH_4OAc (0.96 g, 12 mmol), and the resulting solution was heated at 100 °C for 2 h. The reaction mixture was cooled to room temperature and poured into water and ice (100 mL) and carefully neutralized with aqueous 4 M NaOH. The resulting precipitate was collected by filtration and was dissolved in THF again. After drying over magnesium sulfate, the solvent was removed by a rotary evaporator to provide black solid. The residue was purified by column chromatography on silica with hexane/ CH_2Cl_2 (2/3) as an eluent

(138 mg, 14%). ^1H NMR (CDCl_3): 8.54 (1H, bs), 7.55 (2H, m), 7.38–7.33 (1H, m), 7.21–7.18 (1H, m), 7.10–7.09 (1H, m), 6.74–6.73 (1H, m), 6.46–6.44 (1H, m), 6.41–6.40 (1H, m) HRMS (APCI) calcd. for $\text{C}_{14}\text{H}_{11}\text{NO}$ [$\text{M}+\text{H}$]: 210.0913, found 210.0910.

Synthesis of 4: 3 (0.53 g, 2.53 mmol) was dissolved in ethanol (3.8 mL), acetic acid (0.96 mL) and acetic anhydride (0.39 mL). NaNO_2 (87 mg, 1.3 mmol) dissolved in H_2O (0.4 mL) was added into the mixture. The solution was stirred for 1 h. The resulting solution was extracted with CH_2Cl_2 and washed with water. After drying over magnesium sulfate, the solution was concentrated to give the target compounds as a dark blue solid. The residue was purified by flash column chromatography on silica with CH_2Cl_2 (103 mg, 19%). ^1H NMR (CDCl_3): 8.04 (2H, d, $J = 7.3$ Hz), 7.67 (1H, d, $J = 1.4$ Hz), 7.42–7.35 (3H, m), 7.09 (1H, s), 7.05 (1H, d, $J = 3.4$ Hz), 6.64 (1H, dd, $J = 3.5, 1.8$ Hz). HRMS (APCI) calcd. for $\text{C}_{28}\text{H}_{20}\text{N}_3\text{O}_2$ [$\text{M}+\text{H}$]: 430.1550, found 430.1539.

Synthesis of 5: 4 (0.43 g, 1 mmol) was dissolved in dry CH_2Cl_2 (35 mL). Triethylamine (1.5 mL) was added to the reaction mixture, and the resulting mixture was stirred under nitrogen atmosphere at room temperature for 15 min. Then $\text{BF}_3 \cdot \text{OEt}_2$ (1.9 mL) was added, and the mixture was stirred under nitrogen atmosphere at room temperature for 2 h. The resulting solution was extracted with CH_2Cl_2 and washed with water. After drying over magnesium sulfate, the solution was concentrated to give the target compounds as a dark green solid. The solid was purified by column chromatography on silica with hexane/ CH_2Cl_2 (1/3) as an eluent and dissolved in small amount of THF, and the product was reprecipitated from methanol to give pure **5** as a brown solid (32 mg, 6.7%). ^1H NMR (CDCl_3): 8.08–8.05 (2H, m), 7.86 (1H, d, $J = 3.6$ Hz), 7.71 (1H, d, $J = 1.7$ Hz),

Chapter 5

7.48–7.38 (3H, m), 7.34 (1H, s), 6.72 (1H, dd, $J = 3.7, 1.7$ Hz). HRMS (APCI) calcd. for $C_{28}H_{19}BF_2N_3O_2$ [M+H]: 478.1533, found 478.1531.

References

1. (a) Fabian, J.; Nakazumi, H.; Matsuoka, M. *Chem. Rev.* **1992**, *92*, 1197–1226. (b) Kiyose, K.; Kojima, H.; Nagano, T. *Chem. Asian J.* **2008**, *3*, 506–515. (c) Qian, G.; Wang, Z. Y. *Chem. Asian J.* **2010**, *5*, 1006–1029.
2. (a) Loudet, A.; Burgess, K. *Chem. Rev.* **2007**, *107*, 4891–4932. (b) Ulrich, G.; Ziesel, R.; Harriman, A. *Angew. Chem. Int. Ed.* **2008**, *47*, 1184–1201. (c) Ziesel, R.; Ulrich, G.; Harriman, A. *New J. Chem.* **2007**, *31*, 469–501. (d) Bones, N.; Leen, V.; Dehaen, W. *Chem. Soc. Rev.* **2012**, *41*, 1130–1172.
3. (a) Gorman, A.; Killoran, J.; O'Shea, C.; Kenna, T.; Gallagher, W. M.; O'Shea, D. F. *J. Am. Chem. Soc.* **2004**, *126*, 10619–10631. (b) Loudet, A.; Bandichhor, R.; Wu, L.; Burgess, K. *Tetrahedron* **2008**, *64*, 3642–3654. (c) Ge, Y.; O'Shea, D. F. *Chem. Soc. Rev.* **2016**, *45*, 3846–3864.
4. (a) Gresser, R.; Hartmann, H.; Wrackmeyer, M.; Leo, K.; Riede, M. *Tetrahedron* **2011**, *67*, 7148–7155. (b) Zhang, X.; Yu, H.; Xiao, Y. *J. Org. Chem.* **2012**, *77*, 669–673.
5. Gaussian 09, Revision A.1, Frisch, M. J.; Trucks, G. W.; Schlegel, H. B.; Scuseria, G. E.; Robb, M. A.; Cheeseman, J. R.; Scalmani, G.; Barone, V.; Mennucci, B.; Petersson, G. A.; Nakatsuji, H.; Caricato, M.; Li, X.; Hratchian, H. P.; Izmaylov, A. F.; Bloino, J.; Zheng, G.;

- Sonnenberg, J. L.; Hada, M.; Ehara, M.; Toyota, K.; Fukuda, R.; Hasegawa, J.; Ishida, M.; Nakajima, T.; Honda, Y.; Kitao, O.; Nakai, H.; Vreven, T.; Montgomery, Jr., J. A.; Peralta, J. E.; Ogliaro, F.; Bearpark, M.; Heyd, J. J.; Brothers, E.; Kudin, K. N.; Staroverov, V. N.; Kobayashi, R.; Normand, J.; Raghavachari, K.; Rendell, A.; Burant, J. C.; Iyengar, S. S.; Tomasi, J.; Cossi, M.; Rega, N.; Millam, J. M.; Klene, M.; Knox, J. E.; Cross, J. B.; Bakken, V.; Adamo, C.; Jaramillo, J.; Gomperts, R.; Stratmann, R. E.; Yazyev, O.; Austin, A. J.; Cammi, R.; Pomelli, C.; Ochterski, J. W.; Martin, R. L.; Morokuma, K.; Zakrzewski, V. G.; Voth, G. A.; Salvador, P.; Dannenberg, J. J.; Dapprich, S.; Daniels, A. D.; Farkas, Ö.; Foresman, J. B.; Ortiz, J. V.; Cioslowski, J.; Fox, D. J. Gaussian, Inc., Wallingford CT, **2009**.
6. Budhiraja, A.; Kadian, K.; Kaur, M.; Aggarwal, V.; Garg, A.; Sapra, S.; Nepali, K.; Suri, O. P.; Dhar, K. L. *Med. Chem. Res.* **2011**, *21*, 2133–2138.

Chapter 6

Synthesis of the Near-Infrared Light-Absorbing Polymer Based On Thiophene-substituted Aza-BODIPY

ABSTRACT: The strong near-infrared (NIR) light-absorbing conjugated polymer was synthesized based on thiophene-substituted aza-BODIPY. From the optical measurements, it was revealed that the polymer showed the strong absorption band in the deep NIR region with the peak at 864 nm. The cyclic voltammetry (CV) analyses were performed to obtain information on HOMO and LUMO energy levels. The polymer had deep LUMO level (-4.01 eV), and this LUMO level was similar to the monomer.

Chapter 6

Introduction

Near-infrared (NIR) light absorbing materials are useful for various application such as photovoltaics, biological systems, and so on.¹ Aza-BODIPYs which have nitrogen atom on their *meso*-position in the BODIPY structure are candidate for NIR dyes because they have absorption and emission in the long wavelength region.² Recently, thiophene-substituted aza-BODIPYs were reported, and they showed NIR absorption and emission.³ The author also reported furan-substituted aza-BODIPY which showed strong NIR emission in chapter 5.

To achieve deep NIR absorption by aza-BODIPYs, the extension of π -conjugation should be the effective method. Chujo *et al.* reported the conjugated polymers containing aza-BODIPYS in their main chain, and those polymers showed deeply red-shifted absorption and emission bands from their monomers.⁴ In this report^{4a}, it was revealed that conjugation can be expanded more effectively by introducing comonomers at the bottom phenyl group. Moreover, several groups reported the conjugated oligomers in which thiophene-substituted aza-BODIPYs were connected to π -conjugated unit by the Pd-catalyzed coupling reaction.⁵

In this chapter, the conjugated polymer including thiophene-substituted aza-BODIPY as main-chain unit was designed and synthesized. The aza-BODIPY monomer for this polymer had four thiophenes on aza-BODIPY core and two bromines at bottom thiophenes. The polymerization was performed via the Pd-catalyzed Suzuki–Miyaura coupling reaction. The polymer showed the much red-shifted absorption band compared to that of the monomer. The peak in the absorption spectrum was at 864 nm in the THF solution, and the absorption range reached to more than 1000 nm.

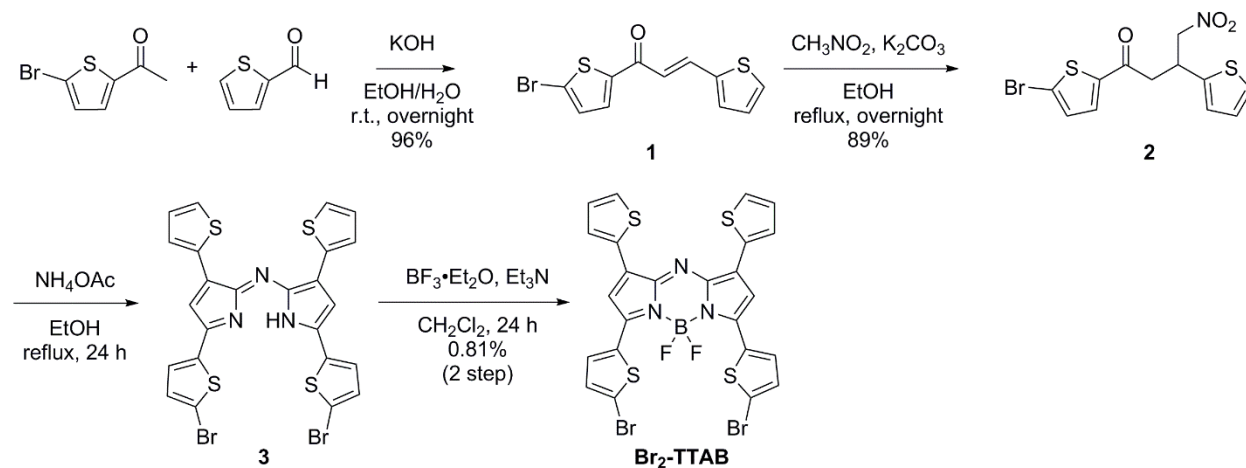
Results and Discussion

The synthetic route of the thiophene-substituted aza-BODIPY monomer (**Br₂-TTAB**) is outlined in Scheme 1. **1** and **2** were produced quantitatively. However, during the reaction for **3**, bromine atoms were removed easily. Since it was difficult to isolate **3**, purification was performed after complexation of boron to obtain the dibromide monomer **Br₂-TTAB**.

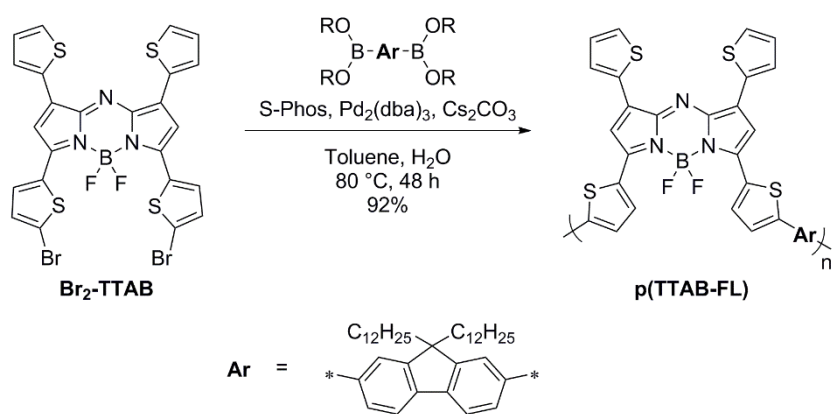
The polymerization of the dibromo monomer (**Br₂-TTAB**) with the fluorene copolymer was accomplished by the Pd-catalyzed Suzuki–Miyaura coupling reaction (Scheme 2). The polymer properties were determined from the GPC analysis toward polystyrene standards in THF ($M_n = 1,500$, $M_w/M_n = 3.4$).

Chapter 6

Scheme 1. Synthetic routes for the BODIPYs dibromide aza-BODIPY



Scheme 2. Synthetic route for the aza-BODIPY polymer



The optical properties of the synthesized polymers were investigated. Tetrathienyl aza-BODIPY (**TTAB**, Figure 1a) and the monomer (**Br₂-TTAB**) were also analyzed for the comparison. **TTAB** was prepared according to the previous reports.³ Figure 1b shows the UV–vis absorption spectra in THF (1.0×10^{-5} mol/L). Both **TTAB** and **Br₂-TTAB** showed strong and sharp absorption bands around 750 nm derived from $S_0 \rightarrow S_1$ ($\pi \rightarrow \pi^*$) transition. The absorption of polymer **p(TTAB-FL)** was observed at longer wavelength region than **TTAB** and **Br₂-TTAB**. Strong $S_0 \rightarrow S_1$ ($\pi \rightarrow \pi^*$) transition was observed in the NIR region with the peak at 864 nm. The peak wavelength was shifted over 100 nm compared to that of the monomer. This result indicates that conjugation should be expanded by the introduction of the fluorene copolymer.

Next, the photoluminescence (PL) properties of products were measured. However, **p(TTAB-FL)** showed almost no emission. **TTAB** and **Br₂-TTAB** showed PL spectra with low quantum yields. These results should be induced by heavy atom effect according to the previous report.³

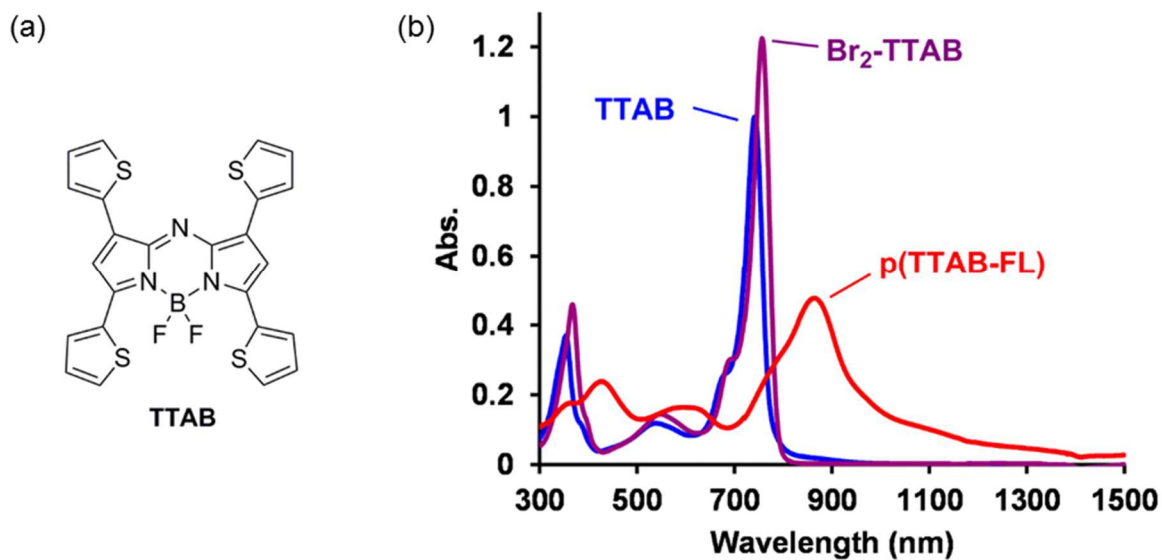


Figure 1. (a) Structure of Aza-BODIPY **TTAB**; (b) UV-vis-NIR absorption spectra of the products in THF (1×10^{-5} M).

Table 1. Optical properties of the compounds^a

	λ_{abs} (nm)	ϵ ($\text{M}^{-1}\text{cm}^{-1}$) ^b
TTAB	741	100,000
$\text{Br}_2\text{-TTAB}$	756	120,000
p(TTAB-FL)	864	48,000

^aMeasured in chloroform (1.0×10^{-5} M). ^bMolar absorption coefficients of the absorption maxima.

To investigate the electronic states, the cyclic voltammetry (CV) analyses were performed. Figure 2 shows cyclic voltammograms of the synthetic products. All three compounds showed two reduction peaks. These results indicate that these BODIPY compounds can easily receive electron. Next, the LUMO energy levels were estimated from the onsets of the first reduction waves by empirical formula.⁶ Their HOMO energy levels were calculated with the LUMO energy levels and optical energy band gaps (E_g^{opt}) of the corresponding compounds (Table 2). The LUMO energy level of the polymer was very similar to the monomer and **TTAB**. However, E_g^{opt} of polymer was smaller than that of the monomer. Therefore, the HOMO energy level was elevated by the expansion of conjugation after polymerization.

Table 2. UV–vis absorption and electrochemical properties of the products.

	$\lambda_{\text{abs.}} \text{ (nm)}^a$	optical band gap ($E_{\text{g}}^{\text{opt}}$)/eV ^b	$E_{\text{red.}}/\text{V}^{c,d}$	HOMO/eV ^e	LUMO/eV ^f
TTAB	741	1.61	−0.76	−5.65	−4.04
Br₂[−]TTAB	756	1.58	−0.69	−5.69	−4.11
p(TTAB-FL)	864	1.27	−0.79	−5.28	−4.01

^a UV–vis spectra of **TTAB**, **Br₂[−]TTAB**, and **p(TTAB-FL)** were measured in THF solution ($c = 1.0 \times 10^{-5}$ mol/L). ^b The optical band gap estimated from the onset wavelength of the UV–vis spectra in THF. ^c CV was carried out in dichloromethane with 0.1 M Bu₄NPF₆ as supporting electrolyte. ^d E_{red} is the onset potential of first reduction wave. ^e Calculated from LUMO and optical band gap ($E_{\text{g}}^{\text{opt}}$) of the synthesized compounds, HOMO = LUMO − $E_{\text{g}}^{\text{opt}}$ (eV). ^f Calculated from the empirical formula, LUMO = − E_{red} − 4.80 (eV).⁶

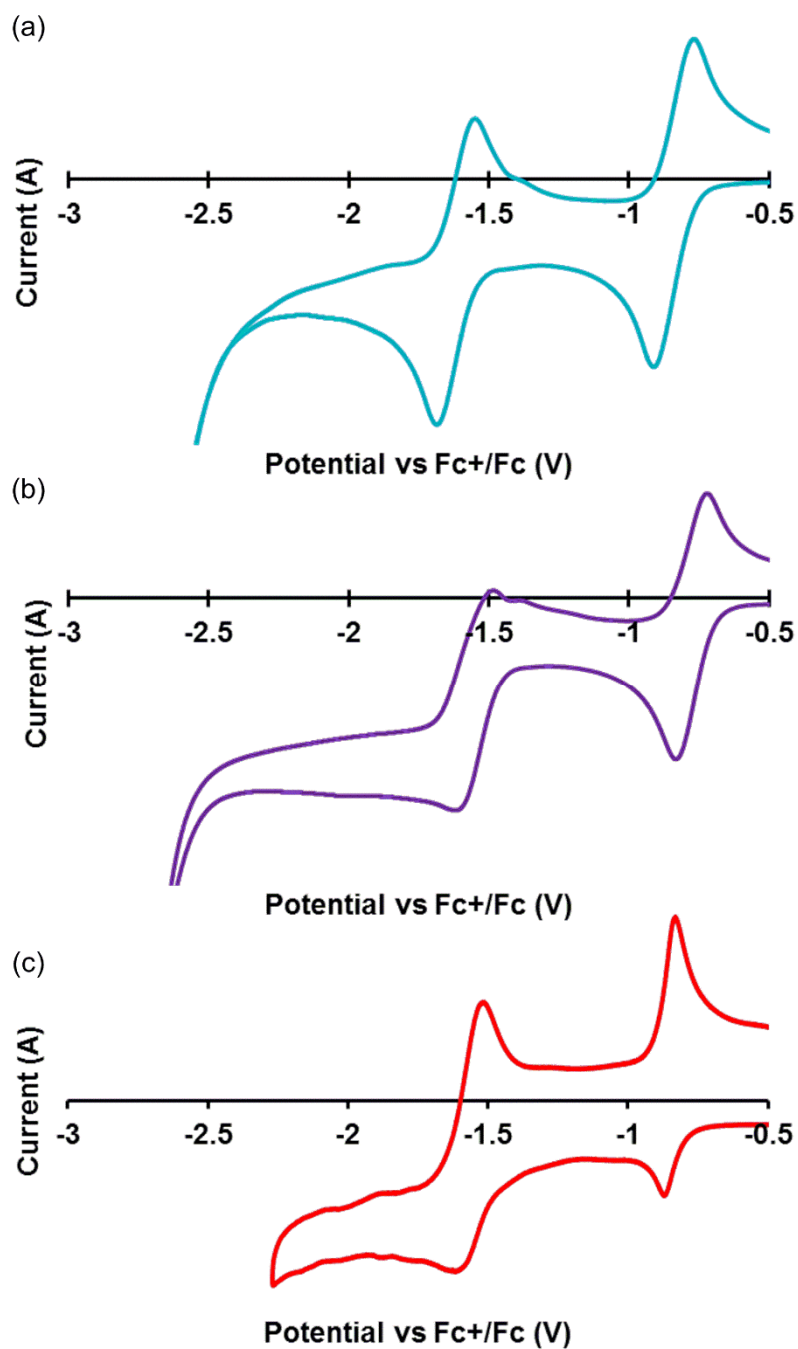


Figure 2. Cyclic voltammograms of (a) **TTAB**, (b) **Br₂-TTAB**, and (v) **p(TTAB-FL)** in dichloromethane ($c = 1 \times 10^{-3}$ M) with 0.1 M Bu_4NPF_6 as supporting electrolyte, AgCl/Ag as reference electrode, glassy carbon as working electrode, Pt as counter electrode, and scan rate at 100 mV/s.

Chapter 6

To receive more information about the electronic states of the synthesized compounds, the computer calculations were performed by the density functional theory (DFT). **TTAB** and **FL-TTAB-FL** which is model of **p(TTAB-FL)** were calculated (Figure 3). It was clearly shown that all HOMOs and LUMOs delocalized through **TTAB** moieties. The HOMO of **FL-TTAB-FL** was spread to the fluorene units, however LUMO was spread within the **TTAB** section. These results should be derived from electron-donating character of the fluorene units. Therefore, the HOMO energy level of the polymer model was higher than that of **TTAB**. On the other hand, the LUMO energy level was similar. These results are corresponded to the results of CV.

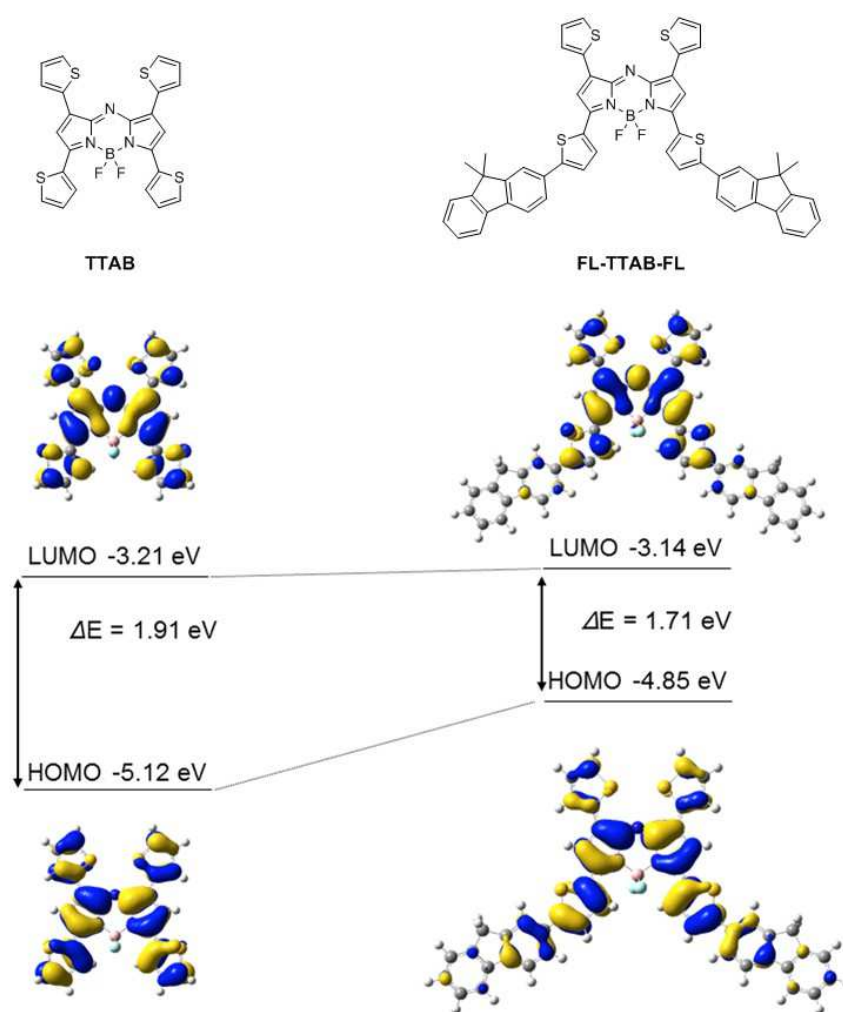


Figure 3. Structures and molecular orbital diagrams for LUMO and HOMO of **TTAB** and **FL-TTAB-FL** calculated with DFT (B3LYP/6-31G(d)//B3LYP/6-31G(d)).

Chapter 6

Conclusion

The deep NIR absorbing polymer was developed. In this chapter, thiophene-substituted aza-BODIPY was chosen as a polymer unit to expand conjugation by introducing the π -conjugated unit via Suzuki–Miyaura coupling polymerization. The synthetic polymer showed strong absorption band in the region with the peak at 864 nm. Furthermore, the LUMO energy level of the polymer was revealed from CV measurements. The low-lying LUMO energy of thiophene-substituted aza-BODIPY was maintained after polymerization. From these results, this NIR absorbing polymer could have potential for various applications.

Experimental Section

General: ^1H (400 MHz) and ^{11}B (128 MHz) NMR spectra were recorded on a JEOL JNM EX400 spectrometer. ^{11}B NMR spectra were referenced externally to $\text{BF}_3\cdot\text{OEt}_2$ (sealed capillary). Analytical thin-layer chromatography (TLC) was performed with silica gel 60 Merck F254 plates. Column chromatography was performed with Wakogel C-300 silica gel. UV–vis spectra were recorded on a Shimadzu UV-3600 spectrophotometer. Fluorescence emission spectra were recorded on a HORIBA JOBIN YVON Fluoromax-4 spectrofluorometer, and the absolute quantum yield was calculated by integrating sphere method on the HORIBA JOBIN YVON Fluoromax-4 spectrofluorometer in chloroform.

Computational Details: The Gaussian 09 program package⁷ was used for computation. The author optimized the structures of BODIPYs in the ground S_0 and excited S_1 states with the density functional theory (DFT) at the B3LYP/6-31G(d)//B3LYP/6-31G(d) level.

Synthesis of 1: 2-Acetyl-5-bromothiophene (5 g, 24 mmol) and 2-thiophenecarbaldehyde (2.7 mL, 3.3 g, 29 mmol) was dissolved in methanol (300 mL). To the solution, aqueous KOH solution (200 mL, 2.5 M) was added dropwise at 0 °C. The reaction mixture was kept under stirred condition at room temperature overnight. After cooling down to 0 °C, the reaction mixture was filtered, and the precipitated solid washed with water at first and then hexane to yield a pale yellow solid (7.0 g, 96%). The obtained **1** was used for the next reaction without further purification. ^1H NMR (CDCl_3): 7.95 (1H, d, $J = 15.1$ Hz), 7.57 (1H, d, $J = 3.9$ Hz), 7.44 (1H, d, $J = 5.1$ Hz), 7.37 (1H, d, $J = 3.4$ Hz), 7.14 (1H, d, $J = 4.1$ Hz), 7.13–7.06 (2H, m) ppm. HRMS (ESI): Calcd. for

Chapter 6

$[M+H]^+$, 298.9194; found, m/z 298.9188.

Synthesis of 2: A mixture of **1** (10 g, 33 mmol), nitromethane (10 g, 9.0 mL, 0.17 mol), and K_2CO_3 (92 mg, 0.67 mmol) were dissolved in ethanol (200 mL) and was heated to reflux for overnight. After cooling to room temperature, the solvent was removed by a rotary evaporator, and the oily residue was dissolved in CH_2Cl_2 and washed with water. The combined organic layers were washed with brine, dried over magnesium sulfate and concentrated to give the target compounds as a dark brown oily residue (11 g, 89%). The obtained **2** was used for the next reaction without further purification. 1H NMR ($CDCl_3$): 7.45 (1H, d, $J = 3.9$ Hz), 7.21 (1H, dd, $J = 4.5, 1.8$ Hz), 7.10 (1H, d, $J = 4.2$ Hz), 6.94–6.93 (2H, m), 4.76 (2H, dq, $J = 46.9, 6.5$ Hz), 4.52–4.45 (1H, m), 3.36 (2H, ddd, $J = 22.8, 15.8, 5.7$ Hz) ppm. HRMS (ESI): Calcd. for $[M+Na]^+$, 381.9178; found, m/z 381.9172.

Synthesis of Br₂-TTAB: A solution of **2** (11 g, 0.07 mol) and ammonium acetate (83 g, 1.1 mol) in ethanol (300 mL) was stirred at reflux temperature for 24 h. After cooling to room temperature, the solvent was concentrated to a half of its original volume by a rotary evaporator, and the suspension was filtered. The isolated solid was washed with ethanol to yield the crude intermediate as a dark blue solid. The crude solid (1.9 g) was dissolved in dry dichloromethane (260 mL). Triethylamine (3.1 g, 4.2 mL, 30 mmol) was then added to the solution, and the resulting mixture was stirred under argon atmosphere at room temperature for 20 min. After stirring for 20 min, $BF_3 \cdot OEt_2$ (6.4 g, 5.6 mL, 45 mol) was added and stirred under nitrogen atmosphere at room temperature for 16 h. The mixture was purified with flash column chromatography with

dichloromethane as an eluent. The silica gel column chromatography with hexane/dichloromethane (1:1) gave **Br₂-TTAB** as a dark blue solid (84 mg, 0.81%). ¹H NMR (CDCl₃): 8.00 (2H, d, *J* = 4.2 Hz), 7.91 (2H, dd, *J* = 3.7, 1.0 Hz), 7.57 (2H, dd, *J* = 5.1, 1.0 Hz), 7.21–7.19 (4H, m), 6.96 (2H, s) ppm. ¹¹B NMR (CDCl₃): δ = 0.93 (t, *J* = 31.3 Hz) ppm. HRMS (ESI): Calcd. for [M+H]⁺, 677.8415; found, *m/z* 677.8416.

Synthesis of p(TTAB-FL): Water (1.4 mL) was added to the solution of **Br₂-TTAB** (0.10 g, 0.15 mmol), [9,9-bis(dodecyl)-9H-fluorene-2,7-diyl]bisboronic acid (87 mg, 0.15 mmol), Pd₂(dba)₃ (1.3 mg, 1.5 μmol), S-Phos (2.4 mg, 5.9 μmol) and cesium carbonate (0.48 g, 1.5 mmol) in toluene (1.4 mL). The reaction mixture was stirred at 80 °C for 48 h under argon atmosphere and poured into a large amount of methanol to collect the polymer by filtration. The precipitate was dissolved in a small amount of THF, and then the product was reprecipitated from ethanol (twice). The polymer collected by filtration was dried in vacuum to give **p(TTAB-FL)** as a black solid (0.14 g, 92%). *M_n* = 1,500, *M_w/M_n* = 3.4. ¹H NMR (CDCl₃): δ = 8.53–7.00 (18H, m), 2.31–1.82 (4H, m), 1.43–0.50 (46H, m) ppm. ¹¹B NMR (CDCl₃): δ = 1.22 (t, *J* = 31.3 Hz) ppm.

Chapter 6

References

1. (a) Fabian, J.; Nakazumi, H.; Matsuoka, M. *Chem. Rev.* **1992**, *92*, 1197–1226. (b) Kiyose, K.; Kojima, H.; Nagano, T. *Chem. Asian J.* **2008**, *3*, 506–515. (c) Qian, G.; Wang, Z. Y. *Chem. Asian J.* **2010**, *5*, 1006–1029.
2. (a) Gorman, A.; Killoran, J.; O'Shea, C.; Kenna, T.; Gallagher, W. M.; O'Shea, D. F. *J. Am. Chem. Soc.* **2004**, *126*, 10619–10631. (b) Loudet, A.; Bandichhor, R.; Wu, L.; Burgess, K. *Tetrahedron* **2008**, *64*, 3642–3654. (c) Ge, Y.; O'Shea, D. F. *Chem. Soc. Rev.* **2016**, *45*, 3846–3864.
3. (a) Gresser, R.; Hartmann, H.; Wrackmeyer, M.; Leo, K.; Riede, M. *Tetrahedron* **2011**, *67*, 7148–7155. (b) Zhang, X.; Yu, H.; Xiao, Y. *J. Org. Chem.* **2012**, *77*, 669–673.
4. (a) Yoshii, R.; Nagai, A.; Chujo, Y. *J. Polym. Sci. A: Polym. Chem.* **2010**, *48*, 5348–5356. (b) Yoshii, R.; Yamane, H.; Nagai, A.; Tanaka, K.; Taka, H.; Kita, H.; Chujo, Y. *Macromolecules* **2014**, *47*, 2316–2323. (c) Tanaka, K.; Yanagida, T.; Yamane, H.; Hirose, A.; Yoshii, R.; Chujo, Y. *Bioorg. Med. Chem. Lett.* **2015**, *25*, 5331–5334.
5. (a) Bellier, Q.; Dalier, F.; Jeanneau, E.; Maury, O.; Andraud, C. *New J. Chem.* **2012**, *36*, 768–773. (b) Khan, T. K.; Sheokand, P.; Agarwal, N. *Eur. J. Org. Chem.* **2014**, 1416–1422.
6. (a) Chen, C. -P.; Chan, S. -H.; Chao, T. -C.; Ting, C.; Ko, B. -T. *J. Am. Chem. Soc.* **2008**, *130*, 12828–12833. (b) Morisaki, Y.; Ueno, S.; Chujo, Y. *J. Polym. Sci. Part A: Polym. Chem.* **2013**, *51*, 334–339.
7. Gaussian 09, Revision A.1, Frisch, M. J.; Trucks, G. W.; Schlegel, H. B.; Scuseria, G. E.;

Robb, M. A.; Cheeseman, J. R.; Scalmani, G.; Barone, V.; Mennucci, B.; Petersson, G. A.; Nakatsuji, H.; Caricato, M.; Li, X.; Hratchian, H. P.; Izmaylov, A. F.; Bloino, J.; Zheng, G.; Sonnenberg, J. L.; Hada, M.; Ehara, M.; Toyota, K.; Fukuda, R.; Hasegawa, J.; Ishida, M.; Nakajima, T.; Honda, Y.; Kitao, O.; Nakai, H.; Vreven, T.; Montgomery, Jr., J. A.; Peralta, J. E.; Ogliaro, F.; Bearpark, M.; Heyd, J. J.; Brothers, E.; Kudin, K. N.; Staroverov, V. N.; Kobayashi, R.; Normand, J.; Raghavachari, K.; Rendell, A.; Burant, J. C.; Iyengar, S. S.; Tomasi, J.; Cossi, M.; Rega, N.; Millam, J. M.; Klene, M.; Knox, J. E.; Cross, J. B.; Bakken, V.; Adamo, C.; Jaramillo, J.; Gomperts, R.; Stratmann, R. E.; Yazyev, O.; Austin, A. J.; Cammi, R.; Pomelli, C.; Ochterski, J. W.; Martin, R. L.; Morokuma, K.; Zakrzewski, V. G.; Voth, G. A.; Salvador, P.; Dannenberg, J. J.; Dapprich, S.; Daniels, A. D.; Farkas, Ö.; Foresman, J. B.; Ortiz, J. V.; Cioslowski, J.; Fox, D. J. Gaussian, Inc., Wallingford CT, **2009**.

Chapter 7

Liquid Scintillators with Near Infrared Emission

Based on Organoboron Conjugated Polymers

ABSTRACT: The organic liquid scintillators based on the emissive polymers are reported. A series of conjugated polymers containing organoboron complexes which show the luminescence in the near infrared (NIR) region were synthesized. The polymers showed good solubility in common organic solvents. From the comparison of the luminescent properties of the synthesized polymers between optical and radiation excitation, similar emission bands were detected. In addition, less significant degradation was observed. These data propose that the organoboron conjugated polymers are attractive platforms to work as an organic liquid scintillator with the emission in the NIR region.

Chapter 7

Introduction

Scintillators which present a luminescence by absorbing radiation are versatile materials not only for quantifying an environmental radiation dose but also for using in the modern medical instruments. Development of higher-performance scintillators has been still required for advanced radiation monitoring such as highly-sensitive detection, precise quantification and discrimination of the radiation species.¹ Most of conventional scintillators are composed of inorganic crystals, and the preparation for the crystals with low cost has been radically explored.² Organic polymers are intrinsically cheap, light and flexible. In particular, polymers have high processability and film-formability which are useful properties for the preparation of the plastic-type sensors. Moreover, color and other optical properties can be readily tuned by altering the chemical structures, the introduction of element blocks which are consisted of heteroatom-containing functional units or groups and the conjugation with various comonomers by employing an alternating copolymer structure according to the preprogrammed design.³ Thus, polymer-based materials are attractive candidates as a platform for developing new series of scintillators. However, even the number of all organic scintillators is much fewer than those of inorganic ones. Although polymers have been used as a matrix in hybrid material-based scintillators or mixture systems, the polymer-based scintillator with the single chemical component is still very few.^{4,5} Especially, the scintillation emissions were observed in the different wavelength regions from the photoluminescence spectra. This fact means that it is still difficult to obtain the scintillation emission at the desired emission wavelength. In addition, there are much room to explore systematic information on the

relationships between chemical structure and scintillation ability. To probe the feasibility of organic materials as a scintillator, fundamental information on the optical properties should be needed. The comparison study on the luminescence by the photon excitation and the radiation irradiation should be essential for receiving expected scintillators based on the molecular design.

Because of the high permeability through air and aqueous media involving vital organs, the NIR is applied in the sensing technology.⁶ The probes with the NIR emission can present the signal at the relatively-deeper spot inside bodies comparing to commodity fluorescence materials. Therefore, the development of efficient NIR-emissive materials is still a topic with high relevance.⁷ Versatility of organoboron conjugated polymers have been revealed from a series of the recent works as a typical example of element blocks.^{3,8} Particularly, various NIR-emissive molecules and polymers have been reported.⁹ For example, it was found that the boron di(iso)indomethene-containing polymers presented strong emission in the NIR region.¹⁰ Especially, the sharp emission bands were observed in the spectra. These properties are feasible for obtaining vivid color from the display and for improving the sensitivity in the bioimaging usages. As another instance, the NIR-emissive boron dipyrromethene (BODIPY) was introduced into the polymer main-chains.^{9,11} Since the resulting polymers also showed high electron-carrier ability, the application of these polymers to the electroluminescent devices progresses.¹¹ Based on the flexibility in the molecular design and various functions derived from a variety of chemical structures, unique characteristics were obtained. Thus, it can be expected that organoboron polymers are a promising platform for producing a new series of advanced scintillators.

Chapter 7

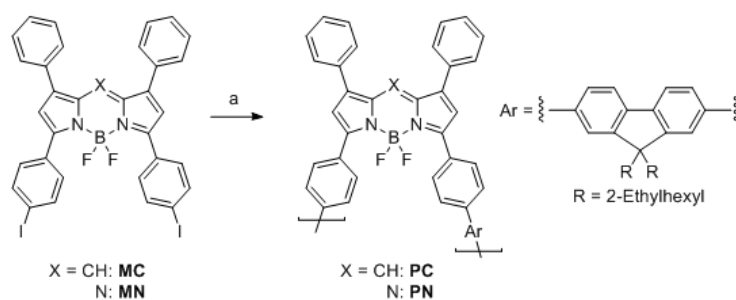
Herein, the NIR-emissive organoboron conjugated polymers were synthesized. Particularly, the author aimed to obtain the similar emission spectra from the polymer solutions with both photo- and X-ray excitations. To fulfill the purpose of this research, the comparison study of the optical properties of the synthesized conjugated polymers with the optical and radiation excitation was performed. Emission efficiencies and the decay times were evaluated. In addition, the stability was also investigated. The structure-property relationship for the application to organic scintillators is mainly discussed.

Results and Discussion

It has been reported that the tetraphenyl-substituted BODIPY and aza-BODIPY derivatives showed bright emissions in deep-red and NIR regions due to the narrow band gaps (Scheme 1).^{9,11} At the *meso*-position in the BODIPY derivatives, the lowest unoccupied molecular orbital (LUMO) was often delocalized.¹² Thereby, by replacing the CH at the *meso*-position to N, only the energy level of LUMO can be lowered, leading to the red-shifted emission.^{9,11} In this study, the author aimed to evaluate the influence of this modification of chemical structures on the scintillation ability. The sharp emission spectra are advantageous for a sensing material. Especially, it was presented from the recent paper that these BODIPYs can have high electron-carrier abilities.¹¹ Thus, it is presumed that the side-reactions or the deactivation of the excitons generated by the higher-energy light irradiation might be suppressed, resulting in efficient scintillation. However, free BODIPYs would readily form aggregation even in the diluted solution state.

Therefore, the chemical modification to maintain solubility should be needed to keep the homogeneous solution state. One of solves to improve solubility is the formation of the polymers. Particularly, by introducing into alternating polymers, the tunability of the electronic states as well as the enhancement of solubility can be expected. Thus, the author designed the BODIPY-containing alternating polymers with alkyl-substituted fluorene which has a superior property for enhancing solubility and light-absorption ability.

The monomers were prepared according to the previous report.¹¹ The polymerization with fluorenyldiboronic acid via Suzuki–Miyaura coupling is illustrated in Scheme 1. To maintain the solubility of the products, the 9-position at the center of the fluorene unit was modified with the alkyl chains. After the reaction and reprecipitation from methanol to remove the metal species and small molecules derived from the monomers, the products were obtained. A series of measurements were performed to characterize the products (Table 1). The number-average molecular weight (M_n) and polydispersity index (M_w/M_n) of the polymer determined from GPC analysis were evaluated, and the values of degree of polymerization (DP) were calculated from the obtained molecular weights. The polymer showed moderate solubilities in conventional organic solvents such as chloroform, dichloromethane, and THF. From the ^1H and ^{11}B NMR spectra, similar signal patterns involving aza-BODIPY and the fluorene units in the polymer were obtained. The author concluded that the polymers should have the designed structures as the author expected.

Scheme 1. Synthetic scheme of the polymers^a

^aReagents and conditions: (a) [9,9-Bis(2-ethylhexyl)-9H-fluorene-2,7-diyl]bisboronic acid, $\text{Pd}_2(\text{dba})_3$, S-Phos, cesium carbonate, toluene, 80 °C, 3 d, (**PC**: 96%, **PN**: 85%).

Table 1. Physical properties of the polymers^a

	PC	PN
M_n	4,300	7,700
M_w/M_n	2.0	2.0
DP^b	4.9	8.7
Yield (%) ^c	85	96

^a Estimated by size-exclusion chromatography (SEC) based on polystyrene standards in chloroform. ^b Degree of polymerization estimated by number-average molecular weight. ^c Isolated yields after precipitation.

The optical properties of the synthesized polymers were investigated. Figure 1 shows the UV-vis absorption spectra in toluene. The results are summarized in Table 2. The largest absorption bands with the peaks at 610 nm and 703 nm assigned to the π - π^* transitions at each complex were observed from **PC** and **PN**, respectively. Comparing the peak positions of the absorption bands to those of the monomers (**MC**: 579 nm, **MN**: 664 nm), the polymers provided the absorption in the red-shifted regions.¹¹ These results indicate that the main-chain conjugation should be expanded in the ground state. In addition, the similar peak shapes were observed from the solutions. The unexpected inter-chain interaction or aggregation could be suppressed in the samples. For the measurements with the optical excitation, the samples were irradiated with the light at the absorption maxima.

Photoluminescence (PL) spectra were gathered with the solutions containing the synthesized polymers in toluene (Figure 2). The optical properties are summarized in Table 2. Typical spectra were obtained from the measurements. Emission bands with the peaks at 654 nm and 750 nm attributable to the S_0 - S_1 (π - π^*) transition were obtained from **PC** and **PN**, respectively. These data mean that the polymers should be NIR-emissive materials. The peak shifts to the longer wavelength regions than those in each monomer were also observed (**MC**: 613 nm, **MN**: 694 nm).¹¹ These data indicate the elongation of the conjugation system through the polymer main-chains in the excited state. The emission lifetimes were measured (Table 2). The kinetics of the emission were evaluated from the time-resolved luminescent spectra. The lifetimes were calculated from the fitting curves to the emission decay. It was confirmed that the emissions of the

Chapter 7

synthesized polymers should be assigned as fluorescence.

Scintillation emission spectrum under X-ray irradiation is shown in Figure 2. X-ray induced radioluminescence spectra of the polymers were evaluated by using the original setup.¹³⁻¹⁷ All samples containing 10^{-5} μM in toluene (10 mL) were sealed into a glass columnar bottle (height: 4.5 cm, bottom diameter 1.5 cm), and X-ray was irradiated from the bottom. The emission bands were observed in the deep red and NIR regions. These data represent that the synthesized polymers should have the scintillation ability in the solution states. In particular, the emission peaks were obtained at 662 nm and 752 nm from **PC** and **PN**, respectively. It is noteworthy that the similar spectra were obtained with the PL spectra. The scintillation decay time profile of the synthesized polymers was measured. The time profiles were well reproduced by a double exponential assumption. Deduced decay times are listed in Table 2 and showed good correlations to those from the PL data. These results strongly support that the scintillation from the synthesized polymers should originate from the S_0-S_1 ($\pi-\pi^*$) transition. In other words, the scintillation properties can be estimated by the PL spectra. In addition, to evaluate the durability against the X-ray irradiation, the author measured the PL spectra again, and similar spectra were obtained from each polymer solution. This result means that the degradation in both polymer samples hardly occurred after the radiation irradiation (360 Gy). It is implied that the synthesized polymers could have stability enough for the application as a scintillator. So far, there are very few scintillators involving inorganic materials with the emission in the NIR regions. Thereby, it is difficult to directly compare and quantitatively evaluate the scintillation ability to the previous materials at this stage. It is

implied that these materials can be used as a standard for evaluating the scintillation ability in the NIR region.

Table 2. Photophysical properties of the polymers^a

	PC	PN
$\lambda_{\text{Abs,max}}$ (nm)	610	703
ϵ (M ⁻¹ cm ⁻¹)	52,000	42,000
$\lambda_{\text{PL,max}}$ (nm) ^b	654	750
Φ_{PL} ^c	0.47	0.028
$\lambda_{\text{X-ray,max}}$ (nm)	662	752
τ_{PL} (ns) ^d	1.64 (0.04), 4.23 (0.96)	1.92
$\tau_{\text{X-ray}}$ (ns)	0.46 (0.90), 2.91 (0.10)	0.36 (0.88), 2.22 (0.12)

^a Measured in toluene (1.0×10^{-5} M). ^b Measured with the excitation light at the maximum peak wavelength of absorption. ^c Absolute quantum yield. ^d Measured with the excitation light at 375 nm. Parentheses mean the proportions of each element in the decay curves.

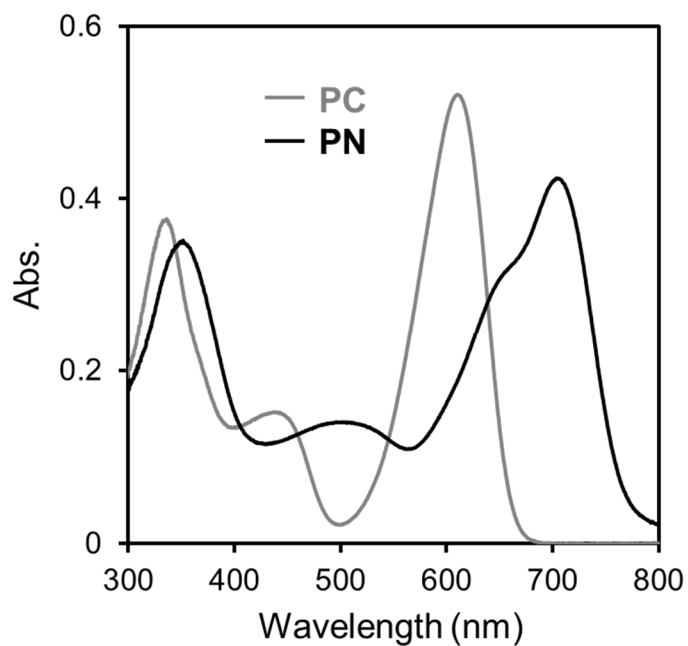


Figure 1. UV-vis absorption spectra of the polymers in toluene (1.0×10^{-5} M).

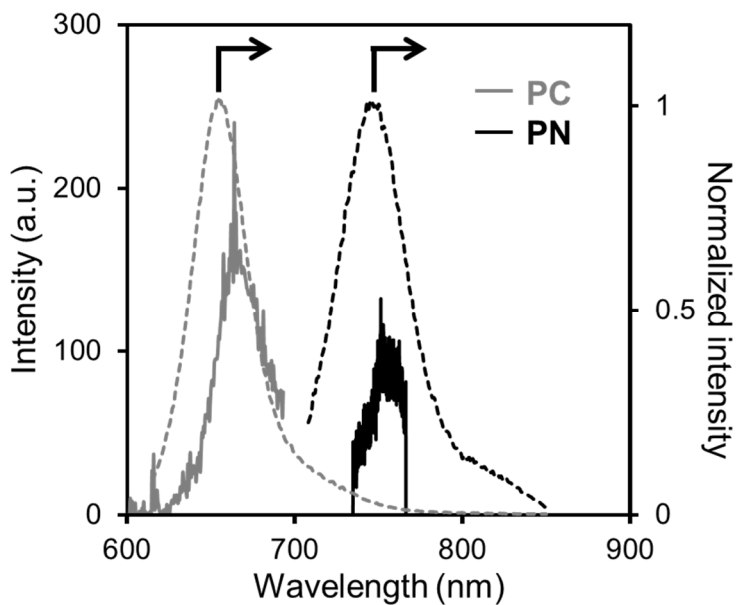


Figure 2. Emission spectra of the polymers in toluene (1.0×10^{-5} M) with the excitation light at the wavelength of the absorption maxima (dot line) and X-ray (solid line).

Conclusion

The conjugated polymers with the similar emission spectra via both photo- and X-ray excitations were demonstrated in this study. The fundamental information on the scintillation abilities of the organoboron NIR-emissive polymers is also presented. It is shown that the organoboron-containing conjugated polymers can work as a liquid scintillator in the organic solvent. It should be emphasized that the scintillation properties showed good correlation to the luminescence by the optical excitation. These facts represent that an expected scintillation ability could be obtained according to the preprogrammed design. Furthermore, organoboron materials involving polymers are paid attention as a neutron-selective scintillator due to the intrinsic reactivity of boron to neutron. Therefore, the findings described here might be useful not only for developing organic-based advanced functional scintillators but also for constructing neutron-selective sensors.

Experimental section

General: ^1H (400 MHz), ^{13}C (100 MHz), and ^{11}B (128 MHz) NMR spectra were recorded on a JEOL JNM-EX400 spectrometer (JEOL Ltd., Tokyo, Japan). In the ^1H NMR spectra and the ^{13}C NMR spectra, tetramethylsilane (TMS) was used as an internal standard in CDCl_3 and CD_2Cl_2 , respectively. In the ^{11}B NMR spectra, $\text{BF}_3 \cdot \text{OEt}_2$ (sealed capillary) was used as an external standard. MASS spectra were obtained on a JEOL JMS-SX102A. Recyclable preparative high-performance

Chapter 7

liquid chromatography (HPLC) was carried out on a Japan Analytical Industry Model LC918R (JAIGEL-1H and 2H columns) using chloroform as an eluent (Japan Analytical Industry Co., Ltd., Tokyo, Japan). The number-average molecular weight (M_n) and the molecular weight distribution [weight-average molecular weight/number-average molecular weight (M_w/M_n)] values of all polymers were estimated by size-exclusion chromatography (SEC), performed on a TOSOH G3000HXI system equipped with three consecutive polystyrene gel columns [TOSOH gels: α -4000, α -3000, and α -2500] and an ultraviolet detector at 40 °C (TOSOH Corp., Tokyo, Japan). The system was operated at a flow rate of 1.0 mL/min with CHCl_3 as an eluent. The system was calibrated with polystyrene standards. UV-Vis spectra were recorded on a Shimadzu UV-3600 spectrophotometer (Shimadzu Corp., Kyoto, Japan). Fluorescence emission spectra were recorded on a HORIBA JOBIN YVON Fluoromax-4 spectrofluorometer, and the absolute quantum yield was calculated with the integrating sphere on the HORIBA JOBIN YVON Fluoromax-4 spectrofluorometer in chloroform (HORIBA, Ltd., Kyoto, Japan). Photoluminescence (PL) lifetime was measured by a Horiba FluoreCube spectrofluorometer system and excitation was carried out at 375nm using UV diode laser (NanoLED 375 nm). Elemental analysis was performed at the Microanalytical Center of Kyoto University.

X-ray induced radioluminescence spectrum of **PC** was evaluated by using the original setup.^{13,14} The excitation source was an X-ray generator supplied with 80 kV bias voltage and 2.5 mA tube current. Scintillation photons were fed into a monochromater (SR163, Andor) via optical fiber and into CCD (DU-420-BU2, Andor). Radioluminescence was evaluated by a transmission-type

measurement assuming actual applications. Then, scintillation spectrum of **PN** was evaluated by using pulse X-ray equipped streak camera system for scintillation characterization which was also developed by us and became a product of Hamamatsu.^{15,16} The mean and maximum end point energy of X-ray were 20 and 30 keV, respectively. Although the system was developed to evaluate timing property, we used it to observe scintillation spectrum since the wavelength sensitivity of the CCD for radioluminescence observation was up to 700 nm. By using pulse X-ray equipped afterglow characterization system¹⁷, we evaluated scintillation decay time profiles. All samples containing 10^{-5} μM in toluene (10 mL) were sealed into a glass columnar bottle (height: 4.5 cm, bottom diameter 1.5 cm), and X-ray was irradiated from the bottom.

Synthesis of PC: Water (2.2 mL) was added to the mixture containing **MC**¹¹ (0.17 g, 230 μmol), [9,9-bis(2-ethylhexyl)-9H-fluorene-2,7-diyl]bisboronic acid (0.11 g, 230 μmol), $\text{Pd}_2(\text{dba})_3$ (2.1 mg, 2.3 μmol), S-Phos (3.7 mg, 9.2 μmol), and cesium carbonate (0.75 g, 2.3 mmol) in toluene (2.2 mL). The mixture was stirred at 80 °C for 3 days under nitrogen atmosphere. After the reaction, the mixture was poured into an excess amount of methanol to collect the polymer as a precipitation by filtration. The precipitate was dissolved again in a small amount of THF, and then the product was reprecipitated from ethanol. After this reprecipitation procedure was carried out twice, the polymer was collected by filtration and dried *in vacuo* to give **PC** as a dark blue solid (0.17 g, 85%). $M_n = 4,300$, $M_w/M_n = 2.0$. ^1H NMR (CDCl_3): $\delta = 8.11$ (4H, br) 7.87–7.32 (21H, m) 6.83 (2H, br) 2.08 (4H, br) 1.00–0.33 (30H, m) ppm. ^{11}B NMR (CDCl_3): $\delta = 1.81$ (t, $J = 31.30$ Hz) ppm.

Synthesis of PN: **PN** was prepared from **MN**¹¹ (0.62 g, 0.84 mmol) in 96% yield (0.71 g, black

Chapter 7

solid) according to the same method for **PC**. $M_n = 7,700$, $M_w/M_n = 2.0$. ^1H NMR (CDCl_3): $\delta = 8.59\text{--}7.27$ (24H, m) 6.99 (2H, br) 1.85 (4H, br) 1.06–0.28 (30H, m) ppm. ^{11}B NMR (CDCl_3): $\delta = 0.91$ (t, $J = 31.50$ Hz) ppm.

References

1. (a) Nikl, M.; Yoshikawa, A.; Kamada, K.; Nejezchleb, K.; Stanek, C. R.; Mares, J. A.; Blazek, K. *Prog. Cryst. Growth Charact. Mater.* **2013**, *59*, 47–72. (b) Li, J.-G.; Sakka, Y. *Sci. Technol. Adv. Mater.* **2015**, *16*, 014902. (c) Yamamoto, Y.; Tasaki, Y.; Kuwada, Y.; Ozawa, Y.; Katayama, A.; Kanemaki, Y.; Enokido, K.; Nakamura, S.; Kubouchi, K.; Morita, S.; Noritake, M.; Nakajima, Y.; Inoue, T. *Ann. Nucl. Med.* **2013**, *27*, 795–801.
2. (a) Masai, H.; Hino, Y.; Yanagida, T.; Fujimoto, Y.; Tokuda, Y. *Opt. Mater. Express* **2015**, *5*, 617–622. (b) Masai, H.; Hino, Y.; Yanagida, T.; Fujimoto, Y. *Opt. Mater.* **2015**, *42*, 381–384. (c) Yanagida, T.; Fujimoto, Y.; Koshimizu, M.; Fukuda, K. *J. Lumin.* **2015**, *157*, 293–296.
3. Chujo, Y.; Tanaka, K. *Bull. Chem. Soc. Jpn* **2015**, *88*, 633–643.
4. (a) Koshimizu, M.; Kitajima, H.; Iwai, T.; Asai, K. *Jpn. J. Appl. Phys.* **2008**, *47*, 5717–5719. (b) Bertrand, G. H. V.; Hamel, M.; Normand, S.; Sguerra, F. *Nucl. Instrum. Methods A* **2015**, *776*, 114–128. (c) Bertrand, G. H. V.; Hamel, M.; Sguerra, F. *Chem. Eur. J.* **2014**, *20*, 15660–15685. (d) Sun, Y.; Koshimizu, M.; Yahaba, N.; Nishikido, F.; Kishimoto, S.; Haruki, R.; Asai, K. *Appl. Phys. Lett.* **2014**, *104*, 174104. (e) Sguerra, F.; Marion, R.; Bertrand, G. H. V.; Coulon, R.; Sauvageot, É.; Daniellou, R.; Renaud, J.-L.; Gaillard, S.; Hamel, M. *J. Mater.*

- Chem. C* **2014**, *2*, 6125–6133. (f) Bertrand, G. H. V.; Sguerra, F.; Dehé-Pittance, C.; Carrel, F.; Coulon, R.; Normand, S.; Barat, E.; Dautremer, T.; Montagu, T.; Hamel, M. *J. Mater. Chem. C* **2014**, *2*, 7304–7312. (g) Nakamura, H.; Shirakawa, Y.; Kitamura, H.; Yamada, T.; Shidara, Z.; Yokozuka, T.; Nguyen, P.; Takahashi, T.; Takahashi, S. *Radiat. Meas.* **2013**, *59*, 172–175.
5. (a) Kamaya, E.; Matsumoto, F.; Kondo, Y.; Chujo, Y.; Katagiri, M. *Nucl. Instrum. Methods A* **2004**, *529*, 329–331. (b) Nakamura, H.; Shirakawa, Y.; Kitamura, H.; Sato, N.; Shinji, O.; Saito, K.; Takahashi, S. *Appl. Phys. Lett.* **2013**, *103*, 161111. (c) Adadurov, A. F.; Yelyseev, D. A.; Titskaya, V. D.; Lebedev, V. N.; Zhmurin, P. N. *Radiat. Meas.* **2011**, *46*, 498–502.
6. Weissleder, R. *Nat. Biotechnol.* **2001**, *19*, 316–317.
7. (a) Yen, S. K.; Janczewski, D.; Lakshmi, J. L.; Dolmanan, S. B.; Tripathy, S.; Ho, V. H. B.; Vijayaragavan, V.; Hariharan, A.; Padmanabhan, P.; Bhakoo, K. K.; Sudhakaran, T.; Ahmed, S.; Zhang, Y.; Selvan, S.T. *ACS Nano* **2013**, *7*, 6796–6805. (b) Pansare, V. J.; Hejazi, S.; Faenza, W. J.; Prud'homme, R. K. *Chem. Mater.* **2012**, *24*, 812–827.
8. Tanaka, K.; Chujo, Y. *Macromol. Rapid Commun.* **2012**, *33*, 1235–1255.
9. Yoshii, R.; Nagai, A.; Chujo, Y. *J. Polym. Sci. Part A: Polym. Chem.* **2010**, *48*, 5348–5356.
10. Yoshii, R.; Nagai, A.; Tanaka, K.; Chujo, Y. *J. Polym. Sci. Part A: Polym. Chem.* **2013**, *51*, 1726–1733.
11. Yoshii, R.; Yamane, H.; Nagai, A.; Tanaka, K.; Taka, H.; Kita, H.; Chujo, Y. *Macromolecules* **2014**, *47*, 2316–2323.

Chapter 7

12. (a) Gresser, R.; Hartmann, H.; Wrackmeyer, M.; Leo, K.; Riede, M. *Tetrahedron* **2011**, *67*, 7148–7155. (b) Tanaka, K.; Yamane, H.; Yoshii, R.; Chujo, Y. *Bioorg. Med. Chem.* **2013**, *21*, 2715–2719.
13. Yanagida, T.; Kamada, K.; Fujimoto, Y.; Yagi, H.; Yanagitani, T. *Opt. Mater.* **2013**, *35*, 2480–2485.
14. Yanagida, T.; Fujimoto, Y.; Fukuda, K.; Chani, V. *Nucl. Instrum. Methods A* **2013**, *729*, 58–63.
15. Yanagida, T.; Fujimoto, Y.; Yamaji, A.; Kawaguchi, N.; Kamada, K.; Totsuka, D.; Fukuda, K.; Yamanoi, K.; Nishi, R.; Kurosawa, S.; Shimizu, T.; Sarukura, N. *Radiat. Meas.* **2013**, *55*, 99–102.
16. Yanagida T.; Fujimoto Y.; Yoshikawa A.; Yokota Y.; Kamada K.; Pejchal J.; Kawaguchi N.; Fukuda K.; Uchiyama K.; Mori K.; Kitano K.; Nikl M.; *Appl. Phys. Exp.* **2010**, *3*, 056202.
17. Yanagida, T.; Fujimoto, Y.; Ito, T.; Uchiyama, K.; Mori, K. *Appl. Phys. Exp.* **2014**, *7*, 062401.

List of Publications

Chapter 1

Simple and Valid Strategy for the Enhancement of the Solid-Emissive Property of Boron Dipyrromethene

Honami Yamane, Kazuo Tanaka and Yoshiki Chujo

Tetrahedron Lett. **2015**, *56*, 6786–6790.

Chapter 2

Preservation of Main-Chain Conjugation through BODIPY-Containing Alternating Polymers from Electronic Interactions with Side-Chain Substituents by Cardo Boron Structures

Honami Yamane, Shunichiro Ito, Kazuo Tanaka and Yoshiki Chujo

Polym. Chem. **2016**, *7*, 2799–2807.

Chapter 3

The Dual-Emissive Polymer Based on BODIPY Homopolymer Bearing Anthracene on Cardo Boron

Honami Yamane, Kazuo Tanaka and Yoshiki Chujo

To be submitted

Chapter 4

Efficient Light Absorbers Based on Thiophene-Fused Boron Dipyrromethene (BODIPY) Dyes

Kazuo Tanaka, Honami Yamane, Ryousuke Yoshii and Yoshiki Chujo

Bioorg. Med. Chem. **2013**, *21*, 2715–2719.

List of Publications

Chapter 5

Synthesis of Furan-Substituted Aza-BODIPYs Having Strong Near-Infrared Emission

Honami Yamane, Shunsuke Ohtani, Kazuo Tanaka and Yoshiki Chujo

To be submitted

Chapter 6

Synthesis of the Near-Infrared Light-Absorbing Polymer Based On Thiophene-substituted Aza-BODIPY

Honami Yamane, Kazuo Tanaka and Yoshiki Chujo

To be submitted

Chapter 7

Liquid Scintillators with Near Infrared Emission Based on Organoboron Conjugated Polymers

Kazuo Tanaka, Takayuki Yanagida, Honami Yamane, Amane Hirose, Ryouyusuke Yoshii and Yoshiki Chujo

Bioorg. Med. Chem. Lett. **2015**, 25, 5331–5334.

Other Publications

QM/MD Simulation of SWNT Nucleation on Transition-Metal Carbide Nanoparticles

Alister J. Page, Honami Yamane, Yasuhito Ohta, Stephan Irle and Keiji Morokuma

J. Am. Chem. Soc. **2010**, *132*, 15699–15707.

π -Conjugated Polymers Composed of BODIPY or Aza-BODIPY Derivatives Exhibiting High Electron Mobility and Low Threshold Voltage in Electron-Only Devices

Ryousuke Yoshii, Honami Yamane, Atsushi Nagai, Kazuo Tanaka, Hideo Taka, Hiroshi Kita and Yoshiki Chujo

Macromolecules **2014**, *47*, 2316–2323.

Synthetic Strategy for Low-Band Gap Oligomers and Homopolymers Using Characteristics of Thiophene-Fused Boron Dipyrromethene

Ryousuke Yoshii, Honami Yamane, Kazuo Tanaka and Yoshiki Chujo

Macromolecules **2014**, *47*, 3755–3760.

Transformation of Sulfur to Organic-Inorganic Hybrids Employed by POSS Networks and Their Application for the Modulation of Refractive Indices

Kazuo Tanaka, Honami Yamane, Koji Mitamura, Seiji Watase, Kimihiro Matsukawa and Yoshiki Chujo

J. Polym. Sci. Part A: Polym. Chem. **2014**, *52*, 2588–2595.

Synthesis and Color Tuning of Boron Diiminate Conjugated Polymers with Aggregation-Induced Scintillation Properties

Kazuo Tanaka, Takayuki Yanagida, Amane Hirose, Honami Yamane, Ryousuke Yoshii and Yoshiki Chujo

RSC Adv. **2015**, *5*, 96653–96659.